ANALYSIS, ASSESSMENT AND OPTIMIZATION OF BIOMASS MIXED HEAVY-OIL DRIVEN INTEGRATED GASIFICATION COMBINED CYCLE FOR MULTIGENERATION

by

SHAHID ISLAM

A Thesis Submitted in Partial Fulfillment

of the Requirements for the Degree of

Doctor of Philosophy

in

The Faculty of Mechanical Engineering

Faculty of Engineering and Applied Science

University of Ontario Institute of Technology

Oshawa, Ontario, Canada

November, 2017

Abstract

There has been increasing interest in employing Integrated Gasification Combined Cycles (IGCC) using various biomasses and low-rank coals for producing multiple outputs. The most of the existing IGCC plants do not conserve the low-grade heat, use air separation unit and the presence of coal produces high amount of carbon based emissions. The production of syngas through gasification of renewable feedstocks, such as biomass, organic food waste and animal manure is an attractive option with less emissions. In this thesis, three novel multigeneration IGCC based on organic and refinery wastes are specifically developed for three sectors; community, food industry and refinery. The systems are simulated using Aspen (Plus) and results are validated through energy and exergy analyses, and research reported in the literature.

The exergy analysis is performed with the help of Engineering Equation Solver (EES). The developed systems can be employed anywhere in the world with some modifications, however, the case studies are performed for Saudi Arabia for assessment. The Genetic Algorithm model is used to optimize the developed systems. A multi-objective optimization approach is applied to achieve the best performances of the developed systems. Three objectives function used in this study include; exergy efficiency, total cost and CO_2 emissions. The developed systems are environmentally benign as the production of CO_2 is low enough to meet the stringent environmental regulations.

The energy and exergy efficiencies of the cold gas, overall, gas turbine and steam turbine for the proposed systems 1 are found to be 58.2% and 57.6%, 55.9% and 32.1%, 29.8% and 26.7%, 34.1% and 60.1%, respectively. The energy and exergy efficiencies of the cold gas, overall, gas turbine and steam turbine for the proposed systems 2 are found to be 62.1% and 61.4%, 57.9% and 33.3%, 29.2% and 25.9%, 33.7% and 61.7%, respectively. The energy and exergy efficiencies of the cold gas, overall, gas turbine and steam turbine for the proposed systems 3 are found to be 68.3% and 68.7%, 60.7% and 34.8%, 27.8% and 24.7%, 34.4% and 60.3%, respectively. The highest magnitude of exergy destruction occurs in combustion chamber. The electrical power output for system 1, system 2, and system 3 is found to be in the order of 461 MW, 433 MW and 466 MW, respectively.

Acknowledgments

I attribute the success of this research to the guidance of my supervisor Professor Ibrahim Dincer whose teachings and supervision have really inspired me to do my best in the thesis research and complete this thesis in correct, complete and consistent manner. I am truly honored by having Professor Dincer as supervisor and inspirational educator.

I would like to thank Professor Bekir Sami Yilbas for his guidance and motivation. I would also like to thank Dr. Abdul Khaliq for his useful advices. Thanks to, Dr. Shuja, Dr. Haider, Dr. Bilal, Dr. Sayem for their support, and Dr. Omer Zahid and Dr. Marianne for their suggestions about simulation and my colleagues at UOIT for their help and excellent suggestions, during the preparation of this report, especially Mr. Farrukh Khalid. I would also like to thank my friends Mr. Israr, Mr. Imtiaz, Mr. Irfan, Mr. Irshad, Mr. Asad, Mr. Rizwan, Mr. Waheed, Mr. Azam, Mr. Pervaiz, Mr. Nadeem Sharif, Mr. Nadeem Ijaz, Mr. Farhan Hussaini, Mr. Samiuddin and Mr. Basit for their encouragement and motivation.

Last but not the least; I would like to express my deepest love and thanks to my deceased parents, my family especially, my wife, daughters (Rumaysa and Wania), elder brother Mr. Abdul Salam and his wife, sisters, mother in law, sisters in law, brothers in law, nephews and nieces for their limitless support, strength, inspiration and reassurance throughout my life, without them this would not have been possible. The honor of this degree truly belongs to them. Their blessings and prayers have always been with me.

To all of whom I have missed during this brief acknowledgement, please rest assure that your support has been vital and it cannot be forgotten.

Table of Contents

Nomenclature

C	carbon atom
$\dot{C}$	cost rate ($/year)
c	specific heat (kJ/kgK)
D_P	depletion factor
$\dot{E}_x$	exergy rate (kW)
E_D	exergy destruction (kJ)
e_x	specific exergy (kJ/kg)
f	gas fraction
G	Gibb's free energy (kJ)
H	enthalpy (kJ)
h	specific enthalpy (kJ/kg)
HHV	higher heating value (kJ/kg)
k	permeability resistance (m s/kgPa)
LHV	lower heating value (kJ/kg)
m	mass (kg)
$\dot{m}$	mass flow rate (kg/s)
M	molar mass (kg/mol)
N_2	nitrogen
n	polytropic index
O_2	oxygen
P	pressure (kPa)
P^{00}	partial pressure
q	compression ratio

R	molar gas constant (kJ/kmol)
r	ratio
s	specific entropy (kJ/kgK)
S	entropy (kJ/K)
T	temperature (K)
T_0	ambient temperature (K)
V	volume (m^3)
v	specific volume (m^3/kg)
w	specific work (kJ/kg)

Subscripts

AM	animal manure
bio	biomass
c	compression
C	compressor
ch	chemical
D	destruction
e	expansion
e	electrical
FV	fuel vaporizer
FW	food waste
g	gas
HE	heat exchanger
i	inlet

k	combustion product components
m	membrane
p	pressure
ph	physical
s	salt
stoic	stoichiometric
T	turbine
th	thermal
w	water
x, y	coefficients of reactants
1, 2,…..,10	state points of proposed system
$1'$- $5'$	state points of four stroke engine

Greek Symbols

α	number of carbon atoms in fuel molecule
β	number of hydrogen atoms in fuel molecule
γ	specific heat capacity ratio
δ	number of nitrogen atoms in fuel molecule
ϑ	number of oxygen atoms in fuel molecule
η	energy efficiency (%)
ϵ_h	regenerator's effectiveness
ψ	exergy efficiency (%)
Δ	difference

Acronyms

AFR	air to fuel ratio

AHT	advanced hydrogen turbine
ASU	air separation unit
ATES	aquifer thermal energy storage system
BGL	British Gas/Lurgi
BIGCC	biomass integrated gasification combined cycle
CC	combustion chamber
CGE	cold gas efficiency
CGEX	cold gas exergy efficiency
CHP	combined heat and power
CI&M	capital investment and maintenance cost
COE	cost of electricity
COLDSYN	cold synthesis gas
COP	coefficient of performance
COS	carbonyl sulfide
CRF	cost recovery factor
DCOALGEN	density model in Aspen
EES	engineering equation solver
ElecNTRL	electrolyte property package
EP	elevated pressure
GCU	gas cleaning unit
GT	gas turbine
HCCI	homogeneous charge compression ignition
HCOALGEN	enthalpy model in Aspen
HE	heat exchanger

HGCU	hot gas cleaning unit
HPP	high pressure pump
HRSG	heat recovery steam generator
HTF	heat transfer fluid
HYPOGEN	hydrogen power generation
IGCC	integrated gasification combined cycle
IGFC	integrated gasification fuel cell
ITM	ion transport membrane
KPI	key performance indicator
KRW	Kellogg Rust Westinghouse
LGCU	low temperature gas cleaning unit
LiBr-H_2O	lithium bromide-water
LP	low pressure
LPP	low pressure pump
MCV	medium calorific value
M	million
MDEA	n-methyl diethanolamine
MON	motor octane number
multigen	multigeneration
NETL	national energy technology laboratory
O&M	operating and maintenance cost (USD)
ORC	organic Rankine cycle
PEM	proton exchange membrane
PLOX	pumped liquid oxygen

ppmw	particles per million weight
PRENFLO	pressurized entrained flow
PTC	parabolic trough collector
PV	photovoltaic
Q-GIBBS	heat stream to Gibbs reactor
RO	reverse Osmosis
RON	research octane number
R-Stoic	stoichiometric reactor
SI	sustainability index
SO	sulfur oxide
STBR	steam to biomass ratio
SWRO	sea water reverse osmosis
Syngas	synthesis gas
TES	thermal energy storage system
VS	venture scrubber
VT	vapor turbine or steam turbine
WD	work done
WGCU	warm gas cleanup
WGR	water gas reaction

LIST OF FIGURES

LIST OF TABLES

CHAPTER 1 INTRODUCTION

1.1 Overview of Energy and Oil Demands

The change in climate and fossil fuel depletion magnify the implication and importance of energy efficient Integrated Gasification Combined Cycle (IGCC) for multigeneration. The enactment of IGCC multigeneration systems is necessary to meet the increasing demand for energy in a safe and environmentally responsible manner. In 2012 and 2013, the contribution of renewable for energy consumption and electricity generation was 19% and 22%, respectively [1]. Modern renewable energy demand is specifically increasing in power generation, heating and cooling, transport fuels, and rural/off-grid energy services. Recent developments like; increased flexibility, diversity and developed global supply chains have enabled renewable energy industries to meet the demands of global markets.

The demand of energy is increasing worldwide due to growing population and higher living standards. The combustion of fossil fuels mainly; coal, natural gas and petroleum, supply most of the energy demand of the world. The utilization of fossil fuels through combustion to meet the increasing energy demand results in fast depletion of fossil fuel reserves and environmental degradation like; acid rain, smog formation, global warming, ozone depletion and health hazards. The energy conservation and search for alternative source of energy is crucial to encounter with energy crisis and pollution. In past, various investigations have conducted on the conservation of energy in fossil fueled power generation systems. It is important to exploit alternative sources of energy to mitigate environmental concerns and global warming.

The petroleum products are the major source of primary energy which had a variable trend of demand in past. The demand of petroleum products rose from about 38% to 45% in 1975 and 1950, respectively, and then declined to about 40% as a result of the energy crises in 1970. The transit sector is almost completely dependent on petroleum products. The prices of petroleum products remained low and steady until 1990, and then recapitulated the unpredictability they had exhibited between 1970 and 1980. In 2004, the perceptions of imminent incompetency of the refineries to meet rising world demand triggered to rapid increase in the prices of petroleum products. The development of nonconventional energy resources increased due to continuous increase in prices of

petroleum products. This process first started in Canadian oil sands followed by shale deposits in the United States. The oil production of U.S. had reached to peak and showed a dramatic increase in 2009. There was a decreasing trend in U.S. imports of oil over this time period and now there are calls to grant more exports. In 1950, the coal consumption was almost equal to oil, with a share of 35% of total primary energy. A decade later, it slumped to 20% and since then it has persisted at about level.

Currently, coal is used almost sovereign for electric power generation and has become controversial due to the concerns about global climate change due to its huge contribution to high production of carbon dioxide [2]. The demand for energy is estimated to increase at a much faster rate in the near future. Fig. 1.1 provides an overview of the energy consumption through previous years and an estimate of the future energy consumption, based on different energy sources [3].

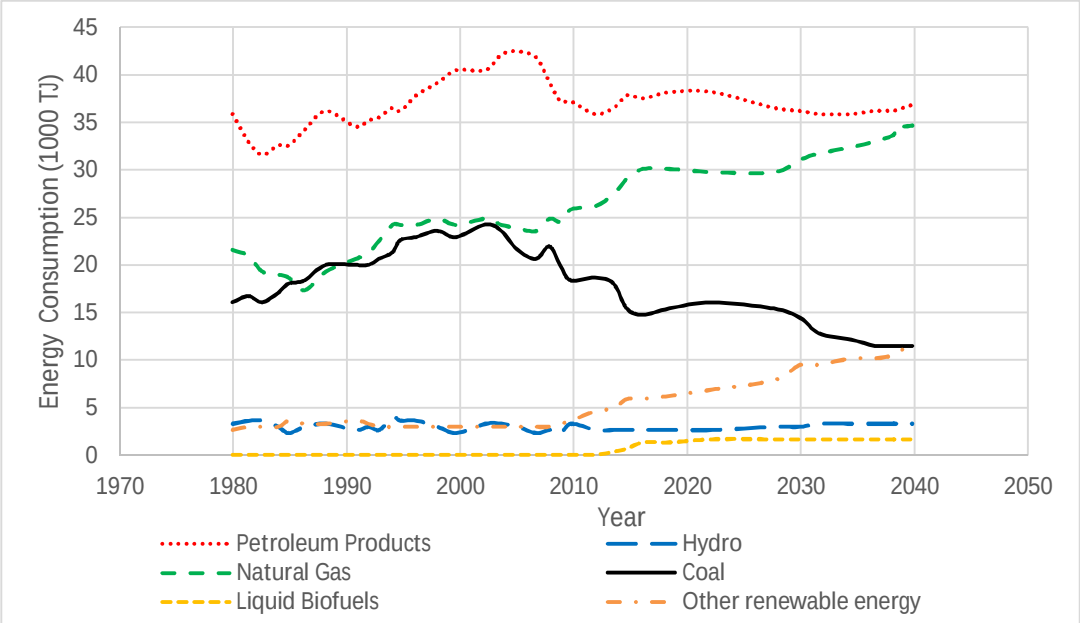

Figure 1.1 Global energy consumption and projection (data from [3])

Renewable energy sources (except hydropower) continue to offer more potential than actual energy production. The conservation and energy efficiency have exhibited compelling results over the past three decades. In addition to this, energy efficient processes offer potential to relieve some of the dependence on the import of petroleum products and compensate increased electric power demand to some extent [2].

The worldwide capacity of gasification is expected to grow 70% in the upcoming years. About 80% of the predicted growth will take place in Asia, and China is expected to contribute a huge portion of this expansion [4]. The energy demand of China is growing at a very fast pace due to rapid development. The main energy source of China is "coal" which is expected to remain dominant [5].

1.2 Overview of Environmental Impact

The energy demand of growing economies and environmental concerns are the challenges of modern times [6]. Clean power, H_2 production from coal, and bio-products (bio-fuels, bio-power) are the main focus of the international community actions. Many IGCC projects were started worldwide in 2006 and 2007 but some of these were abandoned by the end of 2007 because of the new CO_2 legislations, public attention to global warming and the uncertain economic situation [7]. Future-Gen IGCC cancelled the zero-emissions power plant due to ''rapidly escalating construction costs''. Despite this trend, other worldwide projects such as HYPOGEN, Australia's COAL21 National Action Plan and the Canadian Clean Coal Technology Roadmap are still running [4]. Coal fueled power plants generate species like; sulfate, chloride, phosphate, fluoride, cyanide, nitrogen-containing ions and trace organic compounds. These trace substances are emitted through flue gas and aqueous discharges. Chloride and fluoride can exist as acids so, these may appear in the gas phase as well. Significant amount of energy is consumed in gas control equipment. There are some serious health and environmental concerns with the release of trace organic compounds such as dioxins, furans, and formaldehyde [8].

The presence of chemical constituents in the coal depends upon the geological origin and rank. Some potentially toxic metals and metal compounds bound with the coal. These trace species can cause both environmental and human health risk, depending upon their concentration, toxicity, and their final disposal in regional ecosystems integrated with the IGCC system. The impact of these trace species is less in case these are removed with slag or ash but cause significant impact on environment if released with flu gas. The trace metals of greatest environmental concern are reported to be arsenic, boron, cadmium, mercury, and selenium. The existing technologies to clean syngas are not capable of removing theses metals from the emissions of an IGCC system as studies based on thermodynamic equilibrium have reported that these metals are highly volatile. Mercury

has received the most attention from regulators in both combustion and gasification as compared to other particulate matter, because of its existence in vapor phase due to low boiling point [8].

1.3 IGCC for Refinery Applications

In refineries, Integrated Gasification Combined Cycle (IGCC) technology contribute to the commercialization and leadership of IGCC systems for the clean conversion of refinery residues and solid wastes to economical “poly-generation” of power and other high valued by-products. IGCC systems are receiving increased recognition due their advantages like; flexibility, environmentally superior solutions for the conversion of solid and heavy liquid feedstock to power, co-generation steam, and other chemical production purposes. The capability of IGCC systems to use opportunity fuels to produce high value co-products along with power generation, enhances the economic viability of new projects [9]. The key advantages of IGCC technology are the co-production of chemicals and other utility products required by refineries. IGCC systems have achieved exceptional levels of environmental performance, availability, and efficiency at a competitive cost of electricity by fully utilizing the capabilities of modern combined cycle designs [9]. Continuous improvements in system performance and operating characteristics are achieved through advancements in gasification, air separation, syngas cleanup, and gas turbine combined cycle equipment designs. The prospect for continued growth in the IGCC refinery segment has enhanced due to these improvements. Currently, the challenge for IGCC systems is to meet market requirements (which demand lower capital costs, improved operating reliability, and increased fuel flexibility) in combination with increasing efficiency and environmental performance standards.

Biomass integrated gasification combined cycle (BIGCC) plant based on gas turbine is the most commercial system for power generation and possess ability to meet the peak load demand in an efficient and environment friendly manner. This process involves cleaning of gas in pressurized high temperature conditions before it enters the combustion chamber of the gas turbine to avoid exergetic losses. Pressurized (22 bar) air-blown BIGCC using hot gas clean-up with ceramic filters was successfully demonstrated in Varnamo-Sweden from 1996 until 2000. The qualities and characteristics that BIGCC power

generation concept offers could not be found in other contending technologies due to following:

- Environmentally superior to conventional green biomass fired power plants and can be designed to meet the most stringent regulations.
- Surpasses thermal efficiencies of existing conventional technologies.
- Generates power at lowest cost.
- Different kinds of biomass feedstock can be used.
- Requires 20% to 50% less amount of cooling water than conventional coal plant [10].

Table 1.1 Major commercial IGCC plants for producing electricity from coal and/or coke

Company/Country	**Capacity (MW)**	**Start-up Year**	**Gasifier Manufacturer**
Tampa Electric, Polk County	250	1996	GE
Wabash, West Terre Haute	265	1995	CB&I E-Gas™
Nuon, Buggenum	250	1994, shutdown in 2013*	Shell
Elcogas, Puertollano	300	1997	Krupp Koppers
Edward sport IGCC Station, Indiana	618	2013	GE Gasifier
Nakoso IGCC, Japan	250	Experimental 2007, operations in 2013	Mitusbishi
Kemper County IGCC, Mississippi	582	2016	TRIG™ Gasifier

Source [11]

The production of particulate emissions and huge volumes of SO_x and NO_x accumulate due to the combustion of biomass, animal manure, food waste and heavy fuel oils. Heavy fuel oils can be disposed through advance and environmentally friendly process of gasification which converts them into clean and combustible gases. Thermodynamic equilibrium modeling is employed in this study to envision the performance of a gasifier using variety of feedstocks including biomass, refinery and other wastes (food and animal manure). Chemical and thermodynamic equilibriums are combined in the model of the gasification reaction in order to foresee the final species production and distribution in addition to syngas. The composition of the syngas, methanol, ammonia, hydrogen,

chemicals are obtained at the first stage. Then, various attributes of the gasification process, namely, ratio of H_2 and CO, process temperature, heating value of the produced syngas, cold gas efficiency and carbon conversion efficiency of the process are determined. The effects of equivalence ratio, mass flow rate of steam and pressure on the gasification yield are analyzed. The numerical model is validated by comparing the results of simulations with experimental measurements reported in the literature. The detailed thermodynamic investigation are performed on each sub-unit and then overall cycle.

Gasification is recognized as one of the best technologies available that converts waste feedstock to energy and it requires minimum amount of fuel to produce power with high efficiency. Moreover, gasification emits least harmful pollutants in flu gas after combustion of syngas and its expansion in turbine. Since a fair amount of agriculture waste is available in country like Saudi Arabia which creates problem of waste disposal. Utilization of refinery waste, biomass, municipal waste results in the following:

- Waste reduction.
- Reduced pollution.
- Considerable load reduction on fossil fuels and power grid due to additional power generation.

Gasification can be defined as the conversion of variety of carbon based fuels into a gaseous product with a significant heating value whereas; in combustion the product gas has very less amount of heating value. The other technologies like; pyrolysis, partial oxidation and hydrogenation are the other categories of gasification. The different techniques for gasification vary depending upon the fuel source and output products.

The process of gasification regained interest as a result of increased energy prices in the early 2000s. Most of this process has been shifted towards the gasification of coal to produce power through gas turbine by burning synthesis gas. The use of coal for gasification is being limited due to the environmental regulations and awareness about global warming. The gasification of refinery waste and biomass is a neutral alternative which offers opportunities similar to those given by coal gasification.

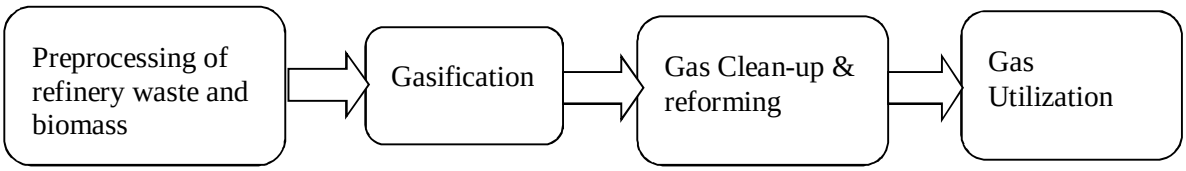

Figure 1.2 The principal steps of gasification

Some common oxidation agents are air, oxygen, steam or any combination of these in the presence of which gasification occurs in a high temperature environment. Direct or indirect heat is added to the process. The combination of heat and oxidizing agent decomposes the large polymeric molecules of the raw feedstock into lighter molecules and finally into permanent gases. The product gas is syngas composed of carbon monoxide (CO), hydrogen (H_2), methane (CH_4) and carbon dioxide (CO_2), ammonia (NH_3) and hydrogen di-sulfide (H_2S) [12]. The syngas will also contain tar, char, and other minor contaminations. The contributing factors on the composition of the product gas are gasification temperature, oxidation agent, reactor type and feedstock. The types of biomass feedstock which can be used for gasification are municipal solid waste, rice husk, saw dust, manure, apple bagasse, sugarcane bagasse, paper mill sludge and straw. The lower heating value (LHV) of the produced gas is influenced by the type of oxidizing agent. The selection of air as an oxidizing agent results in a low calorific value gas (4-7MJ/Nm^3). Oxygen or steam as oxidizer leads to a medium calorific value (MCV) gas (10-20MJ/Nm^3). The later one is more appropriate as a feedstock for synthesis of liquid fuels and chemicals while the previous is more suitable where the heat contents are not critical [13].

There are many different types of technologies for gasification. The type of fuel and the gasifying agent are the main factors in the selection of an appropriate gasification technology. The most common gasification technologies are categorized on the basis of direction of fuel flow and flow speeds.

There are three types of gasifiers on the basis of fuel flow direction in the gasifier as up draft, down draft and cross draft. Gasifiers can further be categorized on the basis of flow speeds as fluidized bed, moving bed and entrained bed.

Table 1.2 Advantages and disadvantages of different gasifiers

Name	Advantages	Disadvantages
Updraft	• Moisture for heat • Good for small scale applications • Ability to handle high moisture • No carbon in ash	• Limits feed size • Tar yields High • Size limitations • Potentials to slag
Downdraft	• Small scale applications • Large scale applications • Low tars	• Sensitive to Moisture • Size limitations • Limited feed size • Gas Producer
Fluidized Bed	• Applicable to large scale • Direct or indirect heating • Feed characteristics • Ability to produce syngas	• Tar yields medium • Particle loading high
Circulating Bed	• Applicable to large scale • Feed characteristics • Ability to produce syngas	• Tar yields medium • Particle loading high
Entrained flow	• Allow to be scaled up • Ability to produce syngas Potential for low tar	• Large contents of carrier gas • Limits of particle size

Source: [14]

The gas clean-up unit (GCU) is very important in order to keep combustion chamber of gas turbine (GT) free of fouling and corrosion of component as a result of burning syngas. Hot or cold gas can be used to drive gas clean-up unit. The use of ceramic filter in hot gas clean-up unit (HGCU) is less reliable because the plant operation is interrupted as a result of cracks in ceramic. Low temperature gas clean-up unit (LGCU) is selected to achieve reliable operation. Ceramic filter is replaced with a metallic filter material in LGCU. Gas is cooled down to below 800 K before being fed into the LGCU unit as a result; the plant thermal efficiency is reduced.

Gas clean-up/conditioning is one of the biggest challenges of IGCC systems. In the sugar industry cogeneration case, the end use application for the product gas is a gas turbine. The level of condensable tars, particulates and alkali metals in the product gas is dependent on the hardware of gas turbine. Sulfur and chlorine are also potential contaminants, but their concentration in biomass feedstocks such as bagasse is low. Figure 1.2 is developed on the basis of standard gas cleaning procedure in the literature.

Raw syngas is passed through ceramic filters which removes dust particles then it passes through Venturi scrubber to remove water and carbonyl sulfide hydrolysis reactor which converts COS into H_2S. Clause plant removes sulfur, sour water stripper removes pollutants and MDEA absorber removes H_2S and clean syngas exits from MDEA absorbers.

Particulates mainly consist of ash and char. These are the main cause of turbine blade erosion. Therefore, there is a stringent particulate limit in gas turbines. Fluidized bed gasifiers produce a product gas with a high particulate concentration of approximately 5000-10000 ppmw. Consequently, IGCC system requires an efficient filtration system that captures the particulates in filter media like ceramic candles or bag house filters. Water scrubbers can also be effective in which the particulates are captured in a spray of water but they create the problem of waste water treatment. Filtration systems are usually consisted of cyclones for the primary particulate removal. Then, the particulates are passed through hot gas filtration units using ceramic candles or bag house filters which operate at temperatures greater than 500^0C or less than 300^0C, respectively.

During biomass gasification, alkali metals such as sodium and potassium present in the biomass fuel are vaporized and leave the gasifier as part of the product gas. Alkali metals corrode turbine blades. The actual concentration of the alkali metals in the product gas far exceeds this limit. The removal of these metals can be carried out by cooling the gas to 350-400^0C before particulate filtering. The alkali metals condense on the solids and are removed along with them in the filter. Alternately, wet scrubbing can be used, which ensures complete removal, but needs an additional step of waste water treatment.

Tars are complex mixture of condensable hydrocarbons and include single ring to five- ring aromatic compounds. Other oxygen containing hydrocarbons and complex polycyclic aromatic hydrocarbons are also included in tars. In a typical fluidized bed gasifier, tars account for 2 to 4 per cent by mass of the fuel or 0.5% to 1.5% by mass of the product gas. Tars can be condensed when the product gas is allowed to cool 400-500^0C and can cause operating difficulties by fouling heat exchanger surfaces in gas coolers, plugging particulate filters, and constricting pipes and valves.

Air separation, gasification, cooling, syngas cleanup and syngas combustion in gas turbine are the five basic steps involved in an IGCC process as represented in Fig. 1.3.

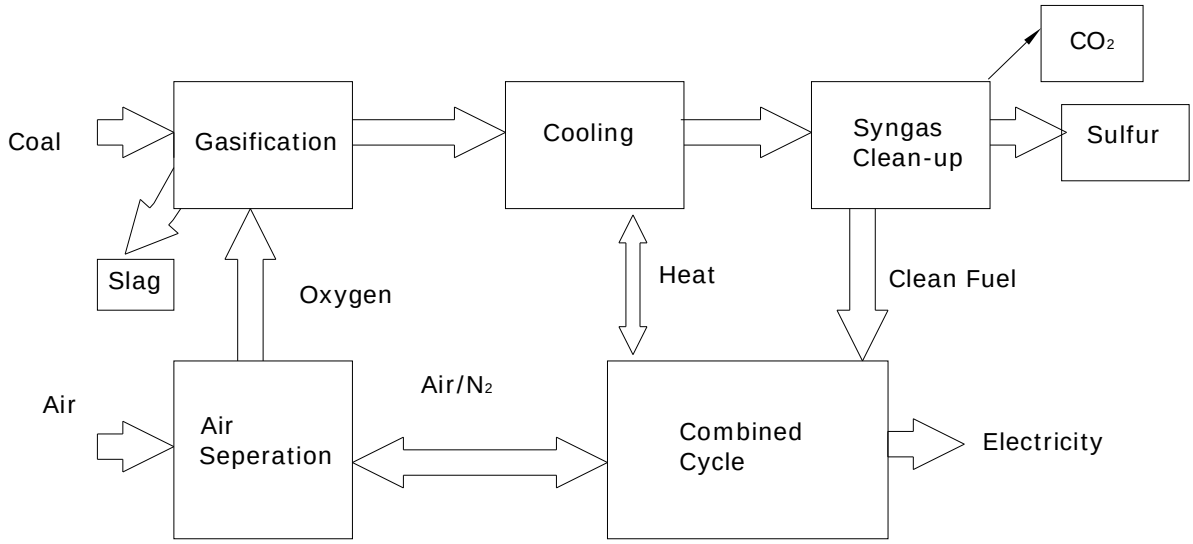

Figure 1.3 Five basic steps of IGCC

Multigeneration concept of IGCC systems along with CO_2 removal is shown in Fig. 1.4. It can be seen that there is a potential to utilize the process steam to run low grade heat driven devices like; organic Rankine cycle and absorption chiller.

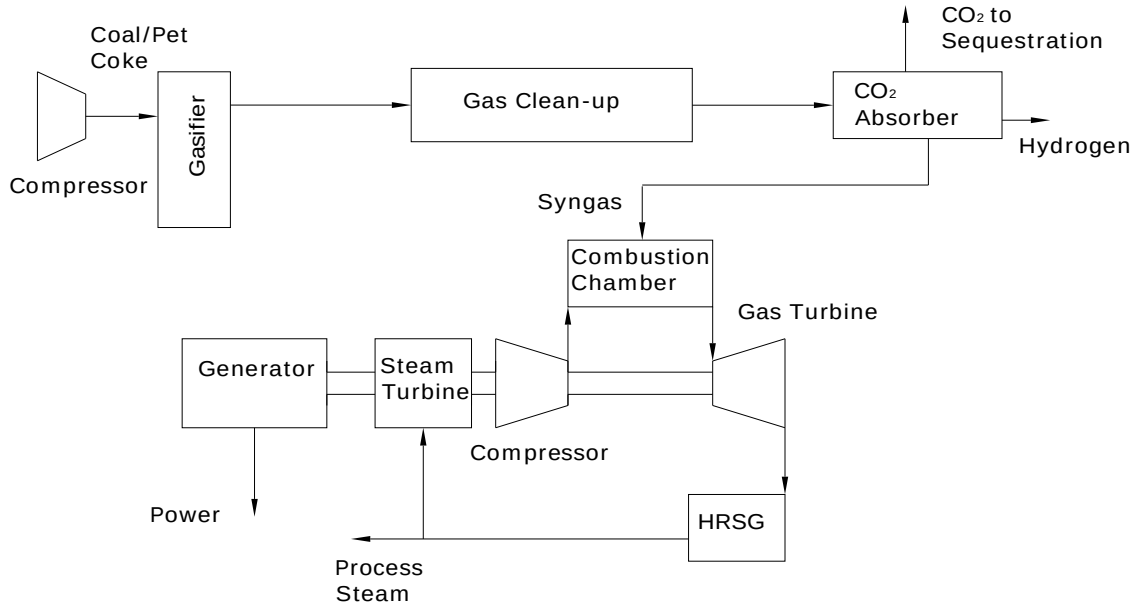

Figure 1.4 Multigeneration process concept of IGCC

1.4 Motivation

The conversion of refinery waste into a valuable feedstock is vital to combat recent huge cutback in the refined oil prices. The development of biomass mixed with food waste, animal manure and refinery waste driven IGCC plants incorporated with multigeneration are of great importance and carry potential to pursue high efficiency at lower emissions per unit energy used. Besides electricity and hydrogen production, the useful products of such a system include hot water, space heating, thermal energy storage, cooling and fresh water supply. In addition to this, global warming and the depletion of fossil fuel resources amplifies the importance of integration of renewable energy resources with conventional ones for multigeneration. Multigeneration energy systems are the most convenient option for meeting the energy demands of new residential applications away from the central grid, food industries located in rural area and oil refineries. These systems are of great interest for researchers. From the literature [15–18], one can see that there are several researches on the analysis of cogeneration and trigeneration energy systems. However, research conducted on IGCC multigeneration energy systems especially, renewable based multigeneration gasification systems is limited. There is a huge lack of the studies of multigeneration systems on exergy, environmental analyses.

1.5 Novelties of the Systems

Three novel waste driven Integrated Gasification Combined Cycles (IGCC) for multigeneration are developed to produce electricity, cooling, heating, fresh water, hot water and hydrogen. The novelties of the developed systems include:

- Specific, new, energy efficient and environmentally benign Integrated Gasification Combined Cycles (IGCC) for the multigeneration are developed based on the availability and composition of specific type of feedstock.
- IGCC multigeneration systems are developed for community, food industry and refinery. The system developed for food industry is integrated with a reverse osmosis plant to meet the demand of fresh water. The system developed for refinery is integrated with homogeneous charge compression ignition (HCCI) engine to generate additional electricity.
- Thermodynamic models based on exergy efficiencies are developed for gasifier, combustor, gas cleanup unit, gas turbine, steam turbine, absorption chiller, organic

Rankine Cycles, thermal energy storage system, reverse osmosis plant, HCCI engine and overall systems. The results are validated through first law and second law of thermodynamics.

- All developed systems convert wastes into useful products especially hydrogen. Then, the produced hydrogen is combusted in homogeneous charge compression ignition engine after blending with methane. The utilization of methane and hydrogen on-site saves huge cost associated with the compression and transportation of these gases.

1.6 Objectives

The aim of this study is to determine the potential of employment of three waste driven integrated gasification combined cycles for multigeneration. The purified syngas is used as a fuel in gas turbines to produce power with high efficiency and less emissions. Three systems are developed to study their operations in three sectors; community, food industry and refinery.

The specific objectives of this research work, in terms of the main objectives and the sub-objectives for each main objective, are as follows:

1. To propose a biomass mixed with heavy oil based Integrated Gasification Combined Cycle (IGCC) and to investigate potential multigeneration through conservation of waste heat by integrating low heat driven devices.

- To propose and develop IGCC for better thermal performance.
- To model a Gibbs free energy equation based reactor for the gasification of feedstock in the presence of steam.
- To develop a novel heat recovery steam generation (HRSG) system for steam turbine and gasification purpose.
- To propose and develop three novel configurations of IGCC based on their applications and feedstock composition.
- To integrate the high temperature stoichiometric reactor for the combustion of biomass to generate heat for gasifier.
- To model another stoichiometric reactor (R Stoic) as a combustion chamber of the syngas to run gas turbine.

- To investigate the performance of the developed model against variety of feedstocks.
- To develop integrated systems for multigeneration including hydrogen production, electricity, cooling, heat, hot water and fresh water.

2. To develop a thermodynamic and chemical reaction models of the developed systems, and conduct comprehensive energy and exergy analyses and performance assessments of the systems.

- To conduct thermodynamic modeling using Aspen (Plus) and Engineering Equation Solver (EES) by writing mass, energy, entropy and exergy balances.
- To evaluate the properties and rates of the various streams, and calculate exergy destructions for the components, subsystems and overall system.
- To find out reaction kinetics of the feed stock in gasifier and produced syngas in combustor.
- To conduct a comprehensive parametric study to observe the effects of varying operating conditions mainly; temperature and pressure on the energy and exergy efficiencies of the proposed configurations, subsystems and overall systems.

3. To perform multi-objective optimization of the integrated systems and determine the ideal operating conditions and limitations.

- To define the three objectives function and constraints for thermodynamic and economic analysis.
- To optimize the integrated systems on the basis of three constraints including; exergy efficiency, total cost and CO_2 emissions using Genetic Algorithm.
- To define the best decision variables among feed composition, gasifying agent, temperature and pressure for each integrated multigeneration system.

4. To validate model for each sub-system of multigeneration system to ensure the correctness of developed codes.

- To validate the syngas composition exiting from Gibbs reactor, energy and exergy efficiencies of the Gas turbine, energy and exergy efficiencies of the steam turbine, energetic and exergetic COPs for the absorption chiller and the performance of the HCCI engine.

5. To perform the environmental impact assessment of each system.

- To calculate carbon and nitrogen based emissions of the systems and compare these with a typical biomass based IGCC.
- To investigate the emissions produced per MWh of the power produced by the all proposed systems.
- To make a comparative assessment of the emissions produced per kg of the mixed feedstock for all proposed systems.

CHAPTER 2 LITERATURE REVIEW

There are several research studies conducted to investigate the performance and feasibility of coal, biomass and heavy oil based integrated gasification combined cycles (IGCC). However, there is a huge lack of studies on the production of multiple outputs from IGCC plants and the integration of homogeneous charge compression ignition engine with integrated gasification combined cycles is not reported in the literature yet. The multigeneration energy systems produce multiple useful outputs. The review of the available literature is done for IGCC and sub-systems used for multigeneration in the studied systems. The literature addresses different recent research works on cogeneration, trigeneration and multigeneration energy systems.

2.1 IGCC Technology

Research and development of IGCC plant technology initiated in the 1970s. Most of the IGCC plants with the capacities of 50-600 MW are for demonstration purpose located in Europe and USA [4]. Technology, availability, reliability and the capital cost are the major challenges in IGCC plants. Chemicals, fertilizers, transportation fuels, substitute natural gas, and electricity can be produced through a commercial gasification manufacturing technology worldwide [19]. Current challenges related to IGCC power plant are CO_2 capture, H_2 purification, integration between units and co gasification of variety of feedstocks. The integration of transportation and storage technologies of CO_2 into IGCC plants are crucial for the future of coal-based power generation plants [20].

2.2 IGCC Modifications

IGCC plants require process modification to remove CO_2 from syngas by adding water gas shift reactors (WGR) to transform CO into CO_2 and an absorption unit to separate CO_2 from the synthesis gas stream. Relatively pure H_2 stream can be obtained after removing CO_2 from syngas which can be burned in a gas turbine or used in fuel cells for generating power. This kind of systems are not found in literature at a high power generation scale. Shoko et al. [21] studied the usage of H_2 production in Integrated Gasification Fuel Cell (IGFC) systems and stated that this technology can only be competitive in scenarios of oil and natural gas depletion and stringent environmental standards. The research in the field of carbon capture is needed as the cost of electricity (COE) is 10% higher in IGCC plants

with CO_2 removal as compared to IGCC plants without CO_2 removal. Jiang et al. [22] stated that the integration is the key to increase the efficiency of an IGCC plant. Moreover, three possible levels of integration can be achieved on ASU–CC: (i) a non-integrated ASU – with no N_2 injection or air extraction; (ii) a partially integrated ASU – with N_2 injection; and (iii) a totally integrated ASU, which combines N_2 injection and air extraction [23].

2.3 Coal and Biomass Mixed IGCC

The gasification of coal with other fuels, usually waste materials and/or biomass is called co-gasification. Hence, the possibilities of all former integration can be used in coal gasification power stations as well as for co-gasification. Valero and Uso´n [24] and Yuehong et al. [25] studied coal co-gasification and concluded that it is an auspicious technology to reduce emissions. The combination of coal/biomass for IGCC applications is technically feasible up to 10% in an oxygen-blown entrained bed gasifier as compared to the fluidized or moving bed. The efficiency of co-gasification decreases [24] due to the pretreatment process of biomass as moisture in straw and/or sewage sludge must be removed upto a certain level before feeding. Bridgwater [26] demonstrated the technical and economic feasibility of biomass to power conversion. The first IGCC plant in the world that uses a feedstock entirely made of biomass is Varnamo, Sweden [27] that produces 6 MW to the grid and 9 MW heat to district heating.

Thermo-chemical conversion processes like pyrolysis and gasification are very attractive to convert biomass into syngas. Biomass is a biological material which is largely extracted from living or dead matter available on the earth [28]. Numerous researchers have studied biomass energy based co-generation systems for numerous industries like; palm oil, rice, wood, sugar, and paper [29]. Assima et al. [30] employed three low cost materials including iron, bone meal and ashes as catalysts for the gasification of urban waste. Landis et al. [31] developed a decision support system to help stakeholders to make decisions about tradeoffs and synergies against alternative landscape composition, configuration, and agronomic management. Martyniak et al. [32] conducted an experimental study of few wild populations of a new bioenergy grass species to determine traits related to biomass quality and quantity.

The pyrolysis is a decomposition process of biomass at high temperature without air and the resulting volatiles include; water, nitrogen (N_2), carbon dioxide (CO_2), oxygen (O_2), hydrogen (H_2), methane (CH_4), hydrogen sulfide (H_2S) and carbon monoxide (CO) [12]. In addition to this, a small amount of unsaturated hydrocarbons like olefins, acetylene, aromatic and char [33]. Steam, air, oxygen and carbon dioxide are commonly used as gasification agents for the conversion of char into gases. The fluidized bed reactors are more frequently used for gasification as compared to the other kinds of reactors because of the high rate of heat and mass transfer which ultimately yields high production of gas. The use of steam as gasification agent is one of the auspicious option for biomass conversion [34, 35]. Thapa and Halvorsen concluded that the contribution of the factors like; de-volatilization, water-gas shift reactions and gasification in the presence of steam are more dominating than others in the product gas heating value [36].

2.4 Modelling of IGCC Gasifiers

The model developed on Texaco IGCC by Frey and Akunuri [37] is very comprehensive work found in the literature that describes variety of gas purification units. Then, Frey and Zhu [23] analyzed different patterns of integration within ASU-CC and enhanced the flowsheet. Ordorica et al. [38] incorporated technology for the removal of CO_2. Perez et al. [5] validated the data from the ELCOGAS Puertollano power plant by developing a conceptual model. Campbell et al. [39] conducted sensitivity analysis of some parameters of IGCC plant whereas, Kanniche and Boullou [40] performed assessment on including or excluding the CO_2 removal train. Arienti et al. [41] presented nine different configurations for the selection of the best integration of the plant. They conducted the study to meet a specific demand of H_2 and excess amount of hydrogen for power production. Desideri and Paullucci [42] included H_2 purification unit as well and calculated the overall efficiency of the plant including the purification of H_2. They also added the modeling of a CO_2 removal train in Aspen (Plus) and compared the results of performance and cost with literature [42]. Descamps et al. [43] calculated the overall efficiency of the integrated CO_2 capture IGCC power station by developing a simulation model.

Zheng and Furinsky [44] performed simulation using Aspen (Plus) to compare the performance of Shell, Texaco, BGL and KRW gasifiers for three different kind of feeds and showed that the performance of IGCC plant greatly depends on the type of gasifier,

biomass and heating value of biomass. Environmental performance and the fuel flexibility are the key bench-marks for designing an IGCC plant [9]. Holopainen [45] concluded that the integration of heavy oil gasification with combined cycle is more economical as compared to coal gasification. Emun et al. [46] improved the energy efficiency and minimized the operation cost through the principles of pinch analysis and process integration. Ashizawa et al. [47] performed gasification analysis of extra heavy oil by using Orimulsion in gasifier. Their results depict that the heavy oil feedstock can be used for design and operation of actual gasifier.

2.5 Thermochemical Equilibrium of Heavy Oil Based IGCC

Davison et al. [48] compared IGCC power plants with and without hydrogen production. Moreover they compared the performance of these plants including and excluding CO_2 capture. Kansha et al. [49] designed an innovative technology called self-heat recuperation for the production of methanol with reduced energy consumption. Vaezi et al. [50] performed gasification of heavy oil through a thermochemical equilibrium methodology and concluded that the gasification of the heavy oil is beneficial for the production of syngas.

2.6 Advanced IGCC with Carbon Capture

Research and developments are being made to improve conventional IGCC technology that will lower the cost of electricity through advanced and efficient power production. In addition to this, performance and cost of an IGCC cycle including carbon capture are under investigations. Gerdes et al. [51] documented the summary and expected benefits of these technological advancements with carbon capture.

The state-of-the-art F-class turbine at Tampa, Wabash River plant is replaced by the advanced hydrogen turbine (AHT). The process efficiency of the gas turbine is improved 45% due to its higher operating temperature (~1450°C). The flow rate of feedstock is also increased which boosts power capacity. The unit capital cost of the plant is reduced due to larger plant units to handle increased power production. The cost of electricity (COE) is decreased 14.5% and efficiency is increased 3% due to this upgrade of turbine [51].

Conventional cryogenic ASU is replaced with the ion transport membrane (ITM) as it separates air more efficiently as compared to ASU but the power consumed in this process is similar to ASU because a compressor is required to compress the inlet air as well as low-pressure oxygen. The real advantage of the ITM is 3% reduction in COE due to the less targeted cost which is about 2/3 of the ASU.

The desulfurization Selexol units for mercury removal process are replaced with warm gas cleanup. The whole cleaning process can be performed at high temperature to avoid the efficiency loss due to cooling and reheating gas stream. The net plant efficiency can be increased by 0.2% by adopting the warm gas cleanup (WGCU) process train. This increase in the efficiency is a result of increased power generation through the steam turbine. COE is also reduced about 4% through this advanced technology [50].

Selexol stage for CO_2 capture from the syngas is replaced by palladium-based 100% hydrogen-selective membrane. The plant efficiency is improved by 0.14% by using palladium membrane which is because of the lower compression costs of CO_2. The COE is also reduced by 3% due to the same reason. The analyses of alternative advanced pre-combustion technologies are being performed at National Energy Technology Laboratory (NETL) for the production of CO_2 at high pressure.

2.7 Multigeneration Systems

Several industries, particularly solar energy had difficult years, but many solar photovoltaics (PV) manufacturers returned to profitability by the end of 2013 [1]. On the other hand, the fast diminution of fossil fuels intensifies the importance of energy efficient integrated multigeneration systems. The adoption of multigeneration systems becomes necessary to meet the rising energy demands in an environmental friendly manner.

The process of multigeneration processes offer numerous potential benefits such as high energy efficiencies, low operating costs and less pollutant emissions [52]. Al-Ali and Dincer [53] developed multigeneration system and showed an increased energy efficiency of 75% as compared to 16.4% in case of single generation. The exergy efficiency was improved by 10% after shifting the system from single generation to multigeneration.

The multigeneration systems do not only mitigate environmental impact and cost but also increase efficiency and sustainability. The quality of the available energy for

multigeneration is highly connected with the reference environment, which is often modeled as the ambient environment. Many modifications have already tested on the multigeneration processes. Dincer and Zamfirescu [54] confirmed that the multi generation renewable energy base system offers better efficiency, cost, sustainability and environment. Al-Sulaiman et al. [55] performed a study on electrical energy efficiency and reported an increase from 14% to 94% when system was shifted from single generation to trigeneration.

Ratlamwala and Dincer [56] performed comparative energy and exergy analyses of two solar based integrated systems for producing hydrogen and found that hydrogen production rate increases from 986 kg/day to 2248.6 kg/day and 1197.4 kg/day to 2672.1 kg/day, respectively, with rise in solar light intensity from 600 W/m^2 to 1200 W/m^2. Bicer and Dincer [57] proposed and analyzed a new combined system for the production of hydrogen, power, cooling and heating through solar and geothermal resources. The overall energy and exergy efficiencies of this proposed system can reach up to 10.8% and 46.3%, respectively, for a geothermal water temperature of 210°C. Islam et al. [58] performed energetic and exergetic analysis of a solar energy based multigeneration system and found that the energy and exergy efficiencies of PV panels increase from 5.6% and 5.9%, to 10.1% and 10.7%, respectively, through the integration of an unique cooling system. Yilmaz et al. [59] performed a review of solar based hydrogen production methods and found that the utilization of solar energy for hydrogen production promises to be one of the most viable options to replace fossil-based hydrogen production. The sub-systems integrated in this study for the multigeneration are as follows

The cost of electricity has a major share in the total cost associated with the hydrogen production through electrolysis. Electricity for the electrolysis can be generated through commercially available renewable energy technologies like solar, but this option becomes less attractive due to the high module cost and low energy efficiency. On the other hand, the system efficiency can be improved by mitigating the distribution cost of the electricity through on-site electricity generation for the electrolyzer; however, it is limited by land-use restrictions and the availability of resource [60]. The fuel demand of 300 cars each day can be met through an electrolyzer capable of making 1500 kg of hydrogen daily [61].

The development of a new and advanced water electrolyzer system becomes necessary to meet the growing demand of hydrogen. The production of hydrogen through electrolysis is one of the practical approaches without the consumption of fossil fuels. The analysis of solar driven large scale hydrogen production plants were performed by Dini [62]. The analysis of solar-energy based hydrogen production plants performed by Ozcan and Dincer [63] shows that the highest exergy destruction occurs in the solar field which accounts for one third of the total exergy destructions of the overall system. Clean and sustainable hydrogen can be produced by coupling renewable energy source, like photovoltaic with water electrolysis processes. The integration of renewable energies in autonomous systems can be facilitated through sustainable hydrogen production processes like electrolysis [64].

Yilanci et al. [65] performed the assessment of solar hydrogen production methods including their current status and concluded that the hydrogen production through the use of solar-energy based systems is an environmentally friendly and sustainable choice. Moreover, efficiency of the overall system can be improved by improving the efficiencies of PV, electrolyzer and fuel cell systems. Photovoltaic driven hydrogen production systems are one of the potential options for overcoming current environmental and sustainability issues. Khalid et al. [18] performed energy and exergy analysis of a solar-biomass integrated cycle for multigeneration and found that the energy and exergy efficiencies increase with the integration of two renewable energy sources.

The imbalance between demand and supply and their intermittent nature arises need for energy storage to avoid such problems. The thermal side of it makes thermal energy storage (TES) an environmentally viable option and a cost effective solution [66]. Dincer [67] performed energy and exergy analysis of thermal energy storage system (TES) for design and optimization. A realistic and meaningful assessment was made by an example of exergy analysis in that study. Dincer and Dost [68] evaluated thermal energy systems for their performances, cost and economic viability, convenience in installation, safety, impact on environment, cleanliness and technological adaptability. AlZahrani and Dincer [69] formulated energy and exergy models for three sub-processes: charging, storing, and discharging, to track changes in energy and exergy quantities with discharging time. They considered some uncertainties like energy recovered from aquifer thermal energy storage

system (ATES) at a low temperature rather than at an ambient temperature and developed a comparison pattern between energy and exergy efficiencies.

The integration of heat pump in multigeneration systems improves the overall energy and exergy efficiencies of the plant. Author [58] performed energy and exergy analysis of heat pump integrated multigeneration system and found that the waste heat can produce a COP 3.3 which results in increased energy and exergy efficiency. Soltani et al. [70] performed thermodynamic analysis and performance assessment of an integrated heat pump system for district heating applications and found that the ambient temperature has a great influence on the exergy destruction. In addition to this they concluded that the increase in the mass flow rate of refrigerant increases exergy efficiency due to the utilization of the waste heat. Comparative performance evaluation of cascaded air-source hydronic heat pumps shows that the exergetic COP is increased by 67% for the single refrigerant cascaded system and 70% for a two-refrigerant cascaded system, at low ambient temperatures [71].

The binary plants including ORC (Organic Rankine cycles) and Kalina cycles have many different technical variations [72]. In power plants the low grade hot fluid is used to heat and vaporize a secondary (organic) fluid which runs turbine. The exhaust fluid and the ORC working fluid circulate in separate closed loops. The organic Rankine cycle is suitable for the low temperature exhausts. Due to the circulation of working fluid in a closed loop organic Rankine cycles (ORC) have zero emissions. Ahmadi et al. [73] performed exergo-environmental analysis of an integrated organic Rankine cycle for trigeneration and concluded that the energy of trigeneration system is greatly influenced by the parameters like; compressor pressure ratio, the gas turbine inlet temperature and the gas turbine isentropic efficiency. The results of a case study about analysis and assessment of a new organic Rankine cycle without cogeneration show energy and exergy efficiencies of 0.05%, and 0.17%, respectively, and energy and exergy efficiencies with cogeneration are found to be 0.87%, and 0.35%, respectively [74].

The exergy analysis of hydrogen blended with methanol fueled HCCI engines is not reported in the literature yet, according to the best knowledge of author. The performance of the methanol fueled engine is affected due to incomplete combustion and

poor charge homogeneity. In addition to this, the properties of methanol like; high latent heat, diffusion characteristics and fuel evaporation are poorer as compared to gasoline. The deficiency in the performance of wet methanol fueled internal combustion engine can be overcome by the blending of hydrogen. Therefore, homogenous charge compression ignition (HCCI) engine are proposed as an interesting compromise between spark ignition and compression ignition engines. Several studies [76–79] have obtained promising results through the use of wet-ethanol as a fuel in HCCI engines. These results of the modeling and experiments show that attractive performance and low emissions are possible to achieve by burning as low as 35% methanol-in-water in HCCI engine.

Desalination of the saline has gained a great importance due to the limited availability of the fresh water on the earth. The demand of fresh water is increasing day by day in domestic, industrial, and agriculture. Reverse osmosis (RO) is one of the most favorable desalination technologies and is suitable for moderate production rate [61-62]. The performance of seawater reverse osmosis (SWRO) against the operating parameters is examined in various studies [80–83]. The permeability of membrane can be increased by increasing the temperature of saline water which causes the reduction in viscosity. Desalination process is sensitive to the salinity in the feed water because of the product flow rate, which decreases with the increasing salinity [63-64]. Several studies have investigated the thermodynamic performance of SWRO based on the second law of the thermodynamics [84–86].

The advantages like reduced emissions, and a high thermal efficiency can be achieved by blending of hydrogen with methanol as a fuel, therefore, thermodynamic modeling and analysis of hydrogen enriched wet-ethanol fueled HCCI engine are highly needed to predict its performance. Moreover, the share of renewable energy should be increased significantly for electricity generation. In addition to this, 24.3% of the input power to RO process is recovered through Pelton turbine [58]. Furthermore, fresh water demand is very high in Middle Eastern countries.

The global waste production was 3.5 million tons/day in 2010 and it is going to increase about more than 6 million tons/day by 2025. The worldwide cost of dealing waste in year 2010 was $205 billion and it is projected to be $375 billion by 2025 [86].The

highest increase is forecasted in developing countries. This sharp increase in waste triggers the environmental concerns because landfills and uncollected waste contribute to climate change through the production of methane, a potent greenhouse gas [86].

The municipal solid waste is a renewable energy source and its conversion to energy is a feasible option. The management and disposal of municipal solid waste is a huge problem in Saudi Arabia and more specifically in urban areas. The municipal solid waste in Saudi Arabia is dumped in open landfill sites. An alternative solution is necessary to overcome environmental issues as a result of landfills. Jeddah has the potential to produce about 180 MW of electricity based on incineration scenario [87]. Saudi Arabia generates most of its electricity demand through burning oil despite the fact that it produces than 200,000 tons of biomass waste each year [88]. Therefore, renewable energy based multigeneration system is developed to meet the electricity demand of the rural areas.

The domestic electricity production of Saudi Arabia currently relies mainly on oil and natural gas. More than 900,000 barrels of oil per day is burnt to meet the electricity demands at peak periods which costs about 16 billion dollars per year according to the recent oil prices [89]. Burning less crude can save much more for Saudi Arabia. The country produces 14 million ton of waste per year. There is need to convert waste into electricity through energy efficient and environmentally benign way. Integrated Gasification Combined cycles (IGCC) have potential to convert the waste feed stock into syngas to drive gas turbine for electricity generation with less emissions.

Animal manure production in Saudi Arabia by a dairy “Almarai” alone is 2.8 million tons/year. In recent years, the Kingdom of Saudi Arabia is facing the problem of food waste. About 40 to 51% of the total waste production contains food waste depending upon the density of population and urban activities of that area. The utilizing of wasted food more efficiently is important. This is part of a broader issue of rational and economically efficient waste management.

The potential of electricity generation through the conversion of food waste alone into biogas is estimated about 3 TWh per year. Likewise, other mixed waste including wood, cardboard, paper, leather and textile can generate 1 to 1.6 TWh per year electricity through pyrolysis and other similar technologies. The current solid waste management

activities of Saudi Arabia require an integrated and sustainable methodology with the employment of waste separation awareness at source, recycling of waste, waste-to-energy and value-added product recovery. The government of Saudi Arabia is targeting to generate about half of its energy requirements which is equivalent to 72 GW from renewable sources such as solar, nuclear, wind, geothermal and waste-to-energy systems by 2032 [90].

Currently, the conversion of wastes into syngas through gasification is environmentally benign solution which allow wastes to be profitably converted into valuable commodities while at the same time solving waste storage problems.

The Kingdom of Saudi Arabia is seeking a renewable energy source with potential to generate electricity and other useful outputs. In this thesis, three case studies are performed to assess the potential of producing multiple outputs through wastes for three sectors; community, food industry and oil refinery.

CHAPTER 3 SYSTEM DESCRIPTION

In this section, three novel integrated gasification combined cycles with multigeneration are introduced specifically for three sectors which include; community, food industry and refinery. The waste feedstock composed of different proportions of biomass, animal manure, food waste and heavy oil is used depending upon their availability in a particular sector. The developed systems produce electricity, cooling, heating, hot water, methane and hydrogen with less CO_2 emissions. The hydrogen blended methane is combusted in homogeneous charge compression ignition engine in system 3 to generate additional amount of electricity for refinery. Moreover, a syngas production system from different feedstocks of biomass is also presented for the comparison of calorific value and composition of the produced syngas.

3.1 Syngas Production System Using Variety of Biomass Feedstocks

The newly developed model that uses two types of feedstock wood (Birch) and olive waste is represented in Fig. 3.1. The composition of the feedstock used in Aspen (Plus) model is converted to mass fraction based on the experimental investigation performed by Zanzi et al. [91] about rapid pyrolysis of different types of biomass. Feed is introduced in a splitter which supplies 75% to the mixer and 25% to the combustion reactor. The hot air at 450ºC enters the combustion reactor where combustion reaction is set to generate heat for the gasifier (Gibbs reactor).

The combustion temperature is set at 55ºC above the temperature of the gases entering the reactor [92]. The heat stream Q-GIBBS generated as a result of combustion is supplied to Gibbs reactor for gasification. The steam at 470ºC is mixed with the feed in mixer and supplied to Gibbs reactor. Thermochemical conversion of the feedstock is done at 8 bar and 905°C in this reactor in the presence of gasifying agent steam under Gibbs minimization energy approach. The produced syngas is directed to the separator which separates waste water from the gases. Then, this high pressure syngas is passed through an expander which recovers and heat of this gas is transferred to the ambient water flowing across the heat exchanger 1 (HE 1). The water enters HE 1 at 25ºC and leaves at 102ºC then this steam is passed through HE 2 where it absorbs more heat from the waste and its temperature is raised to 330ºC.

The heat of the flue gases is recovered at two stages first in HE 3 which heats up the ambient air and this ambient air is supplied to the combustion reactor. Then, the flue gases are passed through the heat exchanger 4 which heats up the steam to the required gasification temperature of 470ºC. Finally the heat of this flue gas is used for the drying purpose of the biomass before pyrolysis.

The lower heating value (LHV), higher heating value (HHV) enthalpy and density of the produced syngas are specified with HCOALGEN and DCOALGEN property models present in Aspen Plus [93]. The Peng-Robinson property method with Boston-Mathias modification is selected for this study. The exiting stream "COLDSYN" represents the final syngas produced through gasification.

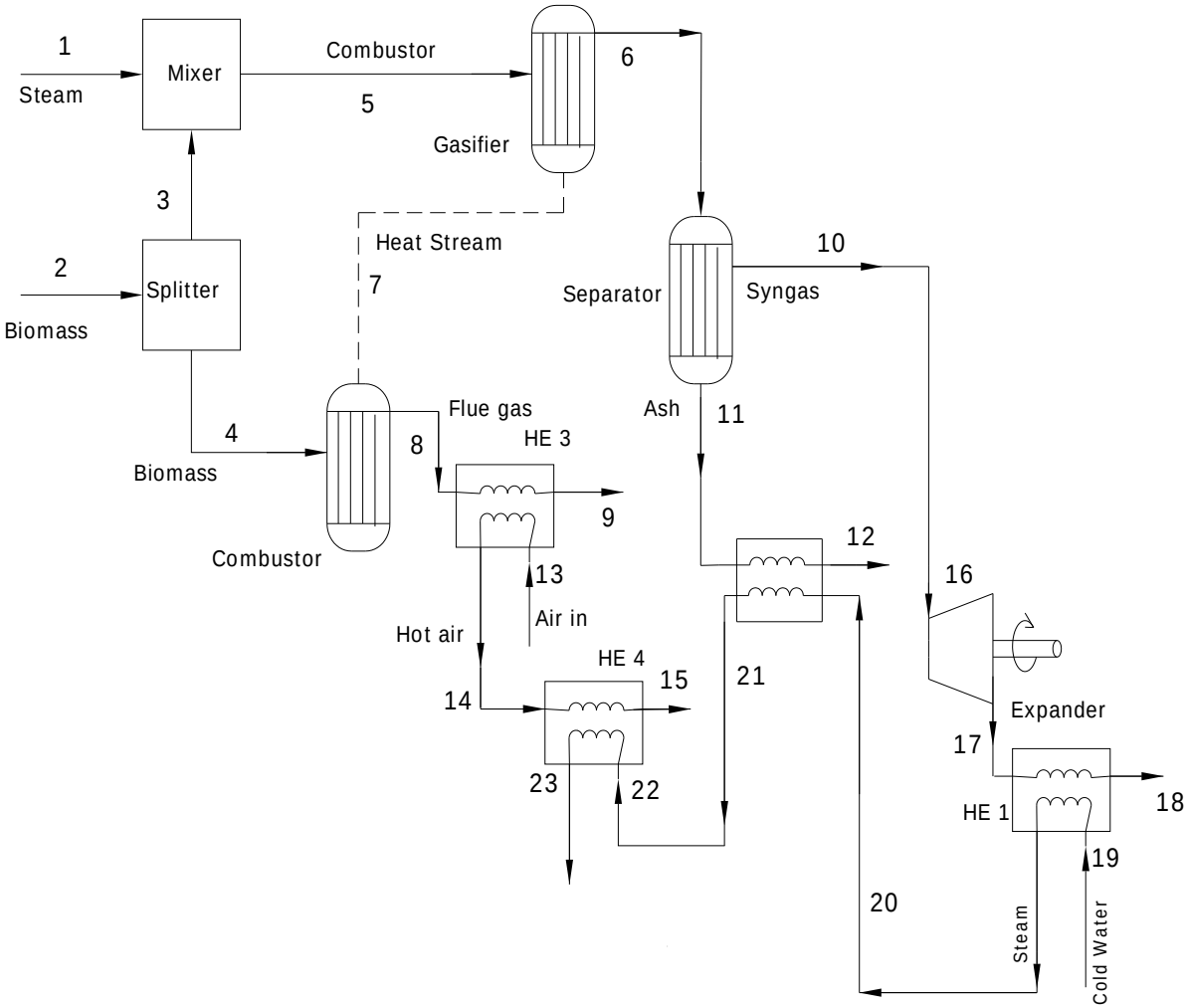

Figure 3.1 Schematic of biomass energy-based system for syngas production

3.2 System 1 for Residential Community

System 1 is developed to produce electricity, cooling, heating and hot water to meet the demands of residential community. The newly developed model uses three types of feedstock biomass, food waste and animal manure as depicted in Fig. 3.2. The composition of the biomass feedstock as discussed in the production of syngas in section 3.1. The composition of food waste and animal manure feedstocks are based on the studies conducted by Reinhart et al. [94], and Haugen et al. [95], respectively. The mass flow rate of biomass, food waste and animal manure is same in the order of 18 kg/s. The biomass is introduced in a splitter which supplies 75% to the mixer and 25% to the combustion reactor.

The hot air at 450 ºC enters the combustion reactor where combustion reaction is set to generate heat for the gasifier (Gibbs reactor). The combustion temperature is set at 55 ºC above the temperature of the gases entering the reactor [92]. The heat stream Q-GIBBS generated as a result of combustion is supplied to Gibbs reactor for gasification. The steam at 470 ºC and 54 kg/s is mixed with the feed in mixer and supplied to Gibbs reactor. Thermochemical conversion of the feedstock is done in this reactor in the presence of gasifying agent steam under Gibbs minimization energy approach. The produced syngas is directed to the separator which separates waste water from the gases. Then, this high-pressure syngas is passed through a heat exchanger which recovers and heat of this gas and generates steam for the gasification. The mass flow rate of air in the compressor is 427 kg/s which compresses it to 8 bar. The air and syngas are inducted to combustion chamber which is the stoichiometric reactor (RStoic) in Aspen database.

The heat of the flue gases is recovered at two stages, first heat exchanger heats up the ambient air and this ambient air is supplied to the combustion reactor. The flue gases are passed through another heat exchanger which heats up the steam to the required gasification temperature of 470ºC. Finally, the heat of this flue gas is used to run R113 based ORC 1. Then, these gases are stored in cylinders after passing through a separator to recover methane and hydrogen from the stream.

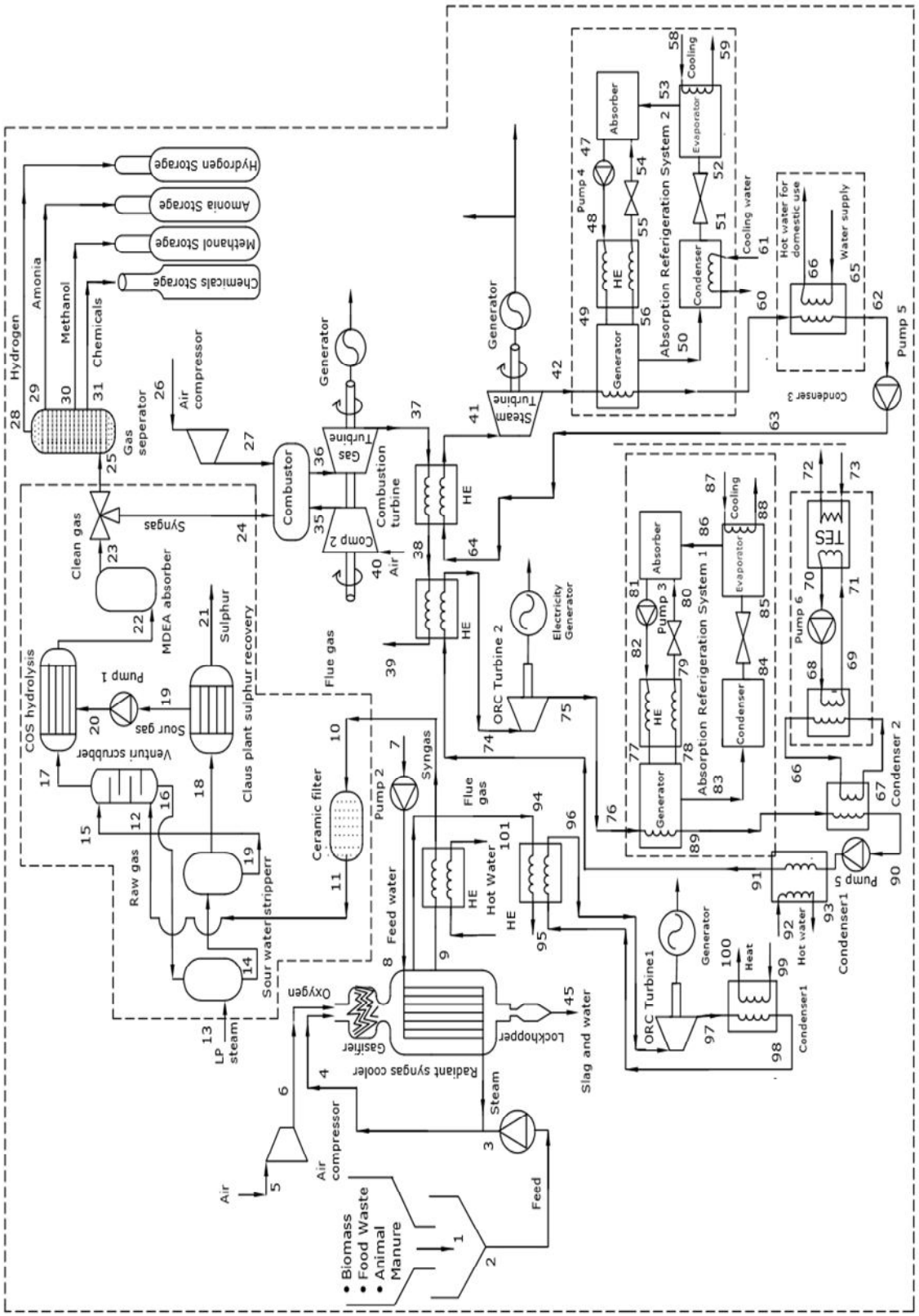

Figure 3.2 Schematic of IGCC multigeneration system for residential community applications

The heat of the flue gases is recovered at two stages, first heat exchanger heats up the ambient air and this ambient air is supplied to the combustion reactor. Then, the flue gases are passed through another heat exchanger which heats up the steam to the required gasification temperature of 470ºC. Finally the heat of this flue gas is used to run R113 based ORC 1. These gas are passed through a separator to recover methane and hydrogen from the stream and these gases are stored in cylinders.

The lower heating value (LHV), higher heating value (HHV) enthalpy and density of the produced syngas are specified with HCOALGEN and DCOALGEN property models present in Aspen (Plus) [93]. The Peng-Robinson property method with Boston-Mathias modification is selected for this study. The exiting stream "COLDSYN" represents the final syngas produced through gasification.

The exhaust of the Gas turbine cycle generates steam to run steam turbine cycle and low grade heat of the exhaust of Gas turbine is recovered through ORC 2 which runs on the working fluid isobutane. The exhaust gases at 491 kg/s and 150°C enter the ORC 2 heat exchanger to evaporate the working fluid. Absorption chiller 1 is placed at the exit of ORC 2 turbine to recover the waste heat and convert it to cooling. Thermal energy storage system is integrated at the condenser of the ORC 2 to further recover the waste heat. The exhaust of the steam turbine leaves at 105°C and passed through a heat exchanger to run the absorption chiller 2. The waste water coming out of the syngas cooler is used for space heating.

The absorption refrigeration cycle uses a heat operated generator, an absorber and a liquid solution pump. The absorption chillers 1 and 2 are integrated at the exhaust of ORC 2 and steam turbine to recover low grade heat. Thermal energy storage (TES) system is incorporated at the exit of the absorption refrigeration chiller 1 which uses water to store the heat for industrial or domestic use.

3.3 System 2 for Food Industry

System 2 is proposed for food industry that requires abundant quantity of fresh water therefore a reverse osmosis plant with energy recovery Pelton turbine is integrated. The system 2 is developed to produce electricity, cooling, heating and hot water and fresh water to meet the demands of a food industry preferably dairy.

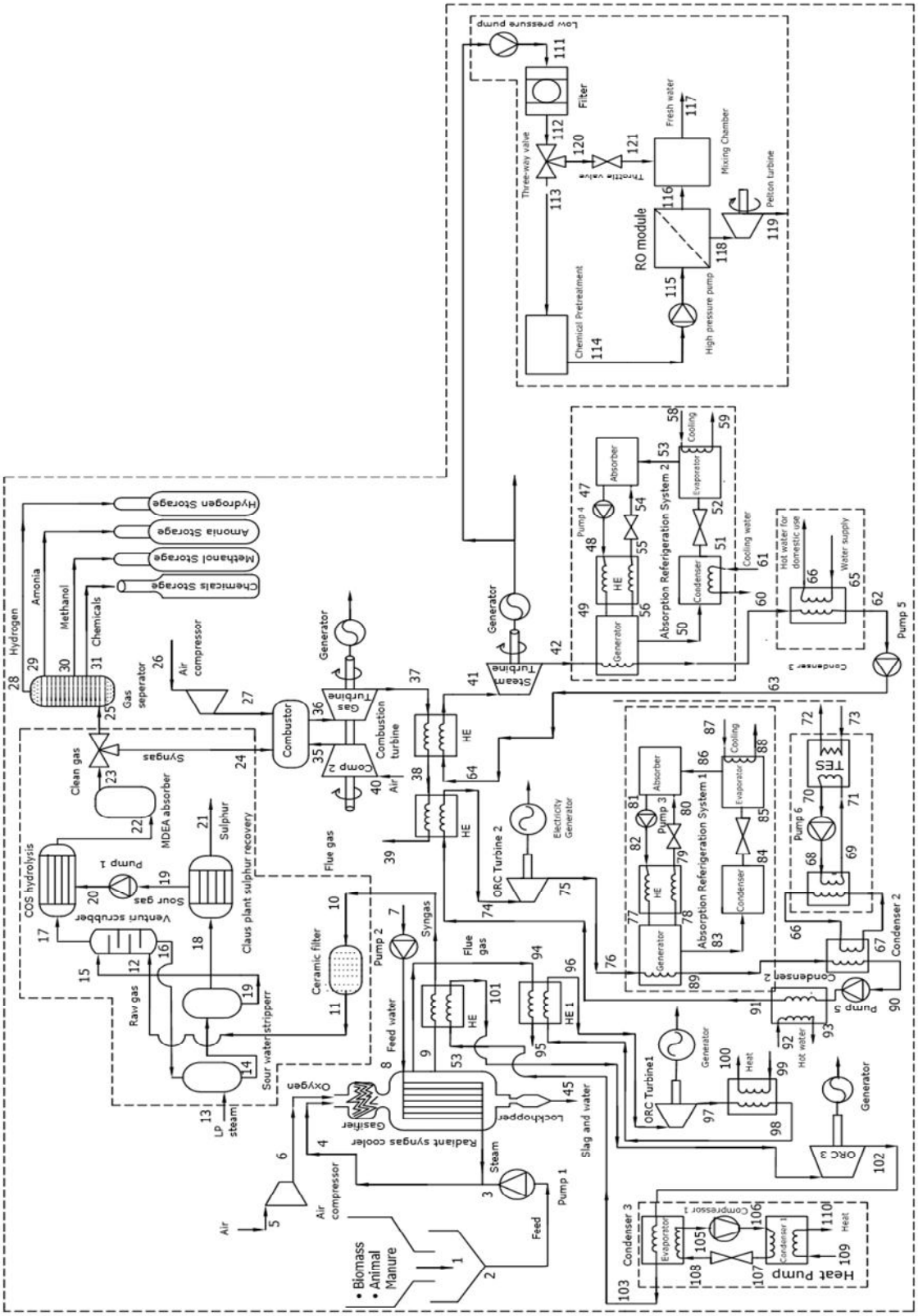

Figure 3.3 Schematic of IGCC multigeneration system for food industry applications

This newly developed system uses two types of feedstock biomass and animal manure as shown in Fig. 3.3. The composition of the biomass feedstock and animal manure is same as discussed in the section 3.2. The mass flow rates of biomass and animal manure are 18 kg/s and 36 kg/s, respectively.

The lower heating value (LHV), higher heating value (HHV) enthalpy and density of the produced syngas are specified with HCOALGEN and DCOALGEN property models present in Aspen (Plus) [93]. The Peng-Robinson property method with Boston-Mathias modification is selected for this study. The exiting stream "COLDSYN" represents the final syngas produced through gasification.

The exhaust of the Gas turbine cycle generates steam to run steam turbine cycle and low grade heat of the exhaust of Gas turbine is recovered through ORC 2 which runs on the working fluid isobutane. The exhaust gases at 487 kg/s and 150°C enter the ORC 2 heat exchanger to evaporate the working fluid. Absorption chiller 1 is placed at the exit of ORC 2 turbine to recover the waste heat and convert it to cooling. Thermal energy storage system is integrated at the condenser of the ORC 2 to further recover the waste heat. The exhaust of the steam turbine leaves at 102°C and passed through a heat exchanger to run the absorption chiller 2. The waste water coming out of the syngas cooler in this system 2 is at 110°C therefore, another isobutane based ORC 3 is integrated to this system to recover the heat of this waste water. The exhaust of ORC 3 is used to run a heat pump for heat production. Some of electricity generated through ORC 1 of this system is supplied to a reverse osmosis plant to generate electricity.

The absorption refrigeration cycle uses a heat operated generator, an absorber and a liquid solution pump. The absorption chillers 1 and 2 are integrated at the exhaust of ORC 2 and steam turbine to recover low grade heat. Thermal energy storage (TES) system is incorporated at the exit of the absorption refrigeration chiller 1 which uses water to store the heat for industrial or domestic use. A device that transfers heat from a low-temperature medium to a high temperature one is heat pump. The heat pump is integrated at the condenser 3 of organic Rankine cycle 3 where, the working fluid of Rankine cycle rejects heat to the working fluid R410 of the heat pump to produce heat between states 109 and 110. The objective of a heat pump is to maintain a heated space at a high temperature.

Food industries require abundant quantity of fresh water therefore, a reverse osmosis (RO) system is incorporated to system 2 to meet this demand. The reverse osmosis plant integrated with this study is designed to provide 100 kg/s of fresh water with less than 500 PPM salinity. Sea water is pumped by a low pressure pump from atmospheric conditions to 650 kPa (state 55). The saline water is then passed through a filter to remove suspended particles. Three- way valve splits small amount of good quality water while the major amount is processed in chemical chamber to make it suitable for the RO membrane modules. The pressure of the process water is raised by a high pressure pump to 6000 kPa based on the osmotic pressure design. The rejected brine at 5100 kPa drives a Pelton turbine and recovers some of the power consumed in RO process. DuPont B10 hollow fiber RO modules are used in this study due to their high salt retention ability as compared to other designs [92–95].

3.4 System 3 for Refinery

System 3 is developed for refinery which requires too much power for refining processes therefore hydrogen and methanol produced onsite are combusted in HCCI engine to produce additional power, and save compression and transportation cost associated with hydrogen and methane as represented in Fig. 3.4. In addition to above, system 3 is developed to produce electricity, cooling, heating and hot water and fresh water to meet the demands of an oil refinery. The newly developed model uses three types of feedstock biomass, food waste and heavy oil. The composition of the biomass feedstock as discussed in the production of syngas in section 3.1 whereas, the composition of heavy oil is based on study conducted by Ashizawa et al. [47]. The mass flow rate of biomass, food waste and heavy oil are 12 kg/s, 12 kg/s and 11 kg/s, respectively.

The input parameters and Aspen (Plus) simulation steps of steam, biomass combustor, gasifier and syngas combustion chamber are the same as discussed in section 3.1 and 3.2.

The lower heating value (LHV), higher heating value (HHV) enthalpy and density of the produced syngas are specified with HCOALGEN and DCOALGEN property models present in Aspen (Plus) [93]. The Peng-Robinson property method with Boston-Mathias

modification is selected for this study. The exiting stream “COLDSYN” represents the final syngas produced through gasification.

The exhaust of the Gas turbine cycle generates steam to run steam turbine cycle and low grade heat of the exhaust of Gas turbine is recovered through ORC 2 which runs on the working fluid isobutane. The exhaust gases at 487.64 kg/s and 150°C enter the ORC 2 heat exchanger to evaporate the working fluid. Absorption chiller 1 is placed at the exit of ORC 2 turbine to recover the waste heat and convert it to cooling. Thermal energy storage system is integrated at the condenser of the ORC 2 to further recover the waste heat. The exhaust of the steam turbine leaves at 157°C and passed through a heat exchanger to run the absorption chiller 2. The waste water coming out of the syngas cooler in this system 2 is at 51°C therefore, it is used to generate hot water for domestic use. Some of electricity generated through ORC 1 of this system is supplied to a reverse osmosis plant to generate electricity. Reverse osmosis plant is coupled with Pelton turbine which recovers the high pressure of the brine leaving the system.

Some mass fraction of produced hydrogen and methane are blended and combusted in HCCI engine to produce more power. The exhaust of the HCCI engine is passed through a heat exchanger to run another R113 operated organic Rankine cycle. Absorption chiller 3 is place at the condenser of this ORC to convert this low grade heat into cooling. The additional by products which include hydrogen, ammonia, methanol and other chemicals can be stored and sold out to industries.

Generally, two types of absorption systems are available based on the refrigerant and absorber combination. These are lithium bromide/water and ammonia water combination system. Lithium bromide /water chillers are appropriate for space cooling. The absorption refrigeration cycle uses a heat operated generator, an absorber and a liquid solution pump. The absorption chillers 1 and 2 are integrated at the exhaust of ORC 2 and steam turbine to recover low grade heat. Thermal energy storage (TES) system is incorporated at the exit of the absorption refrigeration chiller 1 which uses water to store the heat for industrial or domestic use.

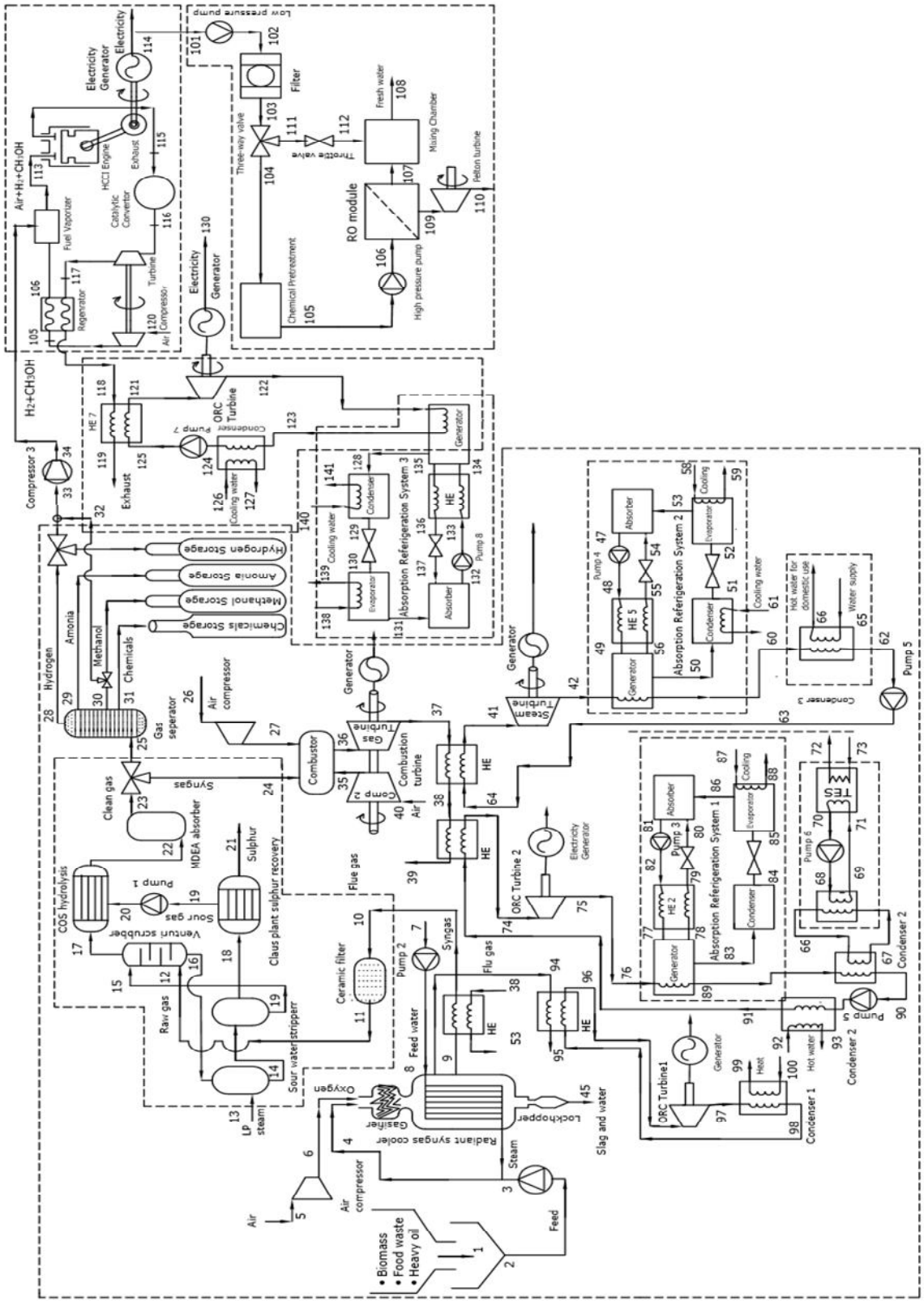

Figure 3.4 Schematic of IGCC multigeneration system for refinery applications

In homogenous charged compression ignition (HCCI) cycle, the ambient air enters the compressor of turbo charger and leaves at high pressure and high temperature. This compressed air enters the regenerator and leaves after absorbing the heat of exhaust gases of the engine. Then, both methanol and hydrogen are injected into the vaporizer where, these are evaporated and mixed with the compressed air. A homogenous mixture of methanol, water, hydrogen and air is produced and injected in the HCCI engine. This homogenous mixture gets heated up after mixing with the residual gases. After combustion, the high temperature exhaust gases enter the catalytic convertor where the unburnt fuel, hydrocarbons and carbon monoxide further react with oxygen and release more heat. The exiting gases from the catalytic convertor enter the turbine, which drive turbocharger compressor. The high temperature exhaust of turbine enters the regenerator where it transfers the heat to the compressed air and then leaves the regenerator.

In this system 3, reverse osmosis (RO) system is coupled with HCCI engine. Refineries also require abundant quantity of fresh water therefore, a reverse osmosis (RO) system is incorporated to meet this demand. The capacity of reverse osmosis plant integrated in this system 3 is same as system 2 and provides 100 kg/s of fresh water with less than 500 PPM salinity. Sea water is pumped by a low pressure pump from atmospheric conditions to 650 kPa (state 55). The saline water is then passed through a filter to remove suspended particles. Three-way valve splits small amount of good quality water while the major amount is processed in chemical chamber to make it suitable for the RO membrane modules. The pressure of the process water is raised by a high pressure pump to 6000 kPa based on the osmotic pressure design. The rejected brine at 5100 kPa drives a Pelton turbine and recovers some of the power consumed in RO process.

The integrated gasification combine cycle (IGCC) can be subdivided into ten main subsystems, namely; air compressor, gasifier, convective syngas cooler, sour water stripper, Sulfur recovery Clause plant, combustor, gas turbine, steam turbine, gas separator and storage system. The other subsystems are incorporated to IGCC cycle are heat pump, organic Rankine cycle unit, absorption chiller and thermal energy storage system. These sub-systems recover low grade waste heat and provide heating, power, cooling and hot water.

Table 3.1 Major subsystems integrated with proposed systems

System1 (For residential Community)	**System 2 (For food industry)**	**System 3 (For refinery)**
• Air Separation Unit	• Air Separation Unit	• Air Separation Unit
• Gasifier	• Gasifier	• Gasifier
• Radiant syngas cooler	• Radiant syngas cooler	• Radiant syngas cooler
• Convective syngas cooler	• Convective syngas cooler	• Convective syngas cooler
• Ceramic filter	• Ceramic filter	• Ceramic filter
• Sour water stripper	• Sour water stripper	• Sour water stripper
• Venturi Scrubber	• Venturi Scrubber	• Venturi Scrubber
• MDEA absorber	• MDEA absorber	• MDEA absorber
• Claus plant	• Claus plant	• Claus plant
• Gas separator	• Gas separator	• Gas separator
• Gas turbine unit	• Gas turbine unit	• Gas turbine unit
• Steam turbine unit	• Steam turbine unit	• Steam turbine unit
• ORC turbines	• ORC turbines	• ORC turbines
• Thermal energy storage system	• Thermal energy storage system	• Thermal energy storage system
• Absorption chillers	• Absorption chillers	• Absorption chillers
-	• Heat pump	-
-	• Reverse osmosis	• Reverse osmosis
-	-	• HCCI engine

Table 3.1 tabulates the major sub-systems integrated with system 1, system 2 and system 3 developed for a residential community, a food industry and a refinery to meet the demand of power, heat, cooling and hot water. The gasification of feedstock also produces other useful by products like hydrogen, methanol, ammonia and chemicals.

The gasifier is designed to have an outer pressure vessel and inner membrane cooled by water which controls the temperature of gasifier by generating saturated steam in case of high temperature. Feedstock, oxygen and steam enter the gasifier to produce raw gas consisting of H_2 and CO which leaves the reactor at approximately gasifier temperature.

The raw gas produced in gasifier is cooled through a recycling gas before entering convective cooler which generates superheated steam. Then, syngas is directed towards

cleaning train for the purification purpose. The detailed cleaning process of the syngas is as discussed below;

The exiting raw syngas from gasifier is purified by passing through the train of Venturi scrubbers (VS), sour water stripper (SWS), carbonyl sulfide (COS) hydrolysis, N-methyl diethanol amine (MDEA) absorber and Sulfur recovery Clause plant. The high operating pressure (8 bar) is maintained in all purification units. The detailed description of this purification process is presented below.

Then, the produced syngas is passed through venturi scrubber where, water absorbs impurities mainly; hydrogen di-sulfide (H_2S), ammonia (NH_3) and hydrogen cyanide (HCN). The acid contaminants and basic contaminants are removed through circulation of steam in two columns of sour water stripper. Both of these units are simulated in ASPEN by considering complex chemical equilibrium. The water stream pressure is reduced from 8 to 1.5 bar in order to facilitate the working conditions of acid stripper column. The pH of SWS is controlled through the induction of sulfuric acid (H_2SO_4) and sodium hydro oxide (NaOH).

The basic function of COS hydrolysis is to convert COS in H_2S by adding water in the presence of a catalyst alumina [100]. Hydrolysis reaction is assumed to follow first order kinetic reaction for carbonyl sulfide with water having zero order behavior [101]. The kinetic reaction properties in the presence of catalyst are taken into account while modelling COS in ASPEN.

The H_2S is highly soluble in $C_5H_{13}O_2N$ therefore, it is selected as liquid washing agent in MDEA absorber. The water solution in MDEA absorbs acid breed in the gas stream and removes H_2S. The gas leaving MDEA absorber is fed into Clause plant. The electrolyte properties package (ElecNRTL) in ASPEN is used to model MDEA absorber. The gas exiting MDEA absorber is directed towards Sulfur recovery Claus plant.

The main objective of this process is to remover sulfur and nitrogen. Sulfur is stored in liquid state while nitrogen is vented. This process occurs in two stages composed of thermal and catalytic. The chemical reaction takes place in the presence of catalyst alumina. The sulfur recovery is increased with the last step of hydrogenation. The sulfur pit collects

the liquid sulfur as a result of condensation process which removes considerable amount of liquid sulfur. The catalytic stages in Clause plant are assumed to be equilibrium reactors.

Thermally activated system replaces compressor in absorption refrigeration systems. Generator, evaporator condenser and absorber are the main components of an absorption cooling system. The absorber is used to convert the vaporized refrigerant back to liquid. Cooling water is circulated through to absorber to absorb the heat. The absorption systems are proficient for producing cooling effect through waste heat. A typical absorption machine requires about 9 kg of steam for 3.5 kW (1 ton) refrigeration effect at about 7°C according to ASHRAE Handbook. Two types of absorption systems are readily available on the basis of refrigerant and absorber combination. The most common absorption systems are a combination of lithium bromide/water and ammonia water [17].

Trichlorotrifluoroethane R113 is selected as a working fluid for ORC coupled with the exhaust of HCCI engine due to its better performance in recovering low temperature waste heat [102]. The high temperature and high pressure fluid is passed through an ORC turbine for power generation. The working fluid rejects its heat to the generator of absorption chiller and then condenser before completing cycle.

CHAPTER 4 SYSTEM ANALYSIS, MODELING AND SIMULATION

In this chapter, the governing equations of the thermodynamics analyses of the syngas production system and three proposed systems based on energy and exergy concepts are documented. Economic analyses based on exergoeconomic concepts are also applied to the developed models. The systems performances are also described by the energy and exergy efficiencies and sustainability indexes.

4.1 Thermodynamic Analysis of Biomass based Syngas Production System

The Aspen (Plus) is selected to develop and perform sensitivity analysis of the syngas produced from two types of biomass feedstocks. The following lists the assumptions made to investigate performance and sensitivities of the proposed system. The equilibrium assumption followed in this study is that no rapid shift occurs when different species exists in a mixture [16].

- The temperature T_0=25ºC and pressure P_0=1 bar are taken as dead state properties of the multigeneration system.
- The operating conditions and all flow processes of the system are of steady state.
- All pumps and turbines are adiabatic [104].
- Tar production is zero and char is composed of solid carbon.
- Negligible or no changes in the kinetic and/or potential energies [104].
- Air is mainly composed of 79% N_2 and 21% O_2.
- The ideal gas properties are chosen for air to perform analysis.
- The isentropic efficiency of 85% is taken for pumps and turbines [105].
- The selected property method is Peng-Robinson (PR) equation of state with Boston-Mathias (BM) modification (PR-BM) [28].
- The lower heating values (LHV) and higher heating values (HHV) for wood (Birch) and olive waste are 31.84MJ/kg and 26.03 MJ/kg, and 17.07 MJ/kg and 19.67 MJ/kg, respectively [91].

The balance equations related to mass, energy, exergy and entropy of the proposed systems are presented here. Moreover, energetic and exergetic performances of sub-systems, and the multigeneration system with irreversibility rates are also discussed.

The Aspen (Plus) is used to calculate the mass and energy magnitudes for all streams however, mass and energy balances for a general process in steady-state can be written as

$$\sum_i \dot{m}_i = \sum_e \dot{m}_o \quad (4.1)$$

$$\sum_i \dot{E}_{in} = \sum_e \dot{E}_{out} \quad (4.2)$$

The overall exergy balance for steady state process can be expressed as

$$\left(\sum \dot{E}x_i\right)_{in} = \left(\sum \dot{E}x_i\right)_{out} + \sum \dot{E}x_{dest} \quad (4.3)$$

where $\left(\sum \dot{E}x_i\right)_{in}$ represents the sum of rate of exergy destruction at inlet

$$\left(\sum \dot{E}x_i\right)_{in} = \dot{E}x_{air} + \dot{E}x_{dry,bio} + \dot{E}x_{bio,moist} + \dot{E}x_{st} \quad (4.4)$$

and the sum of rate of exergy destruction at exit $\left(\sum \dot{E}x_i\right)_{out}$ can be calculated as

$$\left(\sum \dot{E}x_i\right)_{out} = \dot{E}x_{prod,g} + \dot{E}x_{flue,g} + \dot{E}x_{WH2O} + \dot{E}x_{st} + \dot{W}_{net} \quad (4.5)$$

The combustion reactor and gasifier both account physical and chemical exergies at inlet and exit states. Chemical exergies are the exergies associated with combustion process and chemical reactions whereas, only physical exergies are related to heat exchangers as there is no chemical change or reactions. The sum of specific physical and specific chemical exergy is the total specific exergy flow at any specified state which can be found as

$$ex = ex_{ch} + ex_{ph} \quad (4.6)$$

The specific physical exergy can be written as

$$ex_{ph} = (h - h_0) - T_0(s - s_0) \quad (4.7)$$

The gas mixture is assumed to be ideal for the calculations of the specific chemical exergies so the equation can be defined as [106]

$$ex_{ch} = \sum_i x_i(ex_{ch,i} - RT_0 lnx_i) \quad (4.8)$$

where x_i and $ex_{ch,i}$ represent the mole fraction and chemical exergy associated with component "i", respectively. The values of standard chemical exergies are based on the model 2 developed by Szargut et al. [107].

The entropy balance related to the steady flow system can be calculated as

$$\sum \frac{\dot{Q}_j}{T_j} - \sum \dot{m}_0 s_0 + \dot{S}_{gen} = 0 \quad (4.9)$$

The exergy destruction occurring as a result of irreversibilities can be defined as

$$\dot{E}x_{dest} = T_0 \dot{S}_{gen} \quad (4.10)$$

The biomass enters the yield reactor at ambient conditions and hence, the physical exergy is taken zero. Szargut [108] developed a statistical correlation factor to calculate chemical exergy of solid biofuels which is used in this study to find the correlation factor for wood (Birch) and olive waste.

$$\beta = \frac{1044+\frac{0.0160H}{C}-\frac{0.34930}{C}[1+\frac{0.0531H}{C}]+\frac{0.0493N}{C}}{(1044+\frac{O}{C})} \quad (4.11)$$

Equation 4.11 is based on no sulfur contents as the amount of sulfur is very small in biomass. So, the specific chemical exergies of the selected feedstocks can be found as

$$Ex_{ch,drybio} = \beta LHV_{bio} \quad (4.12)$$

The specific heat at constant pressure of the biomass is calculated as [109]

$$C_{p,bio} = 1.5 + 10^{-3}T \quad (4.13)$$

The change in the specific entropy corresponding to the temperature can be expressed as

$$\Delta S = \int_{T_0}^{T} \frac{C_p}{T} dT \quad (4.14)$$

The cold gas energy efficiency (CGE) is a mean to figure out the performance of the gasifier which can be calculated as

$$\eta_{cg} = \frac{\dot{m}_{prodg} LHV_{prodg}}{\dot{m}_{drybio} LHV_{drybio}} \quad (4.15)$$

The energy efficiency of any component at state "i" can be written as

$$\eta_i = 1 - \frac{(\dot{E}_{out})_i}{(\dot{E}_{in})_i} \quad (4.16)$$

The ratio of steam to biomass can be calculated as [110]

$$STBR = \frac{\dot{m}_{st}}{\dot{m}_{drybio}} \tag{4.17}$$

4.2 Mass, Energy and Entropy Balance Equations for Proposed Systems

The mass, entropy and exergy balance equations are applied to a control volume that exchange heat, work and mass with the surrounding environment.

The conservation of mass through the control volume of any system can be described in its general form as follows

$$\frac{dm_{cv}}{dt} = \sum \dot{m}_{in} - \sum \dot{m}_{out} \tag{4.18}$$

For steady state system equation 4.18 can be written as

$$\sum \dot{m}_{in} = \sum \dot{m}_{out} \tag{4.19}$$

where *m* and $\dot{m}$ represents the mass and mass flow rate, respectively. The subscripts *in* and *out* indicate the inlet and exit of the control volume, respectively.

The conservation of energy equation for a control volume can be formulated from the first law of thermodynamics as follows

$$E_2 - E_1 = \delta Q - \delta W \tag{4.20}$$

where *Q* and *W* are the heat and work that the system exchange with the environment in the process from initial state 1 to final state 2, while *E* refers to all forms of energy that the system posses at each indicated state. These forms of energy can be concluded in the following three forms: internal, kinetic and potential energy. Cengel and Boles [111] defined the general energy balance equation in a transient form as follows

$$\frac{dE_{cv}}{dt} = \dot{Q}_{cv} - \dot{W}_{cv} + \sum \dot{m}_{in}\left(h + \frac{V^2}{2} + gz\right)_{in} - \sum \dot{m}_{out}\left(h + \frac{V^2}{2} + gz\right)_{out} \tag{4.21}$$

where *E*, $\dot{Q}$ and $\dot{W}$ are the energy, heat transfer rate and the power exchange through the system control volume, respectively, and *h*, *V*, *z* and *g* represent the specific enthalpy, velocity, elevation and gravitational acceleration, respectively.

From the second law of thermodynamics, the entropy generation associated with the processes that the systems go through can be described as stated in the following general equation:

$$\frac{dS_{cv}}{dt} = \sum \dot{m}_{in} s_{in} - \sum \dot{m}_{out} s_{out} + \sum \frac{\dot{Q}_{cv}}{T} + \dot{S}_{gen} \tag{4.22}$$

where, s stand for the thermodynamics property; entropy and $\dot{S}_{gen}$ is the entropy generation.

The exergy can be defined as the maximum work that can be extracted from a system interacting with a reference environment [106]. The main aim of applying exergy analysis is to evaluate the causes of thermodynamics imperfection and indicate the possible thermodynamics improvements of the process [107]. The exergy balance has the fundamental difference from the energy balance that exergy is exempt from the conservation law. The exergy balance is a statement of law of energy degradation as it describes the irretrievable loss of exergy due to irreversibility of the processes [112]. The exergy balance equation for system components in the general form can be described as follows:

$$\frac{dEx_{CV}}{dt} = \sum \dot{E}x_Q - \sum \dot{E}x_w + \sum_{in} \dot{E}x_{flow} - \sum_{out} \dot{E}x_{flow} - \dot{E}x_d \tag{4.23}$$

where $\dot{E}x_Q$ represents the exergy transfer rate with the heat energy exchange across the system control volume and $\dot{E}x_w$, refers to the exergy transfer rate by the boundary or shaft work applied on or done by the system. The term $\dot{E}x_{flow}$ represents the exergy transfer rate with flow transfer through the system. The exergy destruction, which describes the system irreversibility, is shown in the equation as $\dot{E}x_d$. These terms are described in the following items.

For the heat transfer rate $\dot{Q}$ which occurs at a control surface with boundary temperature T_b, the maximum rate of conversion from thermal energy to useful work, which describes the thermal exergy flow, can be sated as [113]

$$\dot{E}x_Q = \left(1 - \frac{T_0}{T_b}\right) \dot{Q} \tag{4.24}$$

where $(1 - T_0/T_b)$ is the dimensionless exergetic temperature, which is equal to the Carnot efficiency working between the environmental temperature at T_0 and the temperature T_b of the surface at which the heat transfer occurs.

From the simple definition, the work equivalent of a given form or energy is a measure of its exergy. It can be stated that the exergy transfer with shaft or boundary work equals to work and the exergy transfer rate which can also be specified by the power or the work transfer rate [112]. The exergy transfer rate associated with work considering the change of the volume can be described as

$$\dot{E}x_w = \dot{W}_{cv} + P_0 \frac{dV_{cv}}{dt} \tag{4.25}$$

where P_0 is the dead state pressure.

Kotas [112] defined the exergy associated with the flow of matter as the maximum amount of work is attainable when the flow is brought from its initial state to the dead state during a process of interaction with the environment. The exergy transfer by the stream through any system component can be expressed in terms of the specific flow exergy as follows

$$\sum_{in} \dot{E}x_{flow} - \sum_{out} \dot{E}x_{flow} = \sum_{in} \dot{m}_i ex_i - \sum_{out} \dot{m}_i ex_i \tag{4.26}$$

Moran et al. [113] decomposed the flow exergy into four main segments; physical ($e_{x,ph}$), chemical ($e_{x,ch}$), kinetic ($e_{x,ke}$) and potential ($e_{x,pe}$) segments of exergy (Moran et al., 2011).

$$ex_{\text{flow}} = e_{x,ph} + e_{x,ch} + e_{x,ke} + e_{x,pe} \tag{4.27}$$

The kinetic and potential components of exergy in the above equation are assumed to be negligible as the changes in velocities and elevations across the systems components are small as compared to the values of the other terms.

The physical exergy represents the portion of the flow exergy that is caused by physical processes involving only thermal interaction with the environment to bring the flow from its initial condition to the environmental state which is defined by T_0 and P_0. The following equation describes the specific physical exergy components.

$$e_{x,ph} = (h - h_0) - T_0(s - s_0) \quad (4.28)$$

where h and h_0 are the enthalpy values, and s and s_0 are the entropy values at the defined and the reference environment states, respectively.

The chemical exergy is the portion of the flow exergy that is caused by processes involving heat transfer and exchange if substances only with the environment to bring the substance from the environmental state to the dead state [114]. The Chemical exergy for a gaseous mixture can be calculated using the following equation, considering ideal gas assumption [113].

$$ex_{ch,mix} = \sum y_i ex_{ch,i} + RT_0 \sum y_i \ln y_i \quad (4.29)$$

where y_i is the mole fraction of the component *i* in the gas mixture.

The chemical exergy of a solid fuel is calculated based on the following formula

$$ex_{ch,fuel} = \left(LHV + w.h_{fg}\right)\varphi_{dry} + 9{,}417s \quad (4.30)$$

where LHV is the net calorific value of the fuel, w is the moisture content of the fuel, h_{fg} is the latent heat of water at T_0 and s denotes the mass fraction of sulfur in the fuel. The chemical exergy ratio is denoted by φ_{dry} and is defined in terms of the dry organic substances contained in the fuel as follows:

$$\varphi_{dry} = 0.1882\,\frac{h}{c} + 0.061\,\frac{o}{c} + 0.0404\,\frac{n}{c} + 1.0437 \quad (4.31)$$

where *c, h, o* and *n* are the mass fraction of carbon, hydrogen, oxygen and nitrogen in the fuel, respectively. The previous formula works with a mass ratio of oxygen to carbon less than 0.667. For the oxygen to carbon ratio is between 0.667 and 2.67 then the following formula can be used as proposed by Kotas [112].

$$\varphi_{dry} = \left(0.1882\,\frac{h}{c} - 0.2509\left(1 + 0.7256\frac{h}{c}\right) + 0.0404\,\frac{n}{c} + 1.0438\right) / \left(1 - 0.3035\frac{o}{c}\right) \quad (4.32)$$

For liquid fuels, the chemical exergy ratio can be calculated as [112]

$$\varphi = 0.1882\,\frac{h}{c} + 0.0432\frac{o}{c} + 0.2169\,\frac{s}{c}\left(1 - 2.0628\frac{h}{c}\right) + 1.0401 \quad (4.33)$$

The following simplification, which was proposed by Szargut et al. [107] can be also used to calculate the chemical exergy of a fuel:

$$\varphi = ex_{ch,fuel}/LHV \tag{4.34}$$

For a general gaseous fuel, $C_\alpha H_\beta$, the following correlation can be used to calculate the chemical exergy ratio [52].

$$\varphi = 0.0169\frac{\propto}{\beta} - \frac{0.0698}{\alpha} + 1.033 \tag{4.35}$$

So, the specific flow exergy for any component *i* of the inlet and outlet flow streams can be expressed as follows [106]:

$$ex_i = (h_i - h_o) - T_o(s_i - s_o) \tag{4.36}$$

In equation 4.36 the assumption of neglecting the potential and kinetic exergy terms is considered. The exergy destruction rate in any component '*i*' in a system, which appears as $\dot{E}x_d$ in the general exergy balance equation, is proportional to the entropy generation rate across that component, $\dot{S}_{gen}$

$$\dot{E}x_{d_i} = T_o.\dot{S}_{gen,i} \tag{4.37}$$

where $\dot{S}_{gen,i}$ denotes the entropy generation rate in each component.

Hence, the exergy balance equation can be reformulated as [111]

$$\frac{dEx_{cv}}{dt} = \sum\left(1 - \frac{T_0}{T}\right)\dot{Q} - \dot{W}_{cv} + P_0\frac{dV_{cv}}{dt} + \sum\dot{m}_{in}ex_{in} - \sum\dot{m}_{out}ex_{out} - T_0\dot{S}_{gen} \tag{4.38}$$

The efficiency of a system can be defined as the measure of the effectiveness of that system performance. Energy efficiency for a thermodynamics process or system is defined as the ratio of useful output of the system to the energy input to the system.

$$\eta = \frac{\sum useful\ output\ energy}{\sum input\ energy} = 1 - \frac{\sum energy\ loss}{\sum input\ energy} \tag{4.39}$$

The exergy efficiency or second law analysis of thermodynamics systems provides a better insight of system performance. The concept of exergy efficiency provides information about the potential for system improvements.

$$\psi = \frac{\sum useful\ output\ exergy}{\sum input\ exergy} = 1 - \frac{\sum exergy\ loss}{\sum input\ exergy} \tag{4.40}$$

4.3 Chemical Analyses of Gasification Process

The molar quantity of water per one kmol (*w)*of heavy oil can calculated as

$$w = \frac{M_{HFO} \times WC}{M_{H_2O} \times (1 - WC)} \quad (4.41)$$

The stoichiometric air fuel ratio for the fuel with chemical formula $C_\alpha H_\beta O_\vartheta N_\delta$ can be calculated as

$$AFR_{stoic} = \alpha + \frac{1}{4}\beta - \frac{1}{2}\vartheta \quad (4.42)$$

The magnitudes of equilibrium constants can be calculated using Gibbs free energy as follows:

$$lnK = \frac{-\Delta G_T^o}{RT} \quad (4.43)$$

where dependence of Gibbs function is dependent on temperature and can be found as

$$\frac{d(\Delta G_T^o)}{dT} = \frac{h_f^o}{RT} \quad (4.44)$$

The calorific value of a dry-based liquid fuels can be calculated as follows [50]:

$$HHV = 0.3491C + 1.1783H_2 + 0.1005S - 0.1034O_2 - 0.0151N_2 - 0.0211Ar \quad (4.45)$$

4.4 Chemical Reactions in Purification Unit

The chemical reaction that takes place in COS hydrolysis can be expressed as follows

$$COS + H_2O \rightarrow H_2S + CO_2 \quad (4.46)$$

The sulfur removal reaction unit follows the chemical reaction presented below

$$H_2S + (3/2)\ O_2 \rightarrow SO_2 + H_2O \quad (4.47)$$

$$2H_2S + SO_2 \rightarrow 2H_2O + 3S \quad (4.48)$$

The unconverted sulfur can be recovered from the clean gas by passing it Claus plant. The chemical reaction that takes place in this unit can be written as

$$SO_2 + 3H_2 \rightarrow H_2S + 2H_2O \quad (4.49)$$

$$COS + H_2 \rightarrow H_2S + CO \quad (4.50)$$

4.5 HCCI Engine

The mixture of hydrogen, methanol, water and air from vaporizer enters the cylinder where it is compressed by the piston after getting mixed with the residual gases. The air/fuel mixture is heated up by the high compression ratio ($r_c = 16$), which leads to ignition. The bulk auto-ignition process as a result of combustion in HCCI engine is chemical kinetics constrained [115]. The mixed temperature of fresh charge and residual gases is calculated as follows [116] whereas, the cylinder inlet and exhaust pressure ratio is assumed to be 1.4 [117].

Intake process $(i - 1')$

$$T_{1'} = \frac{T_i(1-f)}{1-\frac{1}{(nr_c)\left[{}^{Pe}/_{P_i}+(n-1)\right]}} \tag{4.51}$$

The chemical exergy associated with combustion in HCCI engine can be obtained as [112].

$$e_{x,ch,comb} = -\Delta\overline{h}_0 + T_0\Delta\overline{s}_0 + \overline{R}T_0\left\{xO_2 ln\frac{P_{O2}^{00}}{P^0} - \sum_K x_k ln\frac{P_k^{00}}{P^0}\right\} \tag{4.52}$$

where ex_{ch} is the reference specific chemical exergy, s is the specific entropy at a specified state, subscript 0 represents environment conditions whereas x and y are the molar fraction of the species in the flow and ΔG is the net change in the Gibbs energy. The chemical exergy is calculated by taking the following standard partial pressures;

(O_2) = 0.204, (N_2) = 0.7583, H_2O (g) = 0.0088, (Ar) = 0.00907, and (CO_2) = 0.000294

The stoichiometric air/fuel mixture is inducted in cylinder because the dilution is provided by the water contents in the ethanol. The combustion process in HCCI engine is assumed as the following general combustion equation for all percentages (5% - 20%) of hydrogen is blended in methanol in this study.

$$\alpha CH_3OH + \beta H_2O + \omega H_2 + \lambda(O_2 + 3.773N_2) \rightarrow aCO_2 + bCO + cCH_3OH + dH_2 + eH_2O + fO_2 + gN_2 \tag{4.53}$$

4.6 Overall Efficiencies

The overall energetic efficiency of the system 1 can be expressed as

$$\eta_{ov,1} = \frac{\dot{W}_{net} + \dot{Q}_{cool,net} + \dot{Q}_{heat,net} + \dot{Q}_{hw,net} + \dot{m}_{NH3}LHV_{NH3} + \dot{m}_{H2}LHV_{H2} + + \dot{m}_{CH4}LHV_{CH4}}{(\dot{m}_{bio}LHV_{bio} + \dot{m}_{AM}LHV_{AM} + \dot{m}_{FW}LHV_{FW})} \tag{4.54}$$

The overall energy efficiency of the system 2 can be written as

$$\eta_{ov,2} = \frac{\dot{W}_{net}+\dot{Q}_{cool,net}+\dot{Q}_{heat,net}+\dot{Q}_{hw,net}+\dot{m}_{H2}LHV_{H2}+\dot{m}_{NH3}LHV_{NH3}+\dot{m}_{CH4}LHV_{CH4}}{(\dot{m}_{bio}LHV_{bio}+\dot{m}_{AM}LHV_{AM})} \quad (4.55)$$

The overall energy efficiency of the system 3 can be written as

$$\eta_{ov,3} = \frac{\dot{W}_{net}+\dot{Q}_{cool,net}+\dot{Q}_{heat,net}+\dot{Q}_{hw,net}+\dot{m}_{H2}LHV_{H2}+\dot{m}_{NH3}LHV_{NH3}+\dot{m}_{CH4}LHV_{CH4}}{(\dot{m}_{bio}LHV_{bio}+\dot{m}_{FW}LHV_{FW}+\dot{m}_{heavy\,oil}LHV_{heavy\,oil})} \quad (4.56)$$

The cold gas exergy efficiency of the gasifier can be found as

$$\psi_{cg} = \frac{\dot{m}_{prodg}HHV_{prodg}}{\dot{m}_{drybio}HHV_{drybio}} \quad (4.57)$$

The exergy efficiency of any component at state "i" can be written as

$$\psi_i = 1 - \frac{(\dot{E}x_{dest})_i}{(\dot{E}_{in})_i} \quad (4.58)$$

The overall exergy efficiency of the system 1 can be expressed as

$$\psi_{ov,1} = \frac{\dot{W}_{net}+\left|\dot{Q}_{cool,net}\left(1-\frac{T_0}{T_{cool}}\right)\right|+\dot{Q}_{heat,net}\left(1-\frac{T_0}{T_{heat}}\right)+\dot{Q}_{hw,net}\left(1-\frac{T_0}{T_{hw}}\right)++\dot{m}_{NH3}HHV_{NH3}+\dot{m}_{H2}HHV_{H2}+\dot{m}_{CH4}HHV_{CH4}}{(\dot{m}_{biomass}ex_{ch,bio}+\dot{m}_{AM}ex_{ch,AM}+\dot{m}_{FW}ex_{ch,FW})} \quad (4.59)$$

The overall exergy efficiency of the system 2 can be written as

$$\psi_{ov,2} = \frac{\dot{W}_{net}+\left|\dot{Q}_{cool,net}\left(1-\frac{T_0}{T_{cool}}\right)\right|+\dot{Q}_{heat,net}\left(1-\frac{T_0}{T_{heat}}\right)+\dot{Q}_{hw,net}\left(1-\frac{T_0}{T_{hw}}\right)+\dot{m}_{H2}HHV_{H2}+\dot{m}_{NH3}HHV_{NH3}+\dot{m}_{CH4}HHV_{CH4}}{(\dot{m}_{biomass}ex_{ch,bio}+\dot{m}_{AM}ex_{ch,AM})} \quad (4.60)$$

The overall exergy efficiency of the system 3 can be found as

$$\psi_{ov,3} = \frac{\dot{W}_{net}+\left|\dot{Q}_{cool,net}\left(1-\frac{T_0}{T_{cool}}\right)\right|+\dot{Q}_{heat,net}\left(1-\frac{T_0}{T_{heat}}\right)+\dot{Q}_{hw,net}\left(1-\frac{T_0}{T_{hw}}\right)+\dot{m}_{NH3}HHV_{NH3}+\dot{m}_{H2}HHV_{H2}+\dot{m}_{CH4}HHV_{CH4}}{(\dot{m}_{biomass}ex_{ch,bio}+\dot{m}_{heavy\,oil}ex_{heavy\,oil}+\dot{m}_{FW}ex_{ch,FW})} \quad (4.61)$$

4.7 Sustainability Assessment

Exergy analysis determines the quality of a thermodynamics process and gives an indicator and a potential tool for sustainability achievement. The enhancement of the exergetic performance and efficiency of a system results in a decrease in its environmental impacts and the destructed exergy.

The ecology of the environment is affected by the release of solid, liquid and gas residuals directly to the environment as a result of thermal processes. This concern raises the importance and need of exergy analysis and enhancement in the energy efficiency of the systems. Thermodynamic analyses can be used to calculate the amount of the greenhouse gas emission from a thermal process. Then, the environmental performance of this system can be compared with the similar conventional system on the basis of these results. The rate of fuel consumption is the main driving factor of environmental impact. The ratio of the exergy destruction of a system to the inlet exergy in the fuel characterizes the efficiency of fuel consumption

$$D_{\mathrm{p}} = \frac{\dot{E}x_{\mathrm{d}}}{\dot{E}x_{\mathrm{in}}} \tag{4.62}$$

The sustainability index is another parameter and indicator which illustrates the effectiveness of a process in terms of exergy input and the rate of exergy destruction in the system. Therefore, there are less environmental impacts if the sustainability index, is high as it lowers the exergy destruction in the process. The Sustainability index of a fuel resource can be define as the inverse of the depletion factor

$$SI = \frac{1}{D_{\mathrm{p}}} \tag{4.63}$$

The total cost rate of this newly proposed multigeneration system includes the penalty cost rate of greenhouse gas emissions, operational cost rate and the rate of capital investment and maintenance costs of each system component. Hence, the cost rate of the multigeneration system can be found as

$$\dot{C}_{total} = \dot{C}_{environmental} + \dot{C}_{operational} + \sum \dot{C}_{CI\,\&\,M} \tag{4.64}$$

where $\dot{C}_{CI\,\&\,M}$ represents the rate of capital investment and maintenance costs for each system component. The environmental cost can be calculated as

$$\dot{C}_{environmental} = \dot{m}_{CO2} C_{CO2} \quad (4.65)$$

where $\dot{m}_{CO2}$ and C_{CO2} denotes amount of carbon dioxide emissions and cost to avoid CO_2, respectively. The cost to avoid CO_2 emissions in this study is taken as \$87/ton [118]. The operational cost can be defined as

$$\dot{C}_{operational} = \dot{C}_{fuel} = \dot{m}_{bio} C_{bio} + \dot{m}_{AM} C_{AM} + \dot{m}_{FW} C_{FW} + \dot{m}_{HO} C_{HO} \quad (4.66)$$

where C_{bio} is the cost of biomass and the subscripts AM, FW, HO represent animal manure, food waste and heavy oil, respectively.

The capital investment and maintenance cost rate for each component can be calculated as

$$\dot{C}_{CI\ \&\ M} = \frac{1.06 \times C_{CI\ \&\ M}}{N \times 3600} CRF \quad (4.67)$$

where N represents the number of hours of operation of the component annually and $C_{CI\ \&\ M}$ is the capital cost of the components. The capital investment cost function of major components is tabulated in Table 3. The capital recovery factor (CRF) can be found as [119]

$$CRF = \frac{i_r (1+i_r)^n}{(1+i_r)^{n-1}} \quad (4.68)$$

where n and i_r denote the life of system and annual based interest rate which are taken as 15 years and 14% [120].

4.8 Simulation Study

Three new gasification models of the mixed feedstock composed of biomass, animal manure, food waste and heavy oil are developed using Advanced System for Process Engineering (ASPEN) (Plus). This software is equipped with huge information and strong database of reaction kinetics, chemical reactions and thermodynamic properties. The mass and energy balanced equations are used for calculation purpose by considering the systems in steady state. During the oil crisis in 1970, ASPEN (Plus) software was introduced at Massachusetts Institute of Technology (MIT) to optimize the utilization of energy resources. The political issues between the oil producing countries and western world caused the shortage of oil and gas so the researchers started looking for the alternative energy resources instead of oil and developed ASPEN (Plus) software. The processing time of ASPEN (Plus) software is very short and variety of input feedstocks can be analyzed quickly with less cost. The process engineers can simulate a process and investigate the

impact of various operating conditions using a built-in tool sensitivity analyses in ASPEN (Plus). The optimization and sensitivity tools allow user to find the optimal conditions in no time. It is possible to gain more understanding about the process reactions by studying a wide range of developments. The significant developments and improvements are made in ASPEN (Plus) software during the last decade and now it can be used in a wide range of applications.

In the Aspen physical property system, each property method is based on either the equation-of-state method or the activity coefficient method for phase equilibrium calculations. The phase equilibrium method determines how other thermodynamic properties, such as enthalpies and molar volumes, are calculated. All properties can be derived from the equation-of-state method. The properties of liquid are determined from summation of the pure component properties. Therefore, a mixing term or an excess term is added to the existing property method.

Now, the chemical process industries, and oil and gas producing companies depend heavily on the Aspen (Plus). The presence of many kinds of reactions makes gasification process complex. These reactions include exothermic, endothermic, heterogeneous, homogeneous and partial oxidation etc. Gibbs free energy minimization approach is used to model all three proposed systems. Hence, gasification reactions follow the equilibrium constants required input data of the model is reduced. Simplified overall model yields better results with less uncertainties and inaccuracies associated with the gasification reactions [121]. The Gibbs free energy minimization can be simply represented as in Fig. 4.1.

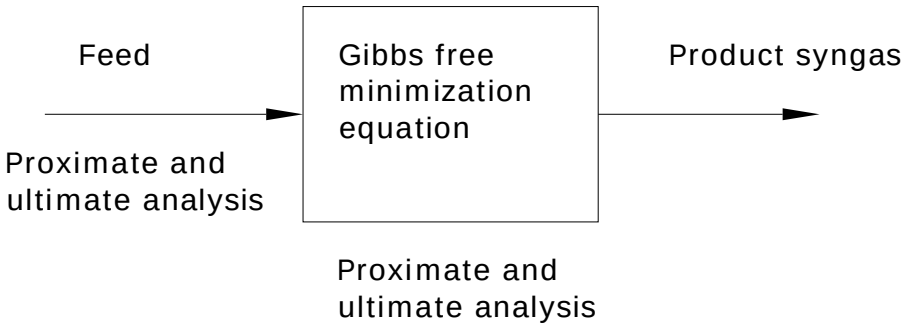

Figure 4.1 A schematic of Gibbs free minimization approach (Source: [115])

4.8.1 Simulation Procedure for System 1

The ASPEN (Plus) software is used to model the mixed feedstock gasification in which the reactants (biomass, food waste, animal manure and steam) are converted to syngas (H_2, CO, CO_2, H_2O, CH_4, H_2S) and impurities as represented in Fig. 4.1. The input parameters in the feedstock streams of biomass, animal manure, food waste and steam are entered as 18kg/s and 18 kg/s, 18 kg/s and 54 kg/s, respectively. An entrained flow gasifier is used in this study because of the reason that the biomass and heavy oil are stable substances which makes them unsuitable to be employed in a fixed (Moving) bed gasifier. A highly reactive feedstock is required for the fixed bed gasifier to sustain the permeability of the bed.

The fluidized bed gasifiers operate at a relatively low temperature (537°C to 982°C) to prevent the ash accumulation and maintain fluidization of the particles in the bed. In addition to this, high temperature range in entrained flow gasifiers increases the carbon conversion of the feedstock with greater efficiency. Despite the high temperature ranges, short residence time between the range 0.5 to 5 seconds in the gasifier yields a good conversion of the feedstock to the syngas with increased efficiency [116, 117]. Particles size, volatile, bulk density, moisture content and energy are the additional factors need to be considered while selecting a gasifier.

The chemical composition of the biomass used in Aspen (Plus) modelling of the syngas production model is based on the experimental study conducted by Zanzi et al. [91] as tabulated in Table 4.1.

Table 4.1 Elemental analysis of Olive waste and wood (Birch) used in Aspen (Plus) modelling

Raw Material	Pyrolysis temperature °C	Mass fraction (%)				CV MJ/kg	Ash	Moisture (%)
		C	H	N	O			
Olive waste	800	71.6	3.9	0.9	23.6	26.03	9.4	4.1
Wood	800	90.0	1.8	0.2	8.0	31.84	4.0	2.5

Source: [91]

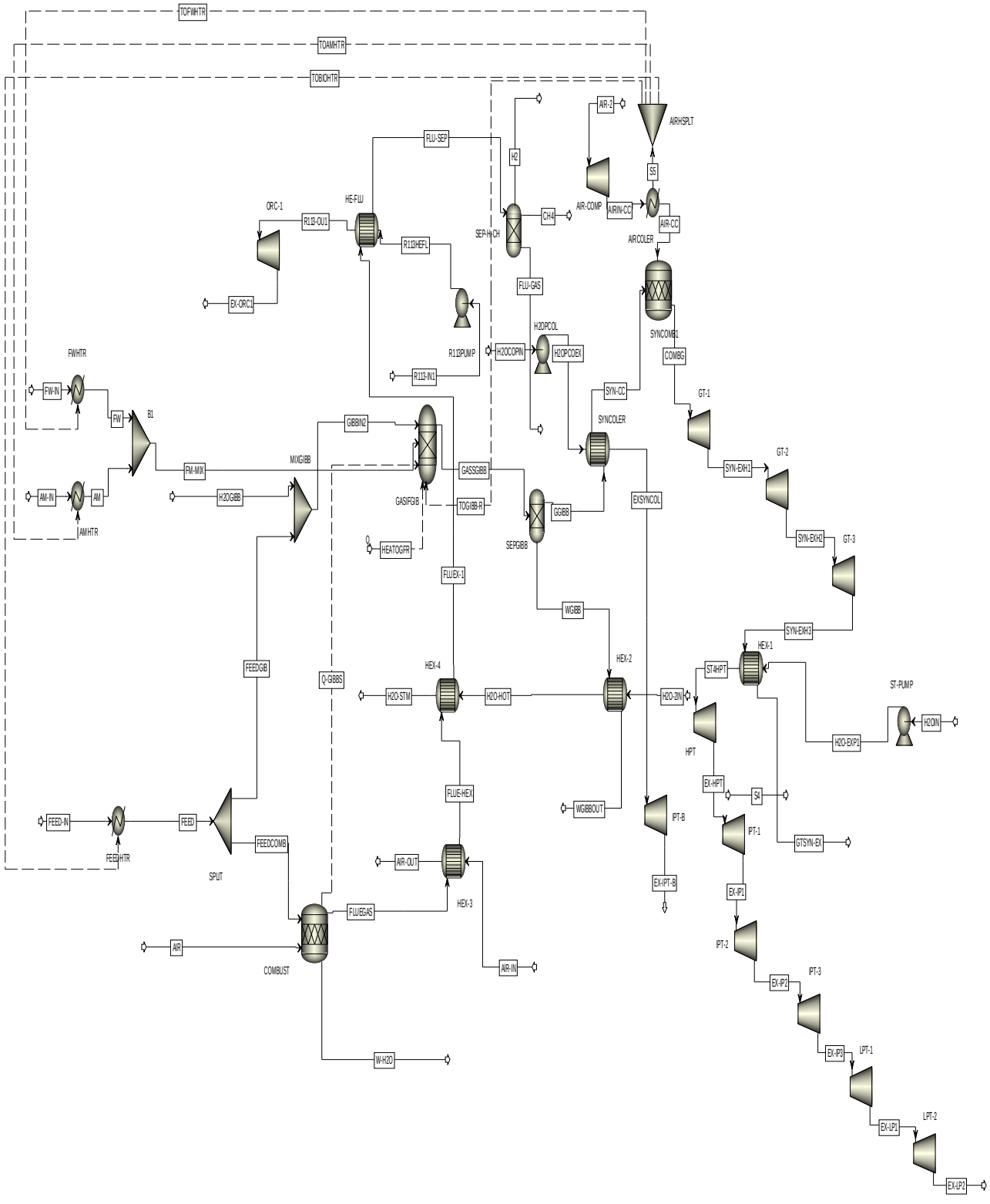

Figure 4.2 Aspen (Plus) model of IGCC multigeneration system for residential community application

The mass fraction of the gas yield as a result of rapid pyrolysis of wood and olive is adopted from Zanzi et al. [91] and tabulated in Table 4.2.

Table 4.2 Mass fraction of Olive waste and wood (Birch) used in Aspen (Plus) modelling

Gas	**Wood (Birch)**		**Olive waste**	
	Mixed (mass fraction)	*CISolid (mass fraction)*	*Mixed (mass fraction)*	*CISolid (mass fraction)*
H_2	0.0125	0	0.0157	0
CO	0.5307	0	0.4962	0
CO_2	0.1365	0	0.2023	0
CH_4	0.0969	0	0.1095	0
C	0	1	0	1
C_3H_6	0.0725	0	0.0483	0
H_2O	0.1509	0	0.128	0

Source [91]

The input parameter used in the syngas production model are tabulated in Table 4.3. The air is injected at 450°C to the combustor.

Table 4.3 Parameters used in Aspen (Plus) simulation

Parameters	**Wood (Birch)**	**Olive waste**
Steam flow rate (kg/hr) @470ºC	112	112
Feed flow rate (kg/hr) @800ºC	112	112
Combustion temperature (ºC)	905	905
Reactor pressure (bar)|	1	1
Air flow rate (kg/hr) @450ºC	31	31

Source: [36]

Chemical composition of the food waste is taken from Rienhart [94] and tabulated in Table 4.4. It is important to note that amount of hydrogen in food waste is more than the amount of hydrogen present on biomass and animal manure.

Table 4.4 Chemical composition of the food waste

Element	**Percent (%)**
Carbon, C	48
Hydrogen, H	6.4
Oxygen, O	37.6
Nitrogen, N	2.6
Sulfur	0.4
Ash	5

Source: [94]

The chemical composition animal manure is taken from Haugen et al. [95] as tabulated in Table 4.5. It can be seen that animal manure has less percentage of hydrogen as compared to the food waste whereas, the amount of carbon is significantly low.

Table 4.5 Animal manure composition used in Aspen (Plus) Modelling

Components	**Percent (%)**
Proximate analyses (wt %)	64.97
Volatile matter	16.07
Fixed carbon	13.46
Ash	21.57
Moisture	27.4
Ultimate analysis (wt %)	
Carbon, C	37.05
Hydrogen, H	5.06
Nitrogen, N	3.66
Sulfur, S	0.45
Chlorine, Cl -	0.97
Ash	21.37
Lower heating value, LHV (MJ/kg)	14.79

Source: [95]

Extra heavy oil (Orimulsion) is selected due to the availability of its technical data. Moreover, chemical composition and physical properties of Orimulsion are almost same as of heavy oil. The physical properties and chemical composition of (Orimulsion) are tabulated in Table 4.6.

It is important to note that the amount of carbon is significantly high as compared to the other elements in heavy oil. The concentration of hydrogen is also high that is why the low calorific and high calorific values of heavy oil are the highest as compared to the other type of waste used in case studies.

The heterogeneous and homogeneous reactions taking place in the stoichiometric reactor (R Stoic) are tabulated in Table 4.7. In reaction number 1 to 3 carbon reacts with hydrogen water and carbon dioxide to produce carbon monoxide, hydrogen and methane. Methane and carbon monoxide react with water and are converted to carbon monoxide and hydrogen in reactions 4 and 5.

Table 4.6 Properties of (Orimulsion)

Physical Properties			
Flash point		>90 ^{0}C	
Pour point		<3–6 ^{0}C	
Density		1.0113 g/ml @ 15 ^{0}C	
Viscosity		560 mPa.s @ 30 ^{0}C	
Chemical Properties			
Proximate analysis		**Ultimate analysis (Dry)**	
Water content	28.8 wt.%	Carbon	84.28 wt.%
Ash Residual carbon	0.18 wt.% 12.84 wt.%	Hydrogen Oxygen	10.33 wt.% 0.55 wt.%
Total-sulfur	2.81 wt.%	Nitrogen	0.64 wt.%
HHV	29.76 wt.%	Sulfur	3.95 wt.%
		Ash	0.25 wt.%
		Cl	70 mg/kg
		F	<10 mg/kg
		Na	20 mg/kg
		K	4.1mg/kg

Source: [47]

Table 4.7 Chemical reactions taking place in the gasifier

Heterogeneous Reactions	1	$C+2H_2$	$\leftrightarrow$ CH_4
	2	$C+H_2O$	$\leftrightarrow$ $CO + H_2$
	3	$C+CO_2$	$\leftrightarrow$ $2CO$
Homogeneous Reactions	4	CH_4+H_2O	$\leftrightarrow$ $CO + 3H_2$
	5	$CO + H_2O$	$\leftrightarrow$ $CO_2 + H_2$

Source: [93]

The reaction kinetics for the major conversion rates and reaction rate expression in the biomass combustor (RStoic) are adopted from the published set of chemical reactions by Xie et al. [124] and Umeki et al. [125]. These set of reactions defines the significant conversion rates in the gasifier as represented in Table 4.8.

Table 4.8 Reactions kinetics for the major conversion rates in a gasifier reactor

Reactions	**Reaction rate**
Water-gas reaction: $C(s) + H_2O \rightarrow CO + H_2$ $CO + H_2 \rightarrow C(s) + H_2$	$r = 1{,}272 * m_s * T * \exp\left(\frac{-22645}{T}\right)[H_2O]$ $r = 1{,}044 * 10^{-4} * m_s * T^2 * \exp\left(\frac{-6319}{T} - 17{,}29\right)[H_2][CO]$
Boudouard reaction: $C(s) + CO_2 \rightarrow 2\ CO$ $2\ CO \rightarrow C(s) + CO_2$	$r = 1{,}272 * m_s * T * \exp\left(\frac{-22645}{T}\right)[CO_2]$ $r = 1{,}044 * 10^{-4} * m_s * T^2 * \exp\left(\frac{-2363}{T} - 20{,}92\right)[CO]^2$
Methanation reaction: $0.5C(s) + H_2 \rightarrow 0.5\ CH_4$ $0.5\ CH_4 \rightarrow 0.5C(s) + H_2$	$r = 1{,}368 * 10^{-3} * m_s * T * \exp\left(\frac{-8078}{T} - 7{,}087\right)[H_2]$ $r = 0{,}151 * m_s * T^{0,5} * \exp\left(\frac{-13578}{T} - 0{,}372\right)[CH_4]^{0,5}$
Water gas shift reaction: $CO + H_2O \rightarrow CO_2 + H_2$ $CO_2 + H_2 \rightarrow CO + H_2O$	$r = 7{,}68 * 10^{10} * T * \exp\left(\frac{-36640}{T}\right)[CO]^{0,5}[H_2O]$ $r = 6{,}4 * 10^{9} * T * \exp\left(\frac{-39260}{T}\right)[H_2]^{0,5}[CO_2]$
Methane-reforming: $CH_4 + H_2O \rightarrow CO + 3H_2$ $CO + 3H_2 \rightarrow CH_4 + H_2O$	$r = 3{,}1005 * \exp\left(\frac{-15000}{T}\right)[CH_4][H_2O]$ $r = 3{,}556 * 10^{-3} * T * \exp\left(\frac{-15000}{T}\right)[CO][H_2]^2$

Sources: [118, 119]

The mass fraction yield of char, tar and moisture as a result of rapid pyrolysis of wood (Birch) and waste olive is documented in Table 4.9. It can be seen the gas yield in case of wood (Birch) feedstock is more as compared to the olive waste feedstock whereas, char yield is high in case of olive waste pyrolysis. The yield of tar and is almost the same in both cases while moisture yield is higher in case of olive waste.

Table 4.9 Yield in the rapid pyrolysis of wood (Birch) and waste olive at 800ºC

Mass fraction (%)	**Wood (Birch)**	**Olive waste**
Gas yield	77.7	51.8
Char yield	7.2	27.6
Tar yield	1.1	0.9
Moisture	14	19.7

Source: [91]

The volume fraction of the resulting gaseous product composition is tabulated in Table 4.10. The comparison the significant fraction of the gases reveals that the volume

fraction of carbon monoxide and ethylene and benzene is high in case of wood (Birch) gasification whereas, yield of methane, hydrogen and carbon dioxide is higher against the gasification of the olive waste feedstock.

Table 4.10 Gaseous product composition resulting a rapid pyrolysis at high temperature of 800 ºC

Gas composition (Vol %)	**Wood (Birch)**	**Olive waste**
CH_4	16.2	18.3
H_2	16.8	21.1
CO	50.7	47.4
CO_2	8.3	12.3
C_2H_6	0.3	0.2
C_2H_4, C_2H_2	6.2	0.5
C_6H_6	1.2	0.2
Other	0.3	-

Source: [91]

The assumptions made for the model and analysis studies are listed as follows:

- The reactants are kept in the gasifier until the chemical equilibrium is attained.
- The carbon in the feedstock is fully gasified.
- The formation of char is neglected.
- The gasifier is considered to be adiabatic.
- The feedstock has chemical formula $CH_xO_yN_z$.

The global gasification chemical reaction can be written as [50]

$$CH_XO_YNz + {}_WH_2O_{(liq)} + SH2O_{(vap)} + m(O_2+3.76N_2) = n_{H2}H_2 + n_{CO}CO + n_{CO2}CO_2 + n_{H2O}H_2O + n_{CH4}CH_4 + (z/2+3.76m)N_2 \quad (5.39)$$

A stream of steam is mixed with the feedstock and linked to the RGIBBS gasifier. The mass fraction basis is selected in the composition window. The input specifications of the steam stream are selected as 100% water at 743 K with a mass flow rate of 54 kg/s for the both system 1 and system 2 whereas, 70 kg/s for system 3 as shown in the Fig 4.2. The sensitivity analysis using built in tool in ASPEN (Plus) simulation is performed for the mass flow rate of steam from 50 to 100 kg/s.

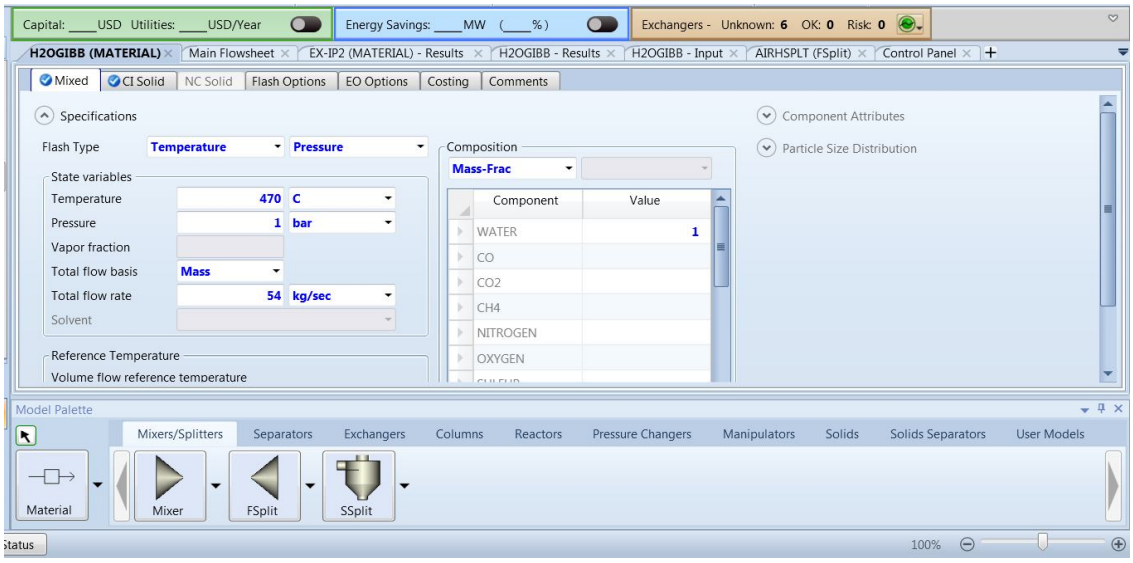

Figure 4.3 Screenshot of Aspen (Plus) input parameters of the steam in the proposed system 1

The stoichiometric reactor (RStoic) is chosen for the combustion of biomass to supply the heat stream to the gasifier. Input parameter include temperature 905°C and pressure 1 bar as shown in Fig. 4.3. Generate combustion reaction option is selected and carbon is fully converted to methane, carbon dioxide and carbon monoxide.

In addition to above, the valid phase selected in this window is Liquid- Vapor- Free Water. The flue gases exiting this combustor are used to heat water and run organic Rankine cycle 1.

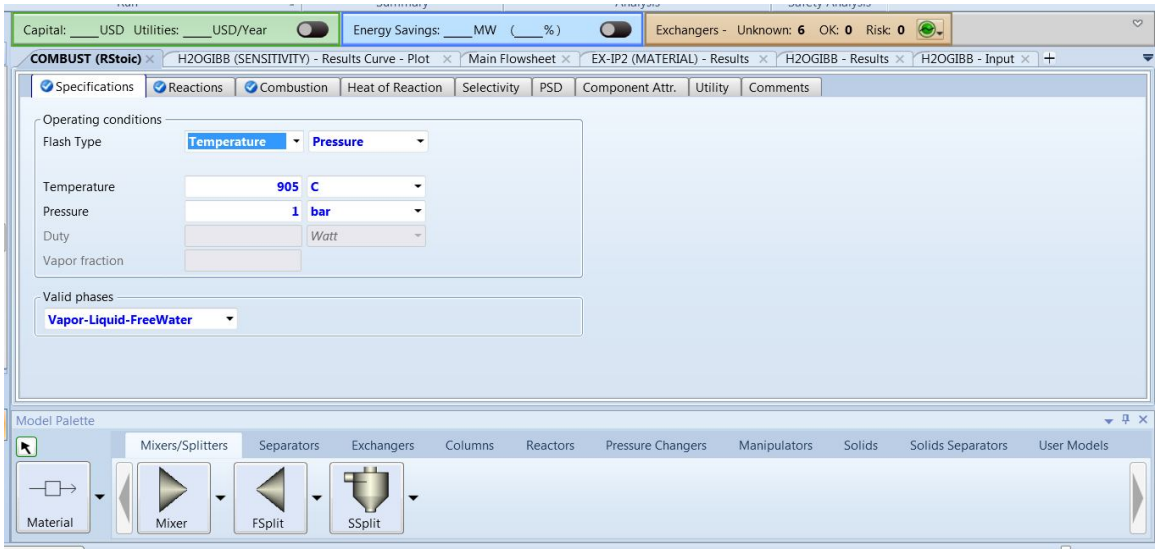

Figure 4.4 Aspen (Plus) input parameters in the combustion reactor in the proposed system 1

The Gibbs reactor is selected for the gasification process. Stream of steam and all mixed feedstock are supplied to reactor. Restricted chemical equilibrium- specify temperature approach or reaction is selected as calculation option in this gasifier. The pressure of the Gibbs reactor is set to 8 bar as depicted in Fig 4.4.

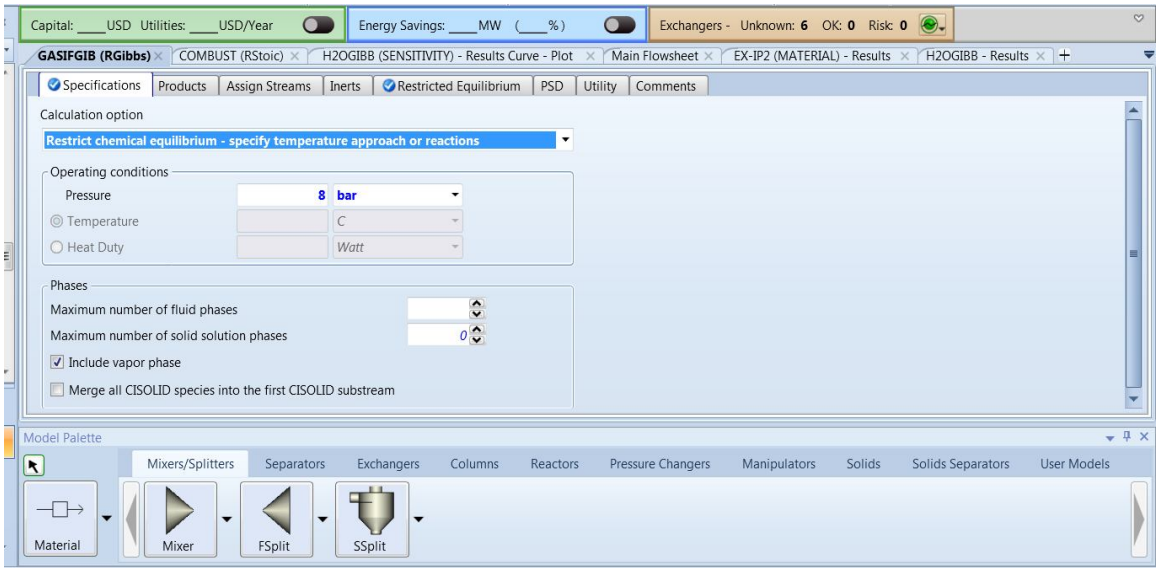

Figure 4.5 Screenshot of Aspen (Plus) input parameters in the gasifier in the proposed system 1

The stoichiometric reactor (RStoic) is chosen for the combustion of syngas to run the Gas turbine and then steam turbine using the exhaust of the Gas turbine. Input parameter of the fractional conversion are represented in Fig. 4.5.

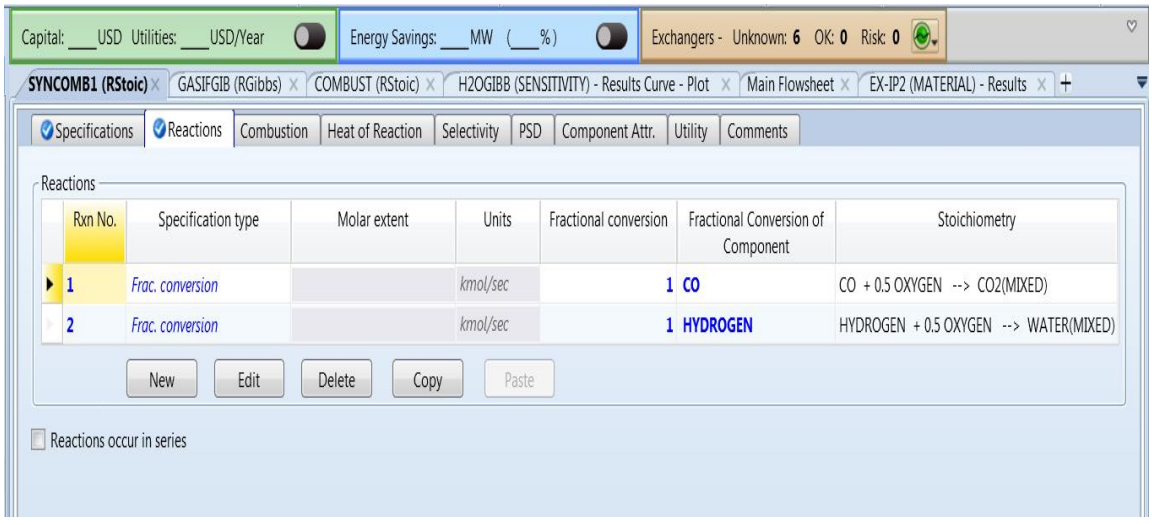

Figure 4.6 Screenshot of Aspen (Plus) input parameters in the gasifier in the proposed system 1

The results of Aspen (Plus) are then fed in Engineering Equation Solver (EES) to calculate the exergy destruction in each sub-system and the overall system. In addition to this, energy and exergy efficiencies of the major sub-units and overall system are also calculated using EES.

4.8.2 Simulation Procedure System 2

The ASPEN (PLUS) software is used to model the mixed feedstock gasification in which the reactants (biomass, animal manure and steam) are converted to syngas (H_2, CO, CO_2, H_2O, CH_4, H_2S) and impurities as shown in Fig. 4.7. The input parameters in the feedstock streams of biomass, animal manure and steam are entered as 18 kg/s and 36 kg/s, and 54 kg/s, respectively. An entrained flow gasifier is used in this study because of the reason that the biomass and heavy oil are stable substances which makes them unsuitable to be employed in a fixed (Moving) bed gasifier. A highly reactive feedstock is required for the fixed bed gasifier to sustain the permeability of the bed. The fluidized bed gasifiers operate at a relatively low temperature (810 K to 1255 K) to prevent the ash accumulation and maintain fluidization of the particles in the bed. In addition to this, high temperature range in entrained flow gasifiers increases the carbon conversion of the feedstock with greater efficiency. Despite the high temperature ranges, short residence time between the range 0.5 to 5 seconds in the gasifier yields a good conversion of the feedstock to the syngas with increased efficiency [116, 117].

Particles size, volatile, bulk density, moisture content and energy are the additional factors need to be considered while selecting a gasifier. The presence of many kinds of reactions makes gasification process complex. These reactions include exothermic, endothermic, heterogeneous, homogeneous and partial oxidation etc.

Gibbs free energy minimization approach is used to model all three proposed systems. Hence, gasification reactions follow the equilibrium constants required input data of the model is reduced. Simplified overall model yields better results with less uncertainties and inaccuracies associated with the gasification reactions [121].

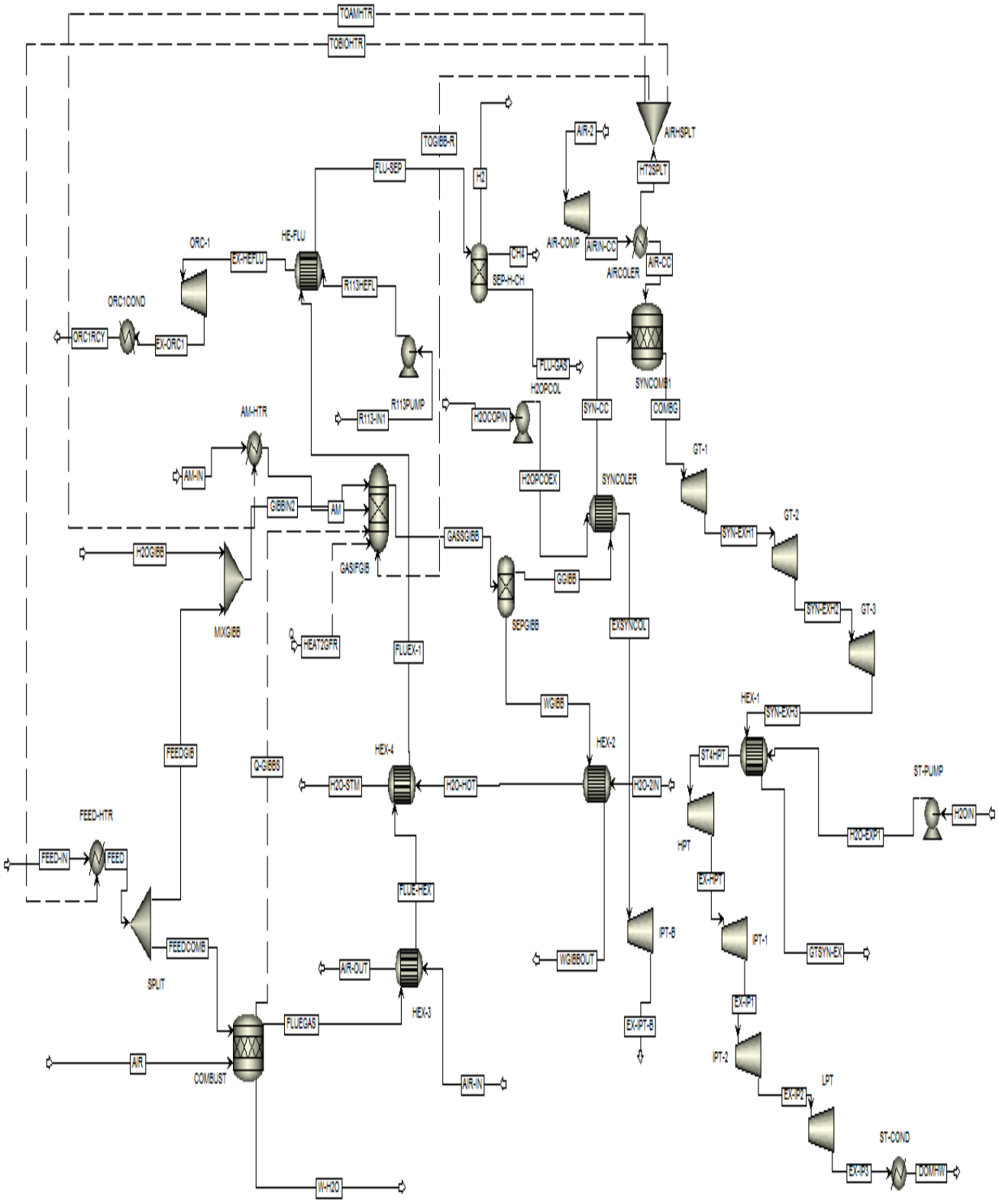

Figure 4.7 Aspen (Plus) process flow sheet of IGCC multigeneration system for food industry applications

The chemical composition of the biomass used in Aspen (Plus) modelling of the syngas production model is based on the experimental study conducted by Zanzi et al. [91] as tabulated in Table 4.1. A stream of steam is mixed with the feedstock and linked to the RGIBBS gasifier. The input specifications of the steam stream are selected as 100% water at 743 K. The sensitivity analysis using built in tool in ASPEN (Plus) simulation is performed for the variations in the mass flow rate of steam from 50 kg/s to 100 kg/s.

The stoichiometric reactor (RStoic) is chosen for the combustion of biomass to supply the heat stream to the gasifier. Input parameter include temperature 905°C and pressure 1 bar. Generate combustion reaction option is selected and carbon is fully converted to methane, carbon dioxide and carbon monoxide.

Gibbs reactor is selected for the gasification process. Stream of steam and all mixed feedstock are supplied to reactor. Restricted chemical equilibrium- specify temperature approach or reaction is selected as calculation option in this gasifier. The pressure of the Gibbs reactor is set to 8 bar.

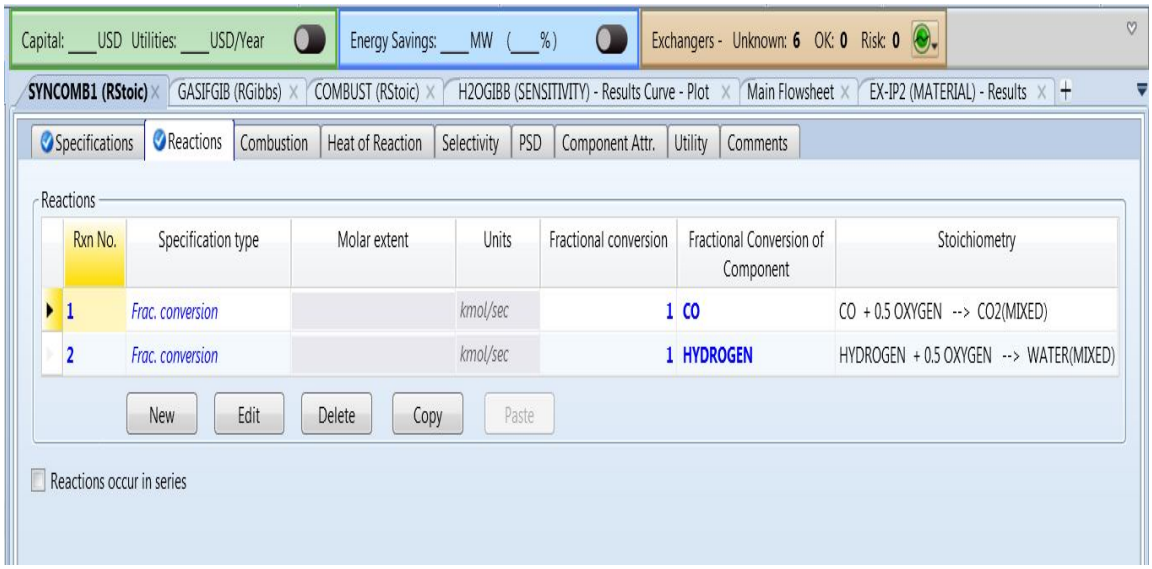

Figure 4.8 Screenshot of Aspen (Plus) input parameters in the gasifier in the proposed system 2

The stoichiometric reactor (RStoic) is chosen for the combustion of syngas to run the Gas turbine and then steam turbine using the exhaust of the Gas turbine. Input parameters of this reactor include 100% conversion of carbon monoxide hydrogen as depicted in Fig. 4.8. The results of Aspen (Plus) are then fed in Engineering Equation

Solver (EES) to calculate the exergy destruction in each sub-system and the overall system. In addition to this, energy and exergy efficiencies of the major sub-units and overall system are also calculated using EES.

4.8.3 Simulation Procedure System 3

The ASPEN (Plus) software is used to model the mixed feedstock gasification in which the reactants (biomass, food waste, animal manure and steam) are converted to syngas (H_2, CO, CO_2, H_2O, CH_4, H_2S) and impurities as depicted in Fig. 4.9. The input parameters in the feedstock streams of biomass, food waste and heavy oil are entered as 12kg/s and 12 kg/s, 11 kg/s and 70kg/s, respectively. An entrained flow gasifier is used in this study because of the reason that the biomass and heavy oil are stable substances which makes them unsuitable to be employed in a fixed (Moving) bed gasifier. A highly reactive feedstock is required for the fixed bed gasifier to sustain the permeability of the bed. The fluidized bed gasifiers operate at a relatively low temperature (810 K to 1255 K) to prevent the ash accumulation and maintain fluidization of the particles in the bed. In addition to this, high temperature range in entrained flow gasifiers increases the carbon conversion of the feedstock with greater efficiency. Despite the high temperature ranges, short residence time between the range 0.5 to 5 seconds in the gasifier yields a good conversion of the feedstock to the syngas with increased efficiency [116, 117]. Particles size, volatile, bulk density, moisture content and energy are the additional factors need to be considered while selecting a gasifier.

The presence of many kinds of reactions makes gasification process complex. These reactions include exothermic, endothermic, heterogeneous, homogeneous and partial oxidation etc. Gibbs free energy minimization approach is used to model all three proposed systems. Hence, gasification reactions follow the equilibrium constants required input data of the model is reduced. Simplified overall model yields better results with less uncertainties and inaccuracies associated with the gasification reactions [121].

The chemical composition of the biomass used in Aspen (Plus) modelling of the syngas production model is based on the experimental study conducted by Zanzi et al. [91] as tabulated in Table 4.1.

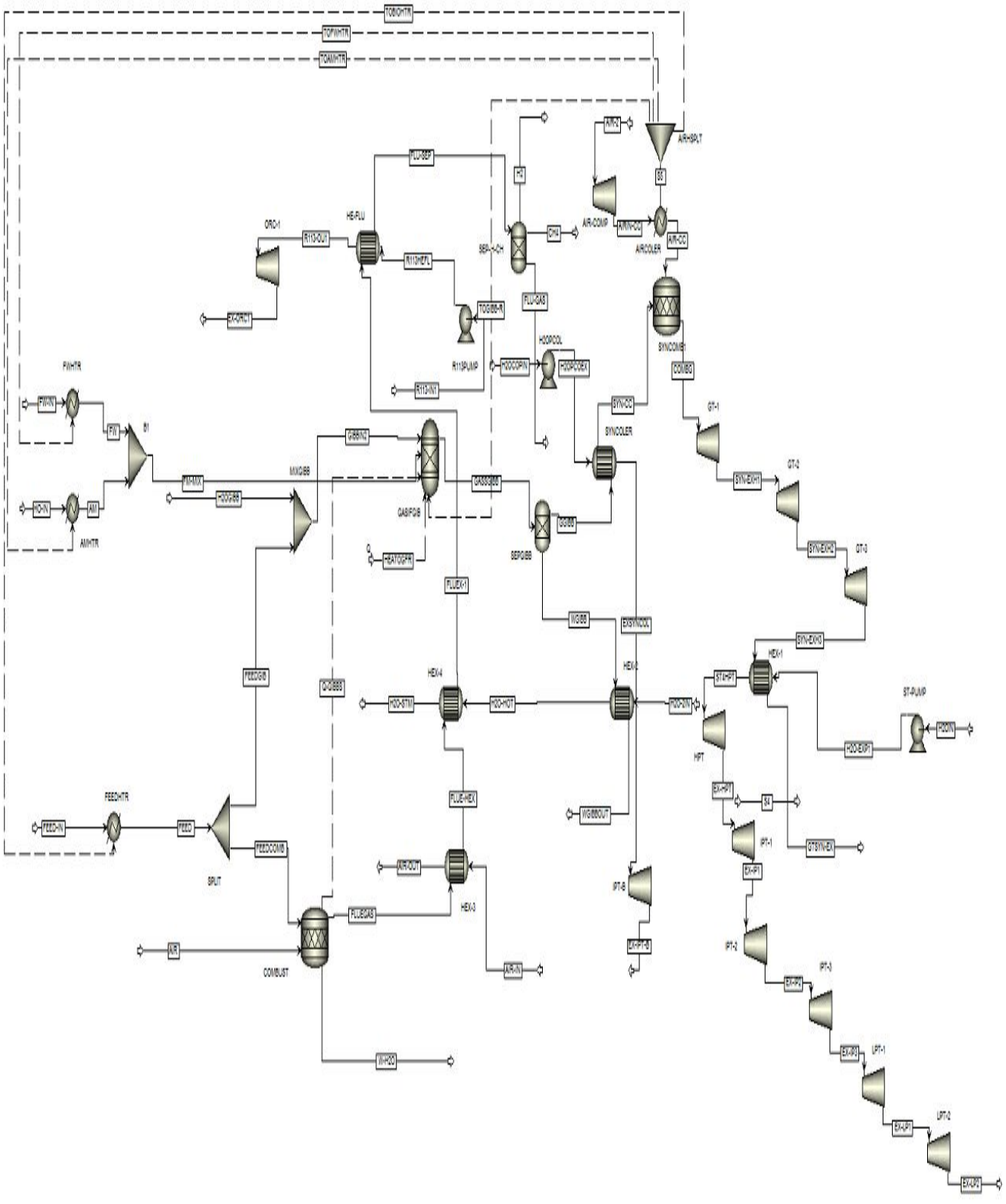

Figure 4.9 Aspen (Plus) process flow sheet of IGCC multigeneration system for food refinery application

A stream of steam is mixed with the feedstock and linked to the RGIBBS gasifier. The input specifications of the steam stream are selected as 100% water at 743 K for system 3 as shown in the Fig 4.10. The sensitivity analysis using built in tool in ASPEN (Plus) simulation is performed for the variations in the mass flow rate of steam from 50 kg/s to 100 kg/s.

The stoichiometric reactor (RStoic) is chosen for the combustion of biomass to supply the heat stream to the gasifier. Input parameter include temperature 905°C and pressure 1 bar. Generate combustion reaction option is selected and carbon is fully converted to methane, carbon dioxide and carbon monoxide.

The Gibbs reactor is selected for the gasification process. Stream of steam and all mixed feedstock are supplied to reactor. Restricted chemical equilibrium- specify temperature approach or reaction is selected as calculation option in this gasifier. The pressure of the Gibbs reactor is set to 8 bar.

The stoichiometric reactor (RStoic) is chosen for the combustion of syngas to run the Gas turbine and then steam turbine using the exhaust of the Gas turbine. Input parameters of the fractional conversion include 100% conversion of carbon monoxide hydrogen as represented in Fig. 4.10.

The results of Aspen (Plus) are then fed in Engineering Equation Solver (EES) to calculate the exergy destruction in each sub-system and the overall system. In addition to this, energy and exergy efficiencies of the major sub-units and overall system are also calculated using EES.

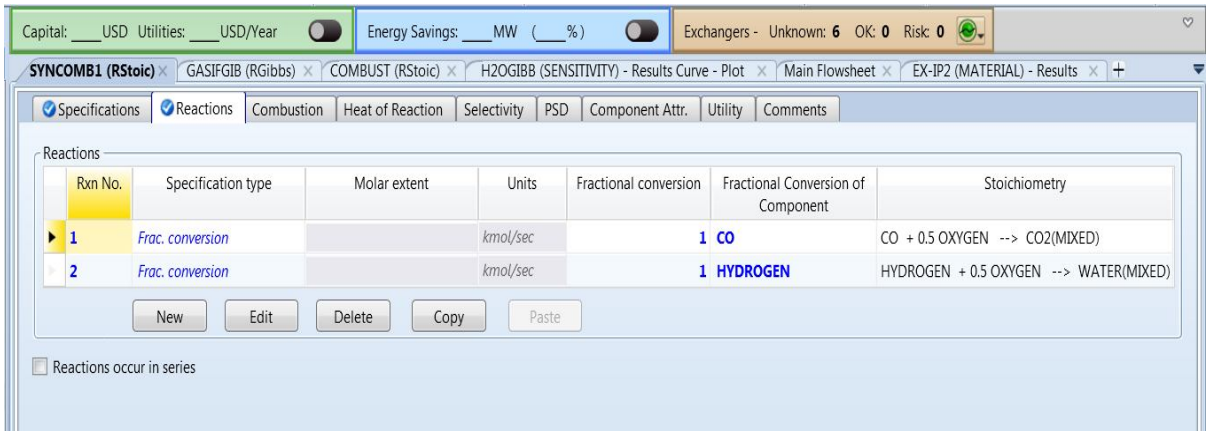

Figure 4.10 Screenshot of Aspen (Plus) input parameters in the gasifier in the proposed system 3

4.9 Optimization Study

Three objectives function based optimization is performed for all proposed systems. The minimization of the costs associated with exergy flows, minimization of CO_2 emissions and maximization of exergy efficiency are the main goals of performing optimization. The objective of such an optimization approach is to find the equipment type, size, configurations, and the ranges of operating pressure and temperature of processes. First of all, system boundary is defined and effective parameters are included. The complex systems can be divided into sub-systems for convenience. The next step is to specify the optimization criteria and define the variables which will govern the optimization. The systems are evaluated on the basis of economy, thermodynamics and environmental performance. These variables are selected on their magnitudes to affect the performance and cost effectiveness.

In addition to this, parameters with lees magnitudes are neglected. The selected variables for optimization are considered as decision variables, and should be prominent from fixed value parameters of the process. Then, a mathematical model for the analysis is selected; variables are related this model and the effects of independent variables are defined on the system performance. Major technical constraints and an optimization function are also included to the model. Some examples of typical objective functions are; minimization of exergy destruction, minimization of exergy loss or maximizing the exergy efficiency of the system.

Genetic algorithm (GA) is an approach in computer science and operations research that is used to perform optimization of complex objective function. Generally, the genetic algorithms produce good solutions to optimization and search problems by relying selected constrains. The initialization of populations of solutions is performed by genetic algorithm after defining genetic representation and fitness function. Genetic algorithm improves results through repetitive application of the inversion, crossover, mutation and selection of operators.

Mass flow rates of feed, air fuel mixture at gas turbine inlet and steam at steam turbine inlet are included in constrains. The other selected set of constrain includes; inlet temperatures at the inlet of gas turbines 1, 2 and 3. The highest limit selected for the gas turbine is 1600°C due to the material constrain of the gas turbine blades. The results of the optimization study are tabulated in Tables 6.12-6.14, respectively.

CHAPTER 5 RESULTS AND DISCUSSION

5.1 Results of Biomass Based Syngas Production System

This section includes detailed performance analysis of a syngas production system based on two types of biomass feedstock of biomass. The dead state properties of pressure and temperature for exergy analysis are assumed as P_0=1 bar and T_0=25 ºC, respectively. Aspen (Plus) simulation model is developed and sensitivity analysis is performed to compare the performance of wood (Birch)-based and olive waste-based systems as presented in Fig. 3.1. The model configuration, operating pressure and temperature for both feedstocks are kept same for the best comparative results. The performance of both models is assessed against variation in several design parameters. Simulation of each component is done with the help of a numerical solver called Aspen (Plus). The thermodynamic analyses of both models are performed with respect to the working fluid properties and reference state points as presented in Fig. 3.1.

The percentage volume fraction based yield of the syngas composition, cold gas energy efficiency (CGE), cold gas exergy efficiency (CGEX), and energy and exergy efficiencies of both feedstocks are presented in Fig. 5.1. It can be seen that the use of wood (Birch) yields more volume fraction of hydrogen and carbon monoxide whereas, the yield of methane and carbon dioxide is more in case of olive waste. In addition to this, cold gas energy efficiencies (CGE) and overall energy efficiencies of the wood (Birch)-based system and olive waste-based system are found to be 38% and 46.5%, and 36% and 45%, respectively. It is important to note that both CGE and overall energy efficiencies of the wood (Birch)-based system are more as compared to the olive waste-based system. This is because of the reason that these values are based on the lower heating values of feedstock and syngas produced, and the LHV of wood is much higher than the LHV of the olive waste whereas, there is no significant difference between the LHV's of the syngas produced by the systems running on two different feedstocks. It is also important to note that overall energy efficiencies of both feedstock are not much lower than the CGE's this is due to the fact the waste heat of the water coming out of the gasifier and the flue gases are used to produce required amount of steam and to heat up the required amount of air.

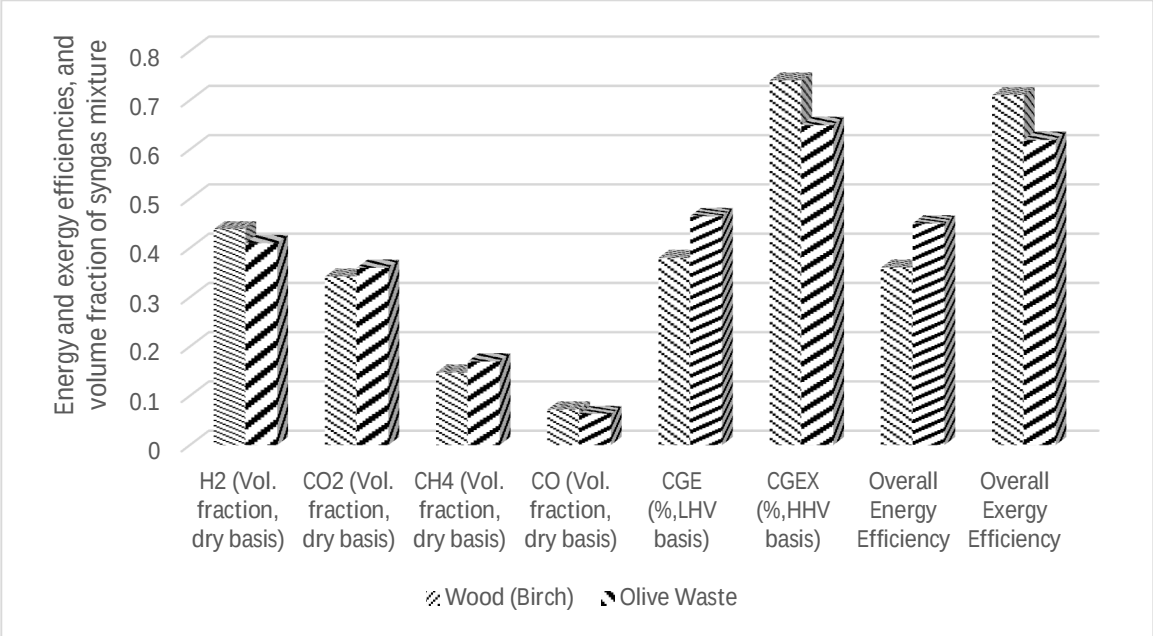

Figure 5.1 Comparison of elemental yields of syngas and energy and exergy efficiencies

The cold gas exergy efficiencies (CGEX) and overall exergy efficiency for the wood (Birch) and olive waste based feedstocks are found to be 71% and 62%, and 74% and 65%, respectively. It can be noted that the exergy efficiencies follow the opposite trend. This is due the fact that the higher heating value (HHV) of the wood (Birch) is less as compared to the HHV of the olive waste.

The influences of operating modes and conditions on volume fraction based yield of the syngas, CGE, CGEX, and overall energy and exergy efficiencies of the both feed are discussed as below.

5.1.1 Effects of Mass Flow Rate of Steam on Syngas Composition

The effects of fluctuation of mass flow rate of steam in the gasifiers of wood (Birch)-based model and olive waste-based model on the volume fraction based composition of the syngas are illustrated in Figs. 5.2 and 5.3, respectively.

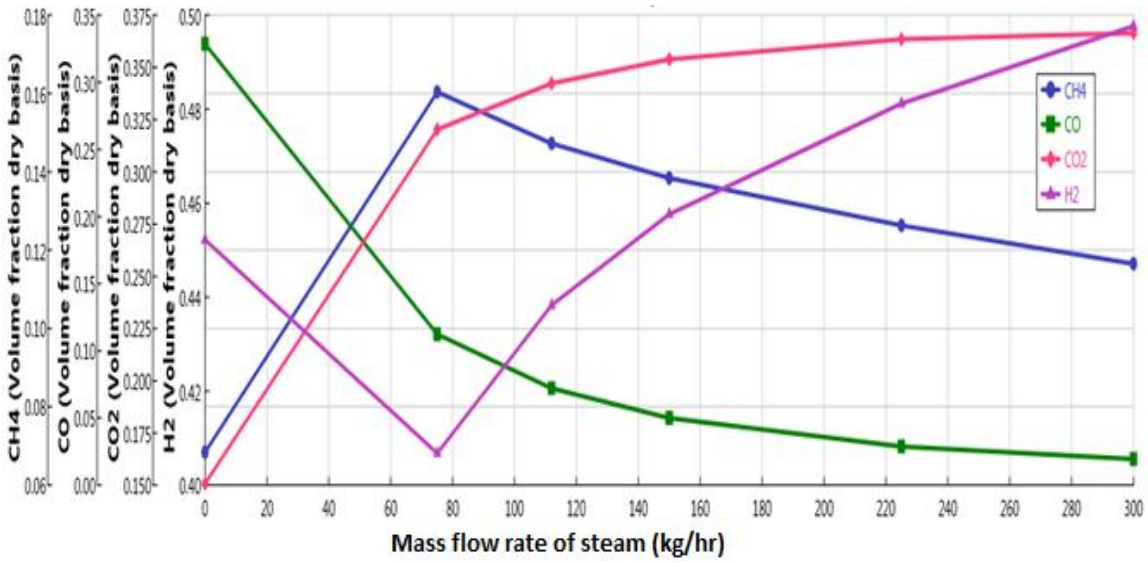

Figure 5.2 Effects of variation in the mass flow rate of steam on volume fraction using wood (Birch)

The yield of methane and carbon mono oxide in both models decreases when the mass flow rate of steam is increased upto 50 kg/hr whereas, the yield of carbon dioxide and hydrogen are enhanced with the increase in mass flow rate of steam. This trend is because of the reason that homogeneous reaction 5 in Table 4.7 is much favored with the increase in the mass flow rate of steam as compared to the other reactions.

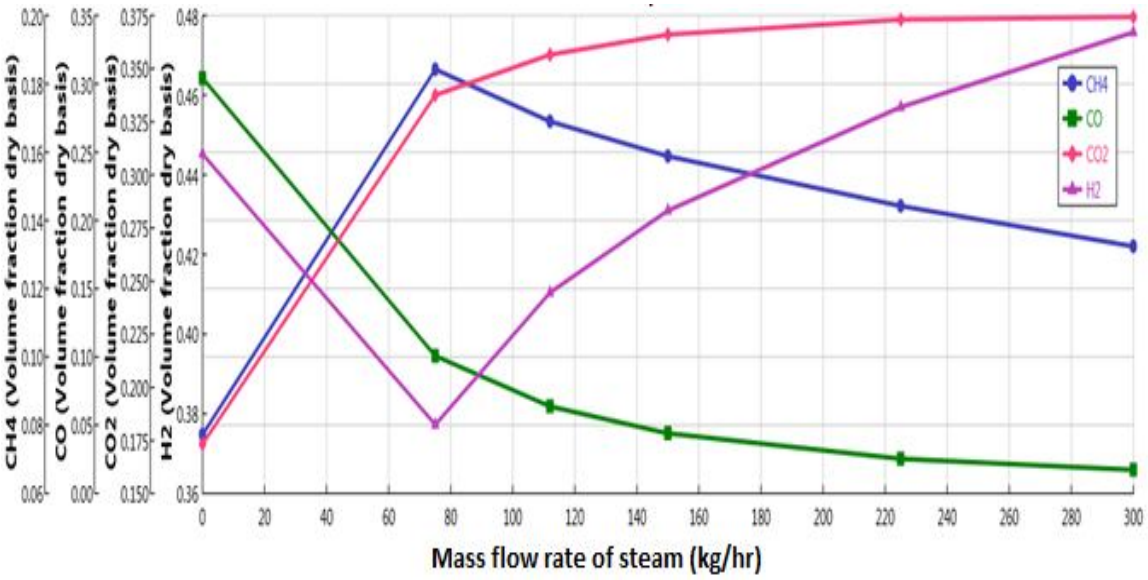

Figure 5.3 Effects of variation in the mass flow rate of steam on volume using olive waste

5.1.2 Effects of Gasifier Pressure on Syngas Composition

The effects of variation in the pressure of gasifiers of wood (Birch)-based model and olive waste-based model on the volume fraction based composition of the syngas are illustrated in Figs. 5.4 and 5.5, respectively.

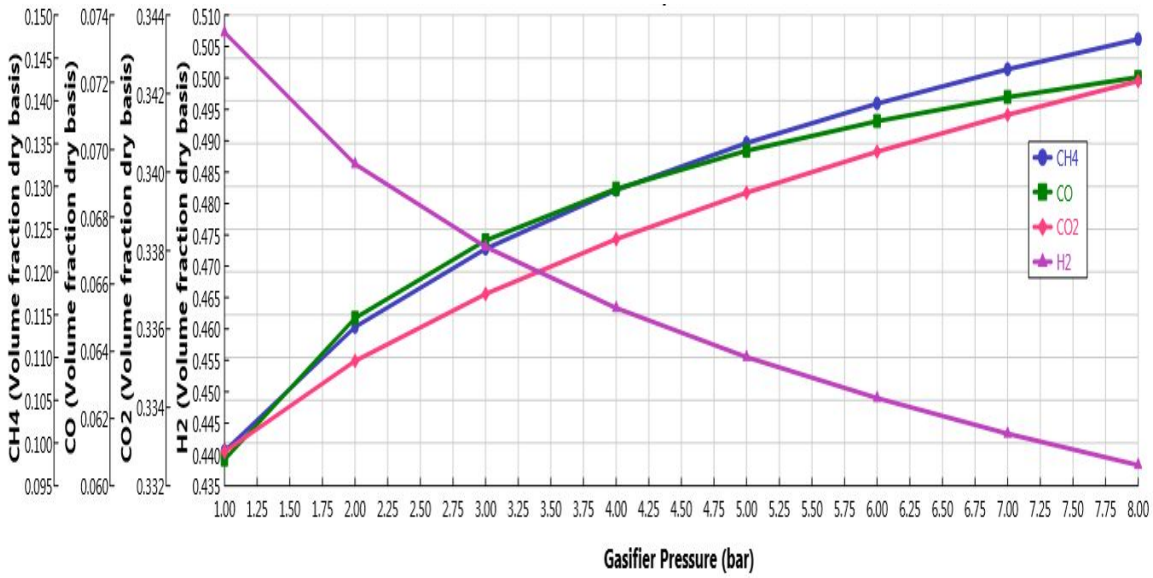

Figure 5.4 Effects of variation in the gasifier pressure on volume fraction using wood (Birch)

The pressure of the gasifier is varied from 1 bar to 8 bar to observe its effects on the composition of the syngas. The yield of methane and carbon mono oxide and carbon dioxide in both models are increased with the increase in the pressure of the gasifier. Conversely, the yield of hydrogen in both models decreases with the increment in the pressure. It is significant to note that the trend of decrease in the yield of hydrogen is more in wood (Birch)-based system as compared to the olive waste-based system. It is also important to note that the yield pattern of carbon monoxide and methane is almost same whereas, the yield of carbon monoxide slightly deviates from CO and CH_4.

The curves of methane and carbon monoxide shows in case of wood (Birch) are almost overlaps whereas, in case of olive waste these are at some distance. The yield of carbon dioxide is same in both cases with slight variation.

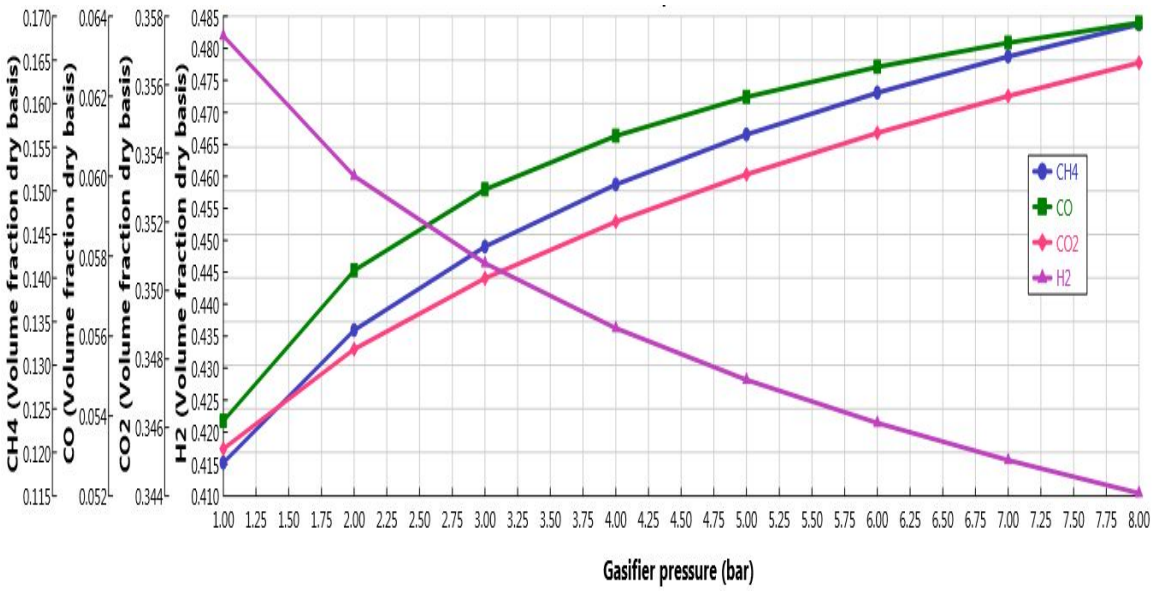

Figure 5.5 Effects of variation in the gasifier pressure on volume using olive waste

5.1.3 Effects of Combustion Temperature on Syngas Composition

The temperature in the combustion reactor is varied from 500ºC to 1500ºC to investigate its effects on the composition of the syngas as shown in Figs. 5.6 and 5.7, respectively.

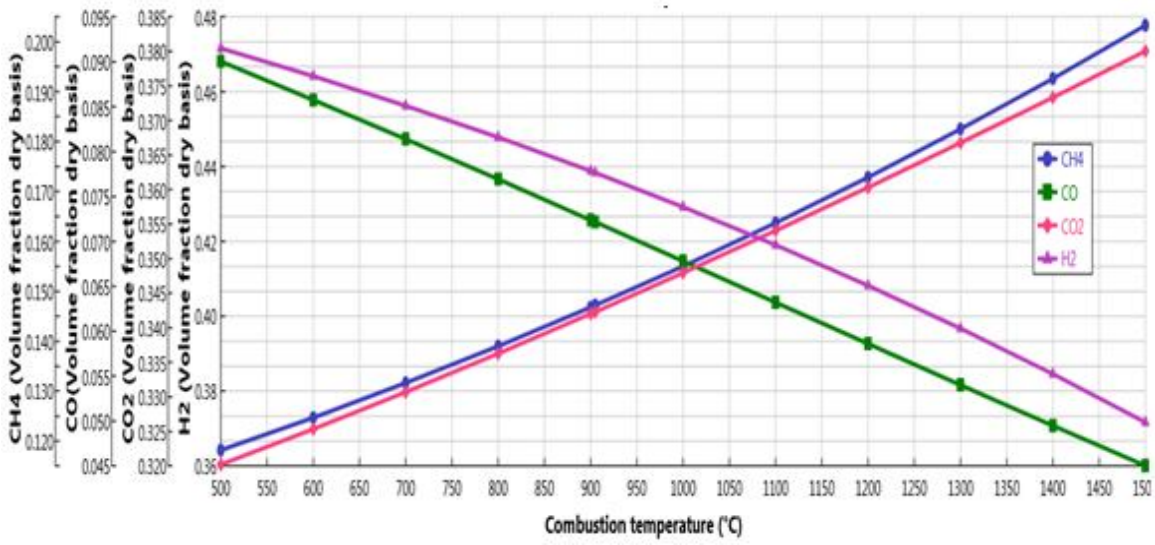

Figure 5.6 Effects of variation in the combustion temperature on volume using wood (Birch)

The yield of methane and carbon dioxide in both models is enhanced with the rise in the temperature of combustion reactor whereas, the yield of carbon monoxide and hydrogen decreases with the increase in the combustion reactor. This is because of the

reason that heat of the combustion reactor is the driving factor of the gasifier and the temperature of the gasifier increases with the increase in the combustion temperature which in turn favors the heterogeneous reaction 1 in Table 5 as compared to the other reactions. On the other hand, the yield of hydrogen and carbon monoxide decreases with the increase in combustion temperature which means forward homogeneous reaction 4 in Table 4.7 is more favorable at low temperature.

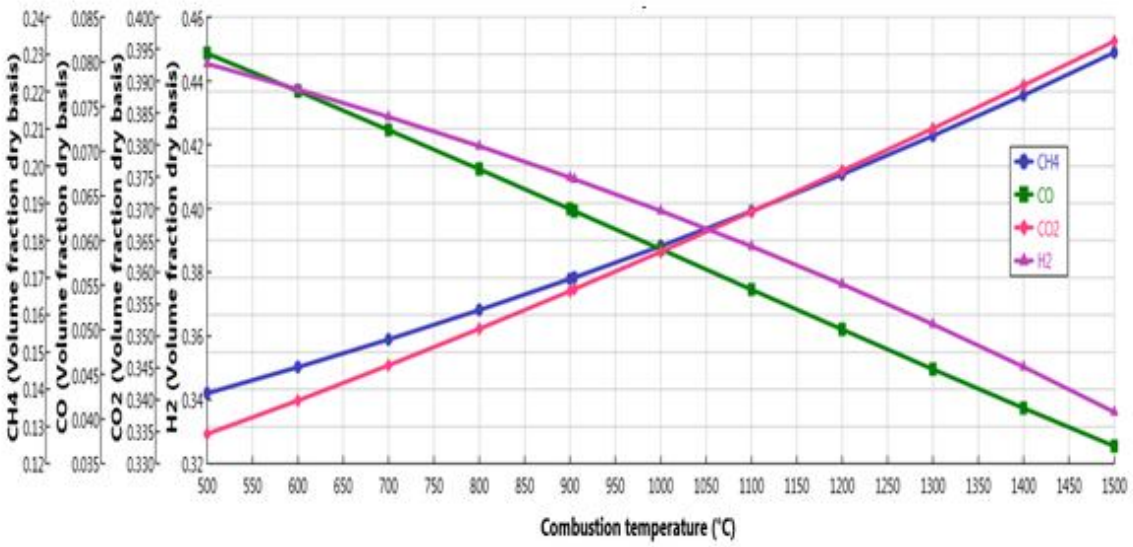

Figure 5.7 Effects of variation in the combustion temperature on volume fraction using olive waste

5.1.4 Effects of Combustion Temperature on LHV, HHV, CGE and CGEX

The sensitivities of low heating values, high heating value, cold gas efficiency and cold gas exergy efficiency are observed against the combustion temperature range between 900ºC and 1200ºC as depicted in Figs. 5.8 and 5.9, respectively. It can be noted that LHV increases with the increase in the combustion temperature whereas, HHV decreases upto 1140ºC then it increases sharply upto 1200ºC for wood (Birch) based system.

It is important to note that there is a considerable increase in the lower heating value and higher heating of the syngas between 1080°C to 1200°C. The cold gas energy and exergy efficiencies follow almost linear decreasing trend due to the decrease in the mass flow rate of the syngas with the increase in the combustion temperature.

The high heating value of syngas remains same between 1020°C to 1080°C temperature. This is an important indicator for heat saving which means combustor should be operated at 1020°C instead of 1080°C if the magnitude of HHV at this temperature is the target.

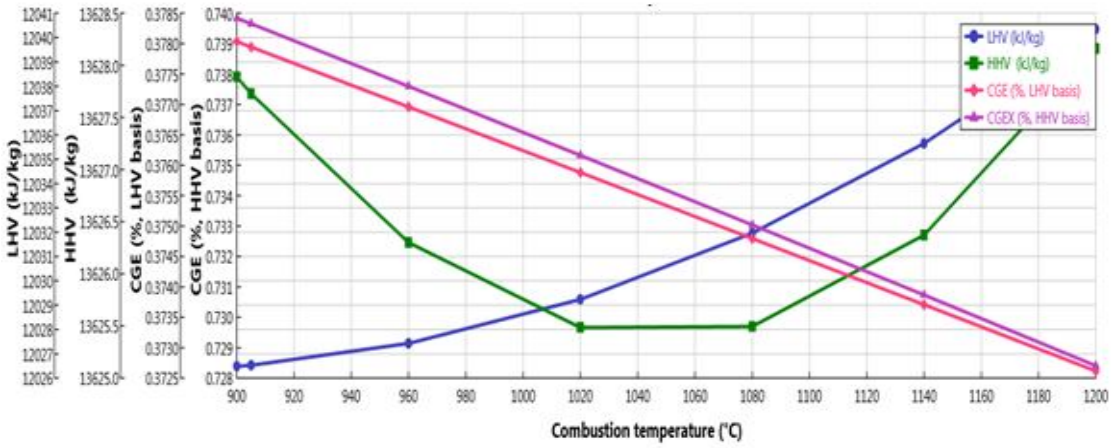

Figure 5.8 Effects of variation in the combustion temperature on LHV, HHV, CGE and CGEX using wood (Birch)

Both LHV and HHV for olive waste based system are enhanced with the rise in the combustion temperature. Moreover, cold gas energy efficiency as well as exergy efficiency of the wood (Birch) based and olive waste based systems are decreased from 37.8% and 74% to 37.2% and 72.8%, and 46.5% and 64.5% to 45.9% and 63.5%, respectively. This trend is found to be almost same for both feedstocks with a slight variation.

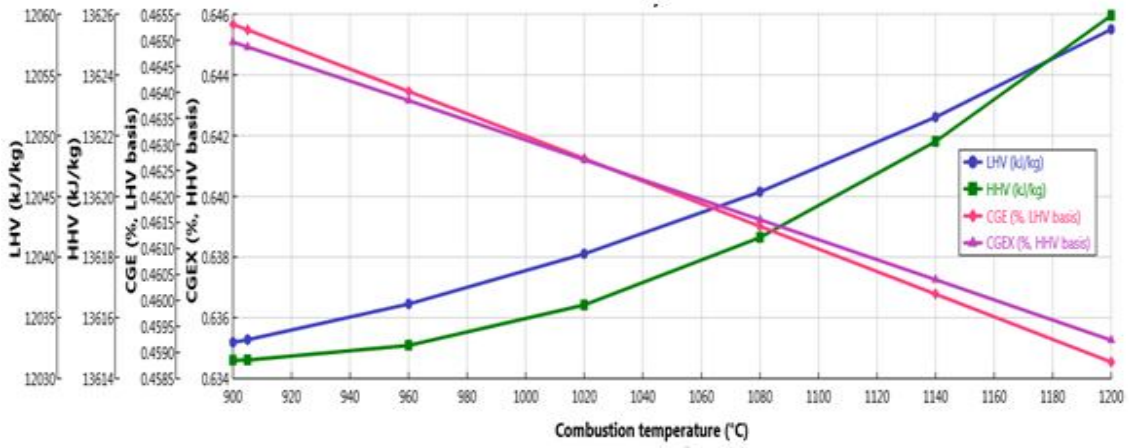

Figure 5.9 Effects of variation in the combustion temperature on LHV, HHV, CGE and CGEX using olive waste

5.1.5 Effects of Combustion Temperature on Overall Efficiencies

The sensitivities of the overall energy and exergy trend/behavior of the wood (Birch) based and olive waste based systems are observed against the variation in the combustion temperature between 900 ºC and 1200 ºC as depicted in Figs. 5.10 and 5.11, respectively.

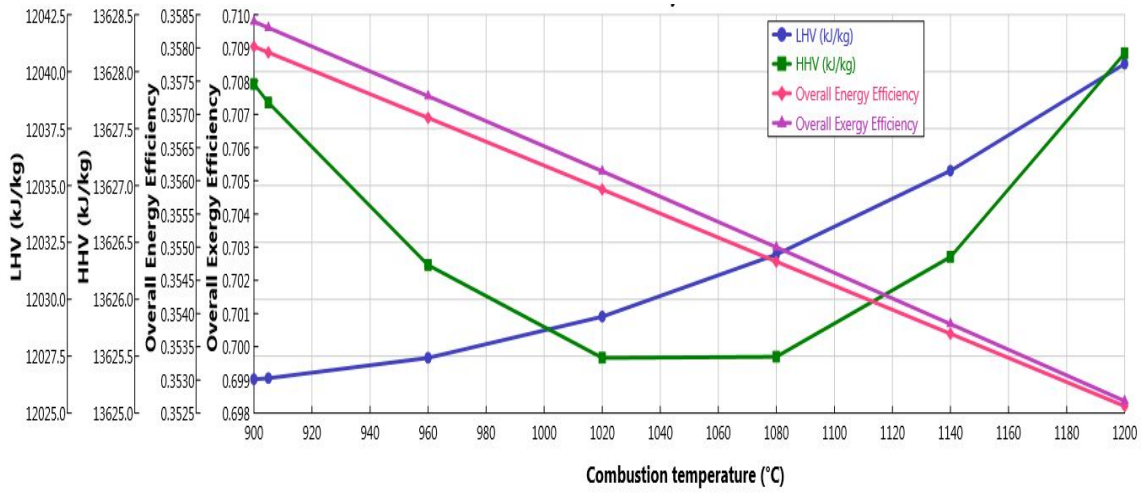

Figure 5.10 Effects of variation in the combustion temperature on LHV, HHV and overall efficiencies using wood (Birch)

The overall energy and exergy efficiencies of wood (Birch) based and olive waste based systems are decreased from 35.8% and 70.1% to 35.2% and 69.8%, and 44.5% and 61.5% to 43.9% and 60.5%, respectively.

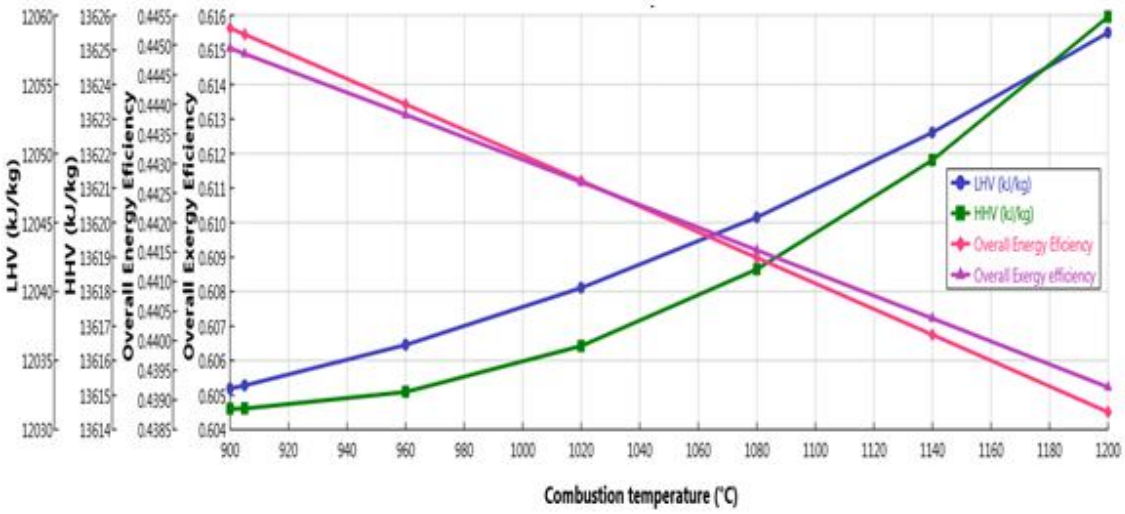

Figure 5.11 Effects of variation in the combustion temperature on LHV, HHV and overall efficiencies using olive waste

5.2 Results of Proposed System 1

This system can be employed to meet the electricity, heating, cooling and hot water demand of a community anywhere in the world but the composition of produced syngas will depend upon the composition of the feedstock available at that location. The performance of the developed system 2 is assessed for community in Saudi Arabia due to the abundant availability of waste feed stock (food waste).

The energy and exergy efficiencies of the major sub-systems of the proposed IGCC system 1 are depicted in Fig. 5.12. The energy and exergy efficiencies of the cold gas, overall, Gas turbine and steam turbine for the proposed systems 1 are found to be 58.2% and 57.6%, 55.9% and 32.1%, 29.8% and 26.7%, 34.1% and 60.1%, respectively.

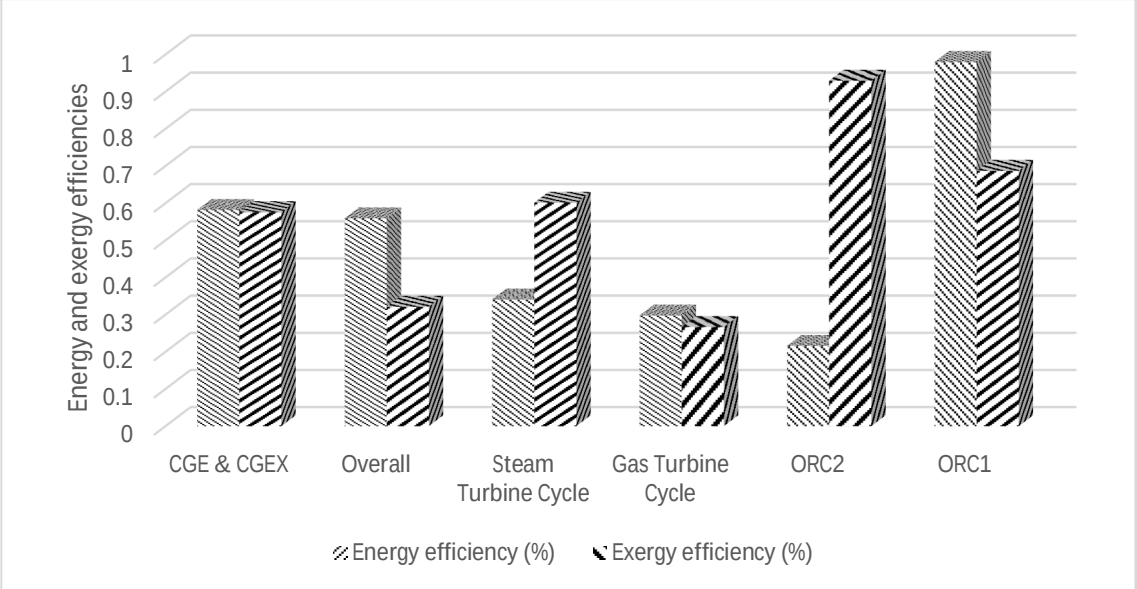

Figure 5.12 Energy and exergy efficiencies of the major sub-systems of the proposed system 1

The rate of exergy destruction in the major components of the proposed IGCC system 1 is represented in Fig. 5.13. The highest magnitude of exergy destruction in the order of 658.6 MW is associated with the syngas combustion chamber followed by the gasifier in the order of 327.1 MW Gibbs reactor in this case. The third and fourth highest amount of exergy destruction are in the order of 98.1 MW and 90.3 MW in space heater and Gas turbine, respectively. The least amount of exergy destruction is found to be 163.5 kW in the evaporator 1 of absorption chiller 1 due to smaller temperature difference

between the inlet and exit of the generator 1. The percentage of exergy destruction is shown in Fig. 5.14. It is important to note that almost half (48%) of the system irreversibilities are associated with combustion chamber followed by about one quarter (27%) in the gasifier.

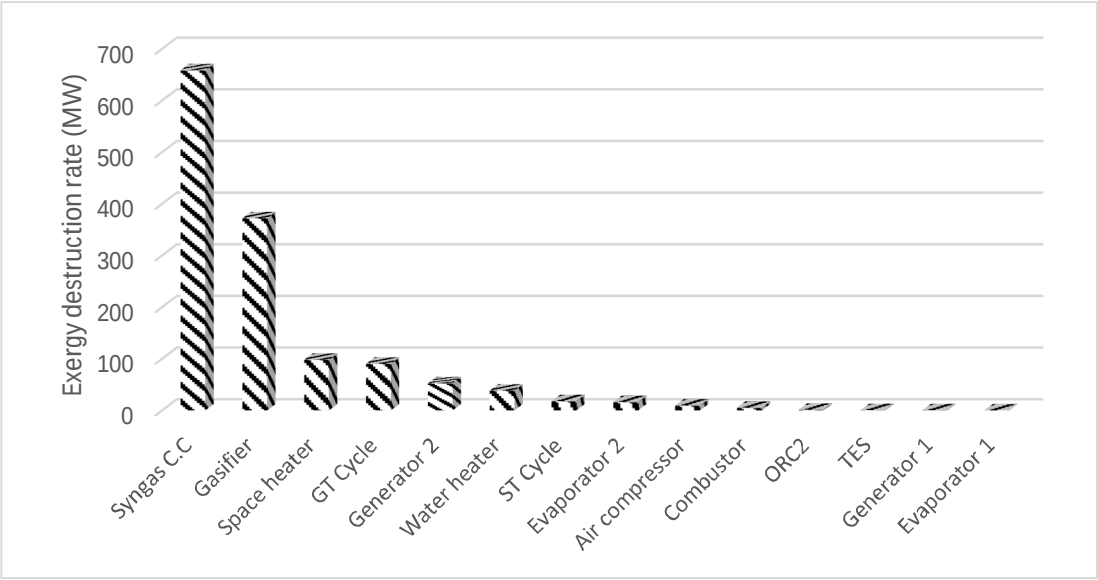

Figure 5.13 Rate of exergy destruction in the major sub-systems of the proposed system1

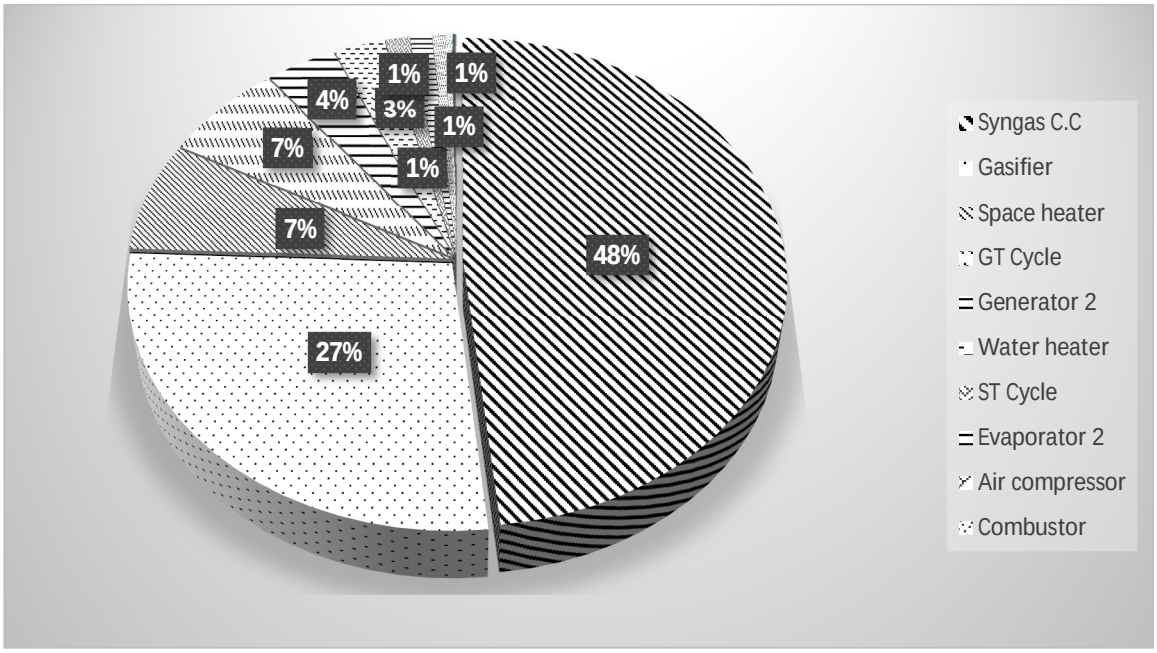

Figure 5.14 Percentage of exergy destruction rate in the major sub-systems of the proposed system 1

The rate of work input required to drive the compressor of the Gas turbine is found to be highest with a magnitude of 121.3MW followed by the pump of steam turbine with a magnitude of 3.13 MW as plotted in Fig. 5.15. The least amount of work rate required is 54 kW associated with the pump of ORC 1.

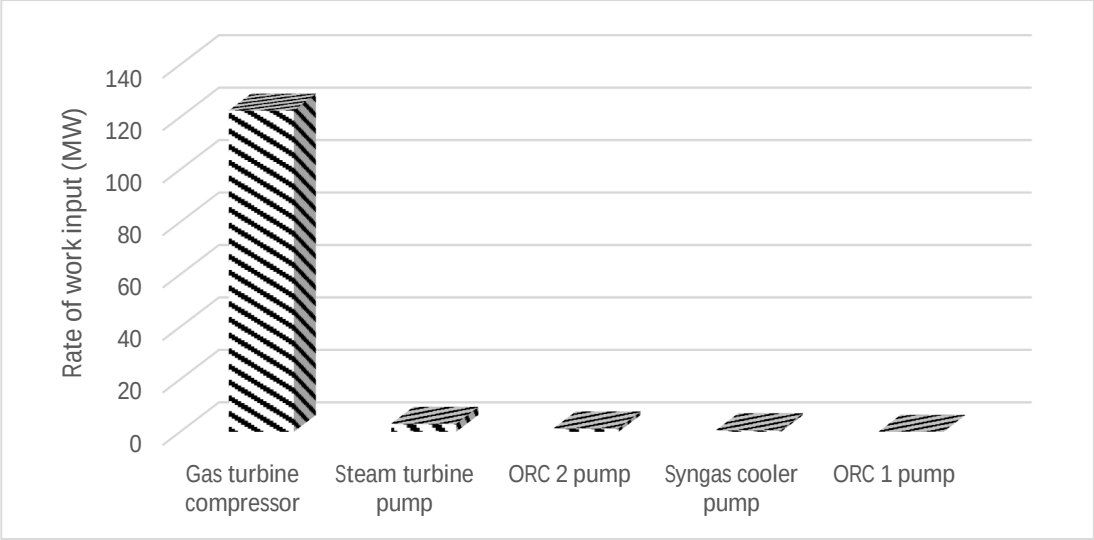

Figure 5.15 Rate of work input required to drive the major sub-systems of the proposed system 1

The rate of work output is found to be highest in the Gas turbine cycle with a magnitude of 269 MW followed by the steam turbine cycle with a magnitude of 177 MW as shown in Fig. 5.16. The ORC 2 has the third highest rate of work output with an amount of 14.32 MW. The least amount of the output work rate is 1308 kW associated with the ORC 1.

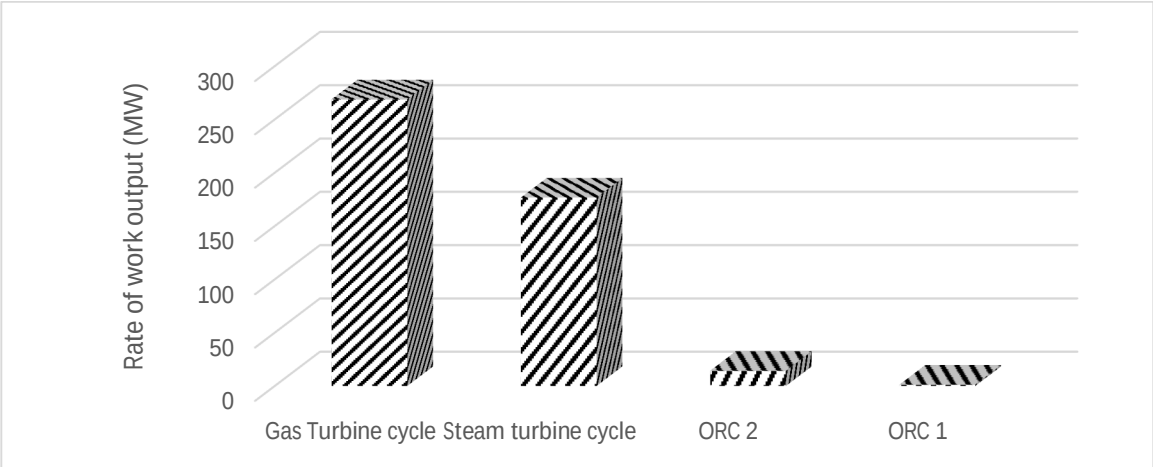

Figure 5.16 Rate of work output by the major sub-systems of the proposed system 1

The effects of fluctuation of mass flow rate of steam in the gasifiers of the proposed system 1 on the volume fraction based composition of the syngas are illustrated in Fig. 5.17.

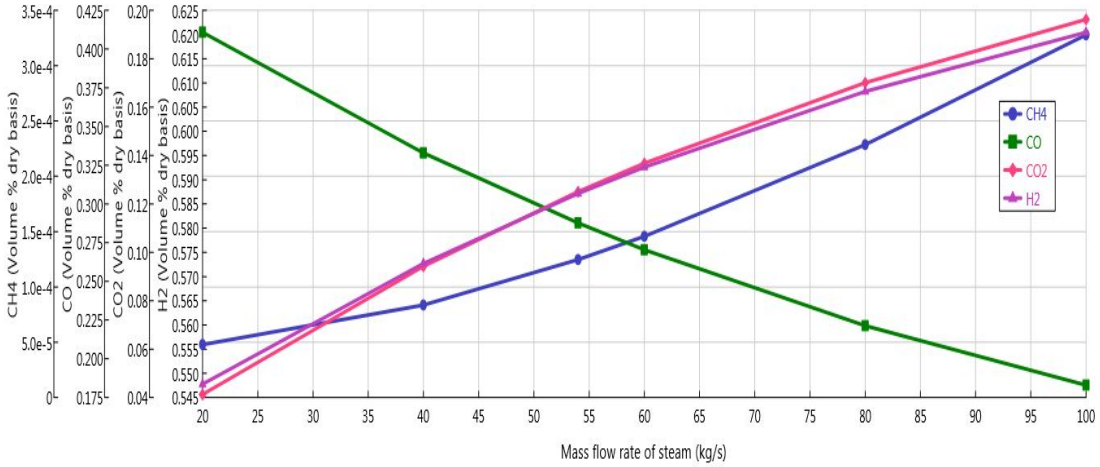

Figure 5.17 Effects of variation in the mass flow rate of steam on gas yield for the system 1

The yield of methane and carbon dioxide and hydrogen in this model increases when the mass flow rate of steam is increased from 20 kg/s to 100 kg/s whereas, the yield of carbon monoxide is decreased with the increase in mass flow rate of steam. This trend is because of the reason that more amounts of hydrogen and oxygen are available in the gasifier to convert these into methane, carbon dioxide and hydrogen.

The yield of methane and carbon dioxide and hydrogen in system 1 is enhanced with the rise in the temperature of combustion reactor whereas, the yield of carbon monoxide decreases with the increase in the combustion reactor as represented in Fig. 5.18. This is because of the reason that heat of the combustion reactor is the driving factor of the gasifier and the temperature of the gasifier increases with the increase in the combustion temperature which in turn favors the heterogeneous reaction 1 in Table 4.7 as compared to the other reactions. On the other hand, the yield of carbon monoxide decreases with the increase in combustion temperature which means forward homogeneous reaction 4 in Table 4.7 is more favorable at low temperature and reaction 5 is more favorable at high temperature.

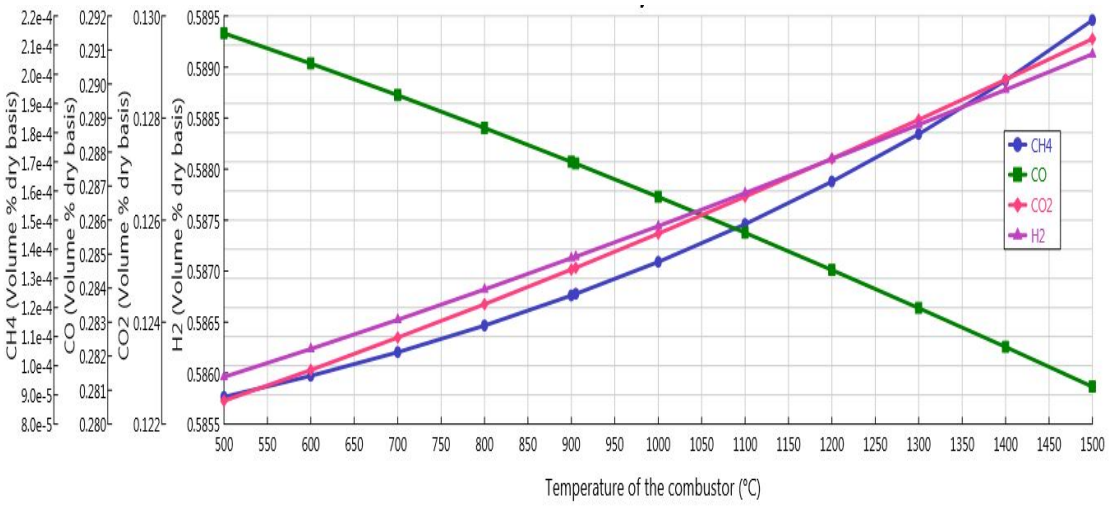

Figure 5.18 Effects of variation in the combustion temperature on gas yield for the system 1

The fluctuations in the LHV and HHV of syngas of the proposed system 1 are observed against the variation in the mass flow rate of the steam from 20 kg/s to 100 kg/s as depicted in Fig. 5.19. The lower heating value and higher heating value of the produced syngas are decreased from 17.2 MJ and 18.9 MJ to 13.4 MJ and 15.3 MJ, respectively.

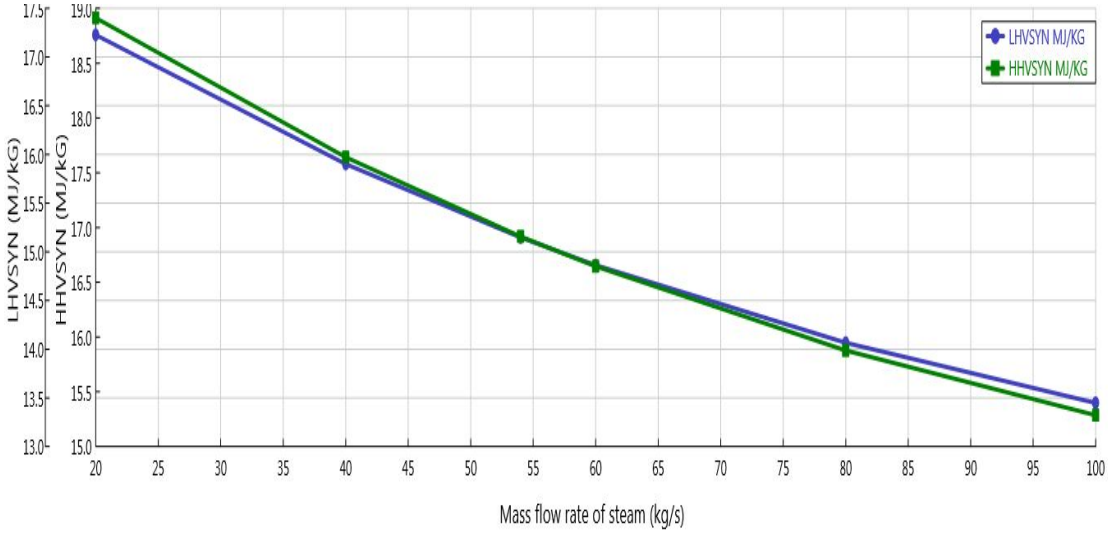

Figure 5.19 Effects of variation in the mass flow rate of steam on calorific values of syngas for the system 1

The cold gas energy efficiency of the syngas and work rate of Gas turbines of the prosed system 1 are plotted against the fluctuations in the mass flow rate of water from 20 kg/s to 100 kg/s as shown in Fig. 5.20. Cold gas energy efficiency and the work rate of

turbines decrease with the increase in the mass flow rate of water. This is because of the reason that the lower heating value of the syngas reduces with the increase in the mass flow rate of the water.

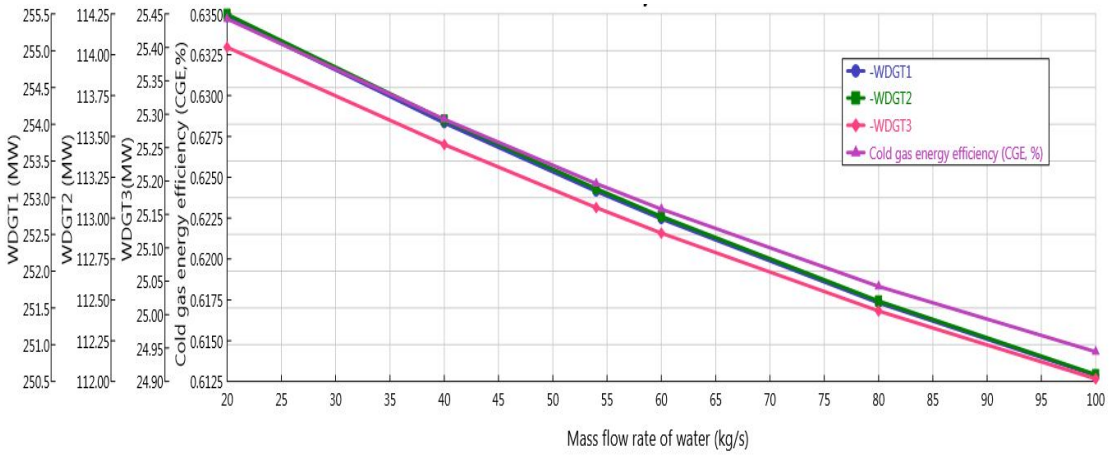

Figure 5.20 Effects of variation in the mass flow rate of steam on the syngas efficiencies and work rate of GT for the system 1

The inlet temperature of gas turbine is varied from 1600 to 1873K to make an assessment of its effects on overall energy and exergy efficiencies of proposed system 1 as depicted in Fig. 5.21. The magnitude of energetic and exergetic efficiencies of the proposed system 1 are increased from 53.7% to 56% and from 30% to 32.3%, respectively, with the rise in temperature from 1600 K to 1873 K. The syngas at high temperature has high enthalpy, which is the main reason for this enhancement.

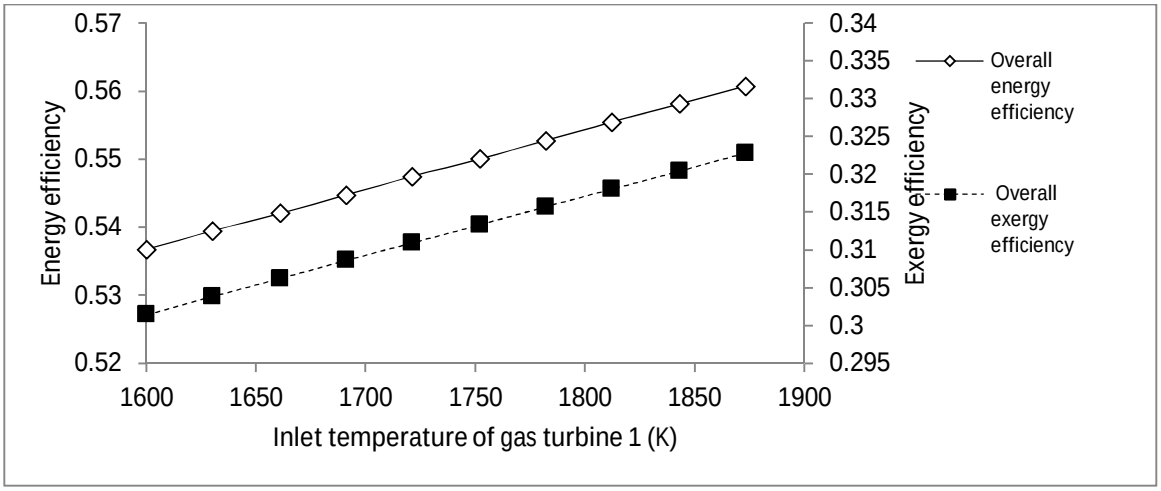

Figure 5.21 Effects of variation in the inlet temperature of gas turbine 1 on overall efficiencies of the system 1

The effects of fluctuation in the ambient temperature are plotted against the exergy destruction rate in the major sub-systems of the proposed system 1 as shown in Fig. 5.22. The magnitude of exergy destruction rate in syngas combustion chamber, biomass combustor, gasifier, gas turbine, organic Rankine cycle 2 and steam turbine decreases with the increase in the ambient temperature. This pattern is observed because of the reduced finite temperature difference between operating temperatures of these sub-systems and ambient.

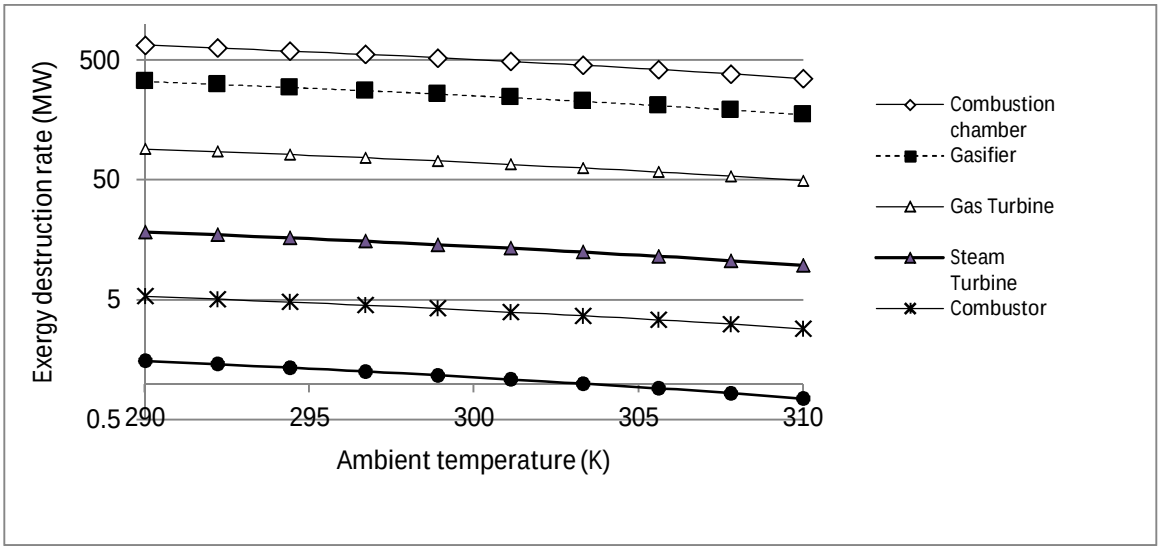

Figure 5.22 Effects of variation in the ambient temperature on the exergy destruction rate in the major components of the system 1

5.3 Results of Proposed System 2

This system can be employed to meet the electricity, heating, cooling, hot water and fresh water demand of a food industry anywhere in the world but the composition of produced syngas will depend upon the composition of the feedstock available at that location. The performance of the developed system 2 is assessed for a dairy in Saudi Arabia due to the abundant availability of waste feed stock (cow manure).

The energy and exergy efficiencies of the major sub-systems of the proposed IGCC system 1 are depicted in Fig. 5.23. The energy and exergy efficiencies of the cold gas, overall, Gas turbine and steam turbine for the proposed systems 2 are found to be 62.1% and 61.4%, 57.9% and 33.3%, 29.2% and 25.9%, 33.65% and 61.66%, respectively.

The energy destruction rate, rate of work input and rate of work out are discussed in this section. In addition to this, sensitivity analysis is carried out against the variations in the mass flow rate of steam, combustor temperature, inlet temperature of gas turbine and ambient temperature.

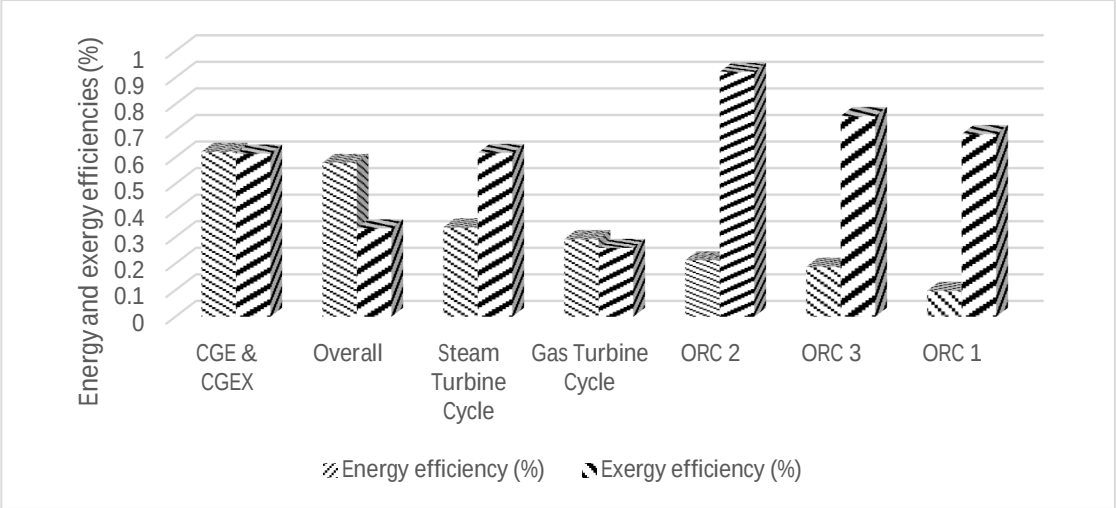

Figure 5.23 Energy and exergy efficiencies of the major sub-systems of the proposed system 2

The rate of exergy destruction in the major components of the proposed IGCC system 2 is represented in Fig. 5.24. The highest magnitude of exergy destruction in the order of 604.5 MW is associated with the syngas combustion chamber followed by the gasifier in the order of 508.7 MW Gibbs reactor in this case. The same amount of exergy destruction occurs in space heater and Gas turbine in the order of 98.1 MW.

The least amount of exergy destruction is found to be 163.5 kW in the evaporator 1 of absorption chiller 1 same as in proposed system 1. This is because of the smaller temperature difference between the inlet and exit of the generator 1. The percentage of exergy destruction is shown in Fig. 5.25. It is important to note that 42% of the system irreversibilities are associated with combustion chamber followed by 35% (about 1/3 of the total) in the gasifier.

The highest amount of exergy destruction rate in combustion chamber is due to the irreversibilities associated with the combustion of syngas. In addition to this, high operating temperature is another important contributing factor in high magnitude of exergy destruction rate.

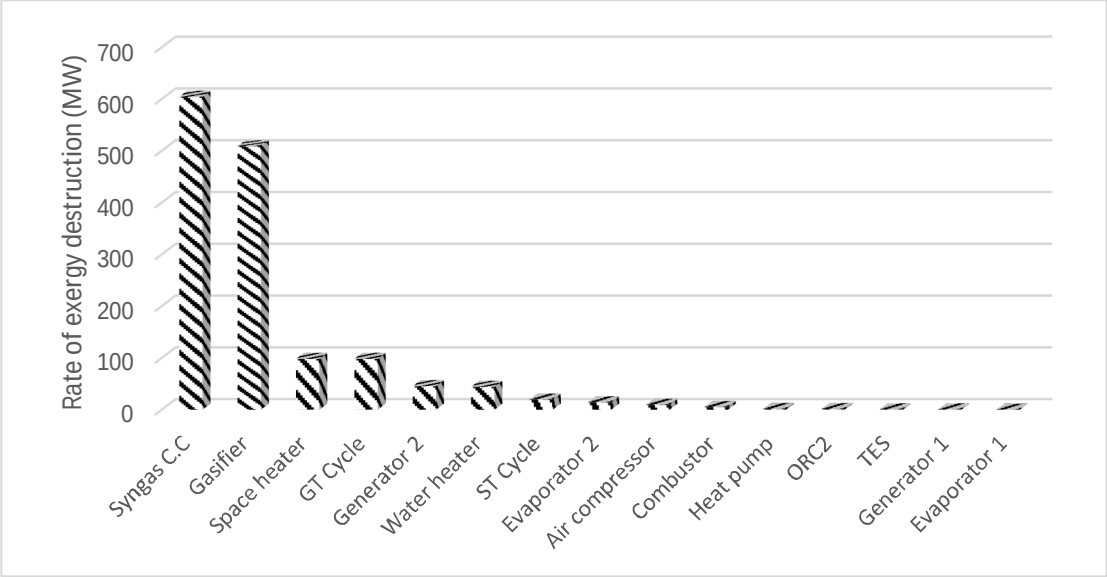

Figure 5.24 Rate of exergy destruction in the major sub-systems of the proposed system 2

Space heater and Gas turbine cycle account for same amount of exergy destruction rate in the order of 7%. The least amount of exergy destruction rate occurs in heat pump due to the less temperature difference between the working fluid R134a and the ambient.

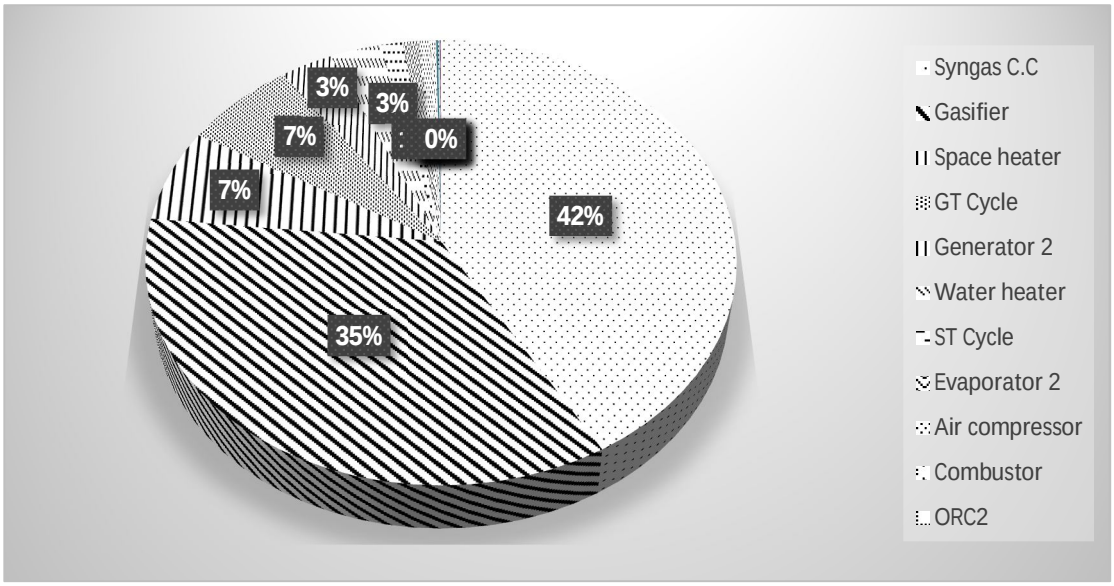

Figure 5.25 Percentage of exergy destruction rate in the major sub-systems of the system 2

The rate of work input required to drive the compressor of the Gas turbine is found to be highest with a magnitude of 121.3MW followed by the pump of steam turbine with

a magnitude of 3.13 MW as plotted in Fig. 5.26 (same as in proposed system 1). The least amount of work rate required is 54 kW associated with the pump of ORC 1.

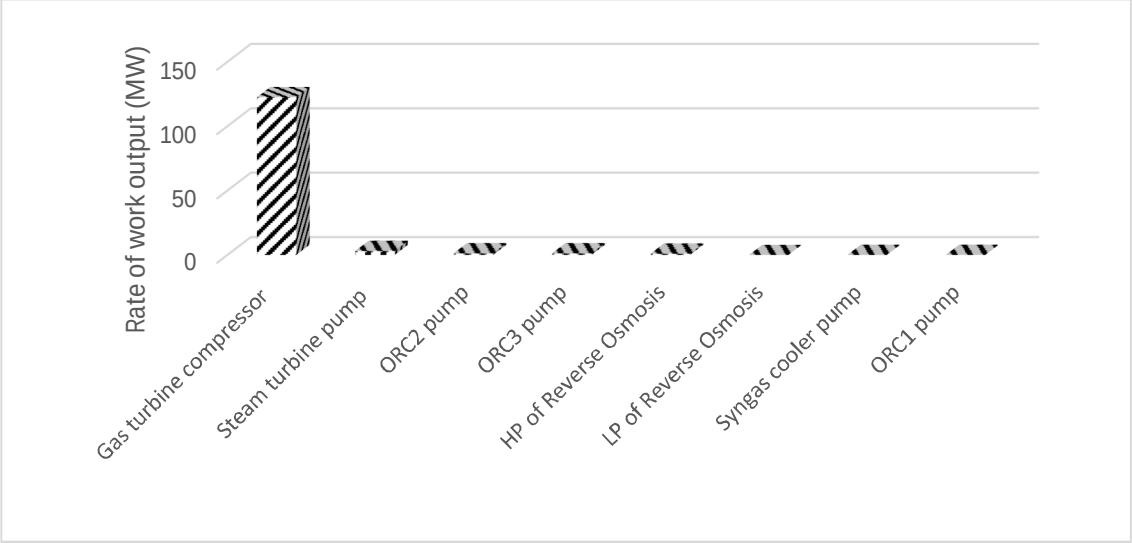

Figure 5.26 Rate of work input required to drive major sub-systems of the proposed system 2

The rate of work output is found to be highest in the Gas turbine cycle with a magnitude of 252 MW followed by the steam turbine cycle with a magnitude of 165 MW as shown in Fig. 5.27. The ORC 2 has the third highest rate of work output with an amount of 14 MW. The least amount of the output work rate is 1308 kW associated with ORC 1.

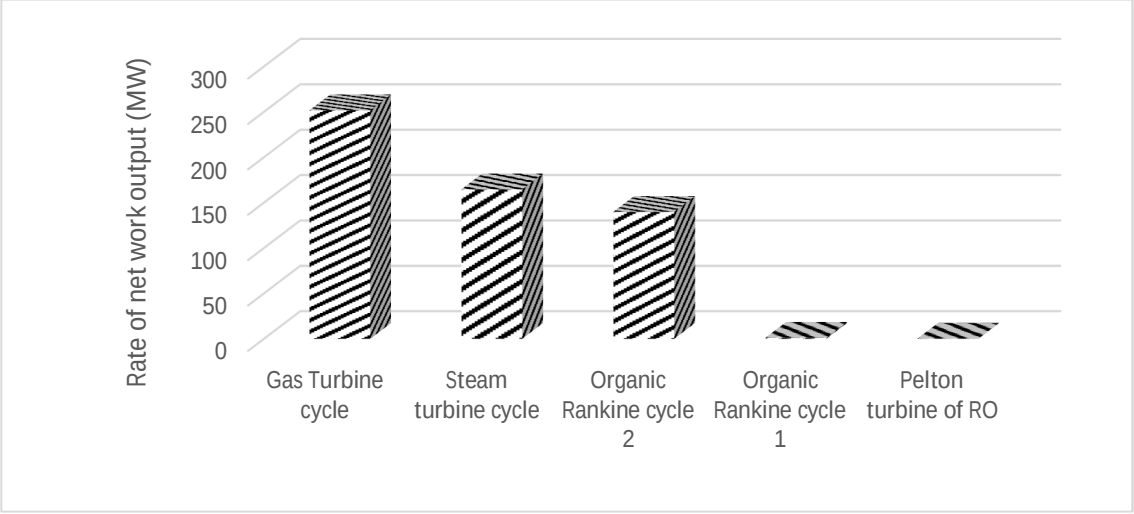

Figure 5.27 Rate of work output by the major sub-systems of the proposed system 2

The effects of fluctuation of mass flow rate of steam in the gasifiers of the proposed system 2 on the volume fraction based composition of the syngas are illustrated in Fig. 5.28.

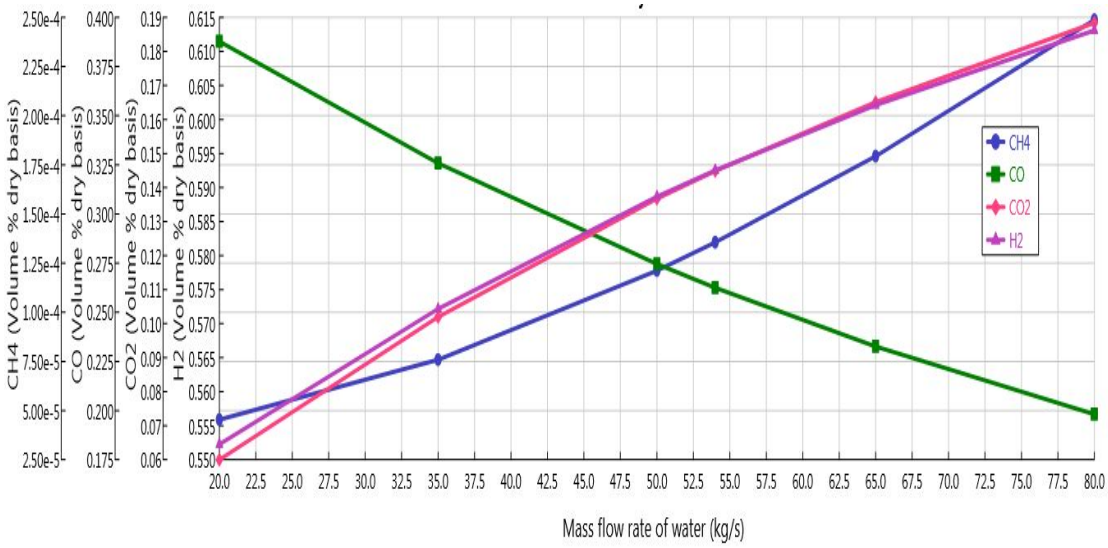

Figure 5.28 Effects of variation in the mass flow rate of steam on gas yield for the system 2

The yield of methane and carbon dioxide and hydrogen in this model increases when the mass flow rate of steam is increased from 20 kg/s to 80 kg/s whereas, the yield of carbon monoxide is decreased with the increase in mass flow rate of steam. This trend is observed because of the reason that more amounts of hydrogen and oxygen are available in the gasifier to convert these into methane, carbon dioxide and hydrogen.

The yield of methane and carbon dioxide and hydrogen in system 2 follow the same trend as in system 1, and is enhanced with the rise in the temperature of combustion reactor whereas, the yield of carbon monoxide decreases with the increase in the combustion reactor as represented in Fig. 5.29. This is due to the same reason heat of the combustion reactor is the driving factor of the gasifier and the temperature of the gasifier increases with the increase in the combustion temperature which in turn favors the heterogeneous reaction 1 in Table 4.7 as compared to the other reactions.

On the other hand, the yield of carbon monoxide decreases with the increase in combustion temperature which means forward homogeneous reaction 4 in Table 4.7 is more favorable at low temperature and reaction 5 is more favorable at high temperature.

The relationship between the combustion temperature and yield of carbon monoxide is almost linear throughout the graph.

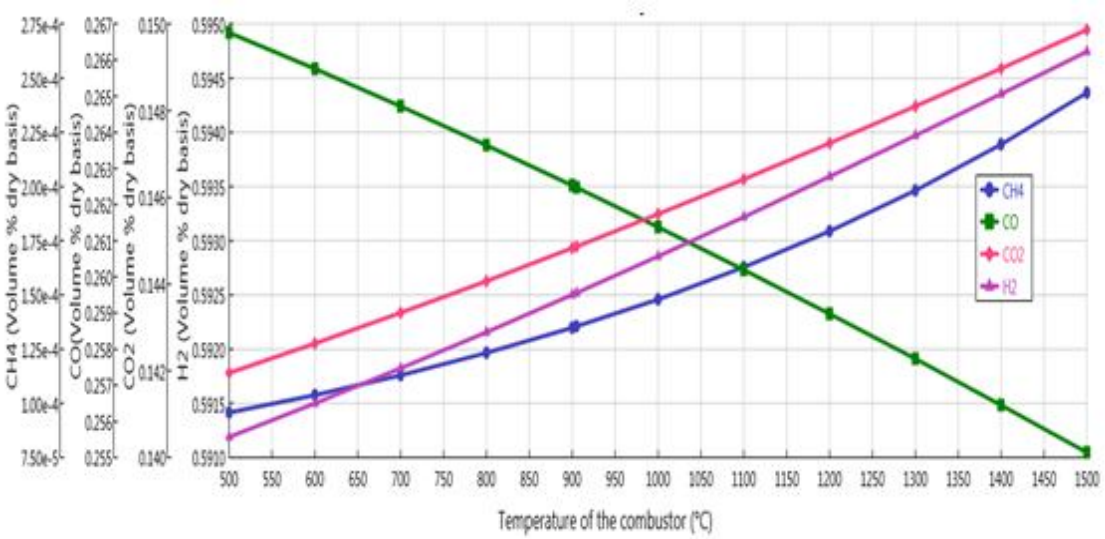

Figure 5.29 Effects of variation in the combustion temperature on volume fraction for system 2

The sensitivities in the LHV and HHV of syngas of the proposed system 2 are observed against the fluctuation in the mass flow rate of the steam from 20 kg/s to 80 kg/s as depicted in Fig. 5.30. The lower heating value and higher heating value of the produced syngas are decreased from 16.64 MJ and 18.32 MJ to 13.55 MJ and 15.36 MJ, respectively.

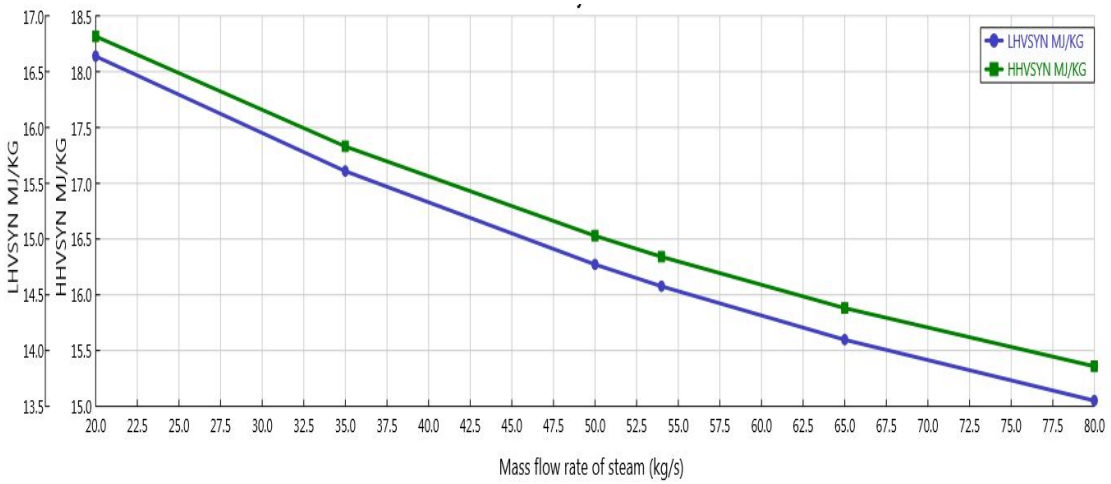

Figure 5.30 Effects of variation in the mass flow rate of steam on the LHV and HHV of the syngas for the system 2

The cold gas energy efficiency of the syngas and work rate of Gas turbines of the system 2 are plotted against the fluctuation in the mass flow rate of water from 20 kg/s to

80 kg/s as shown in Fig. 5.31. Cold gas energy efficiency and the work rate of turbines decrease with the increase in the mass flow rate of water. This is because of the reason that the lower heating value of the syngas reduces with the increase in the mass flow rate of the water.

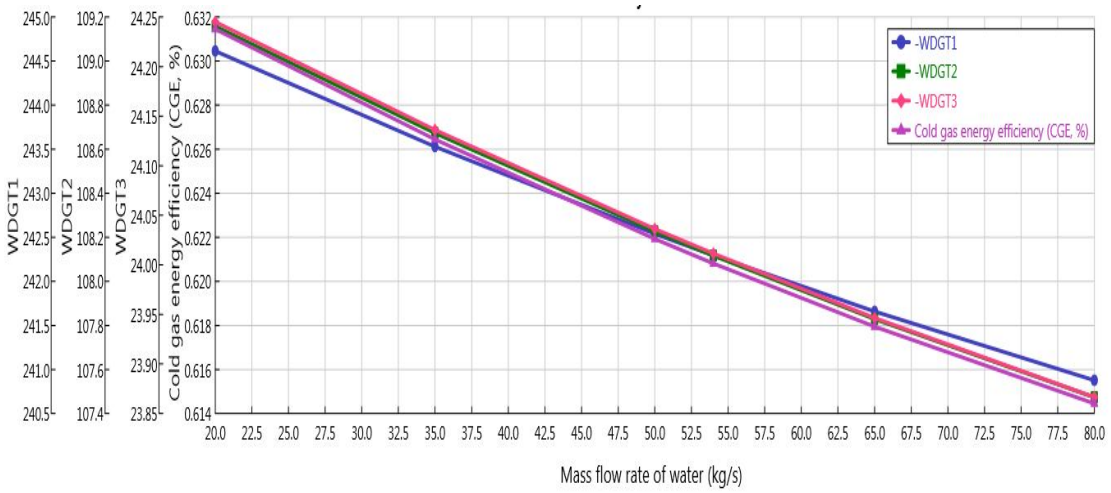

Figure 5.31 Effects of variation in the mass flow rate of steam on the syngas efficiencies and work rate of GT for the system 2

The inlet temperature of gas turbine is varied from 1600 to 1873K to make an assessment of its effects on overall energy and exergy efficiencies of proposed system 2 as depicted in Fig. 5.32. The magnitude of energetic and exergetic efficiencies of the proposed system 3 are increased from 56% to 58.7%and from 31.6% to 34%, respectively, with the rise in temperature from 1600 K to 1873 K. The syngas at high temperature has high enthalpy which is the main reason for this enhancement.

The effects of fluctuation in the ambient temperature are plotted against the exergy destruction rate in the major sub-systems of the proposed system 2 as shown in Fig. 5.33 follows the same pattern as of system 1.

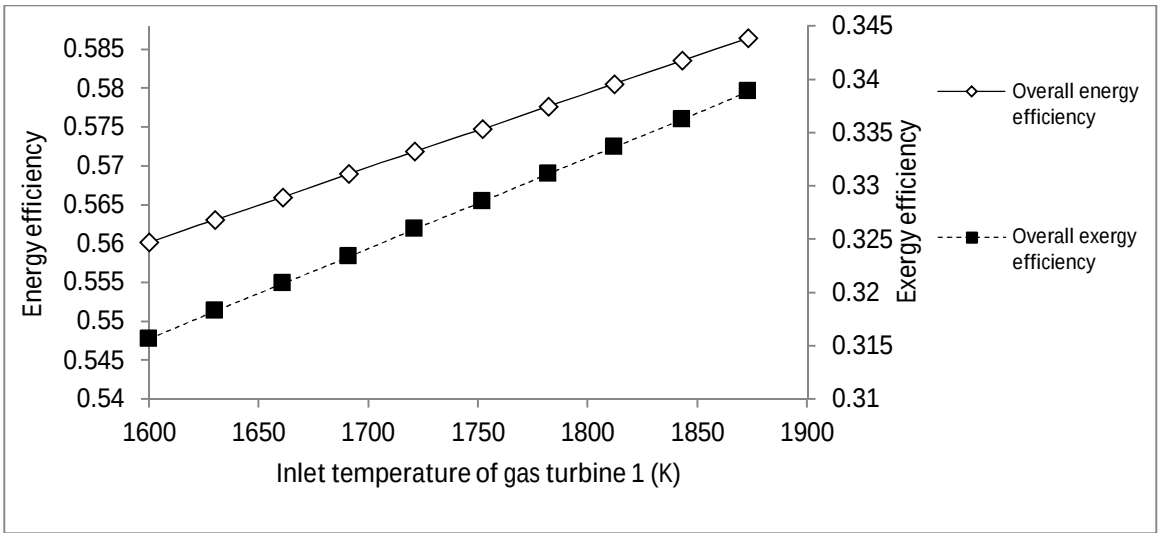

Figure 5.32 Effects of variation in the inlet temperature of gas turbine 1 on overall efficiencies of the system 2

The magnitude of exergy destruction rate in syngas combustion chamber, biomass combustor, gasifier, gas turbine, organic Rankine cycle 2 and steam turbine decreases with the increase in the ambient temperature. This pattern is observed because of the reduced finite temperature difference between operating temperatures of these sub-systems and ambient.

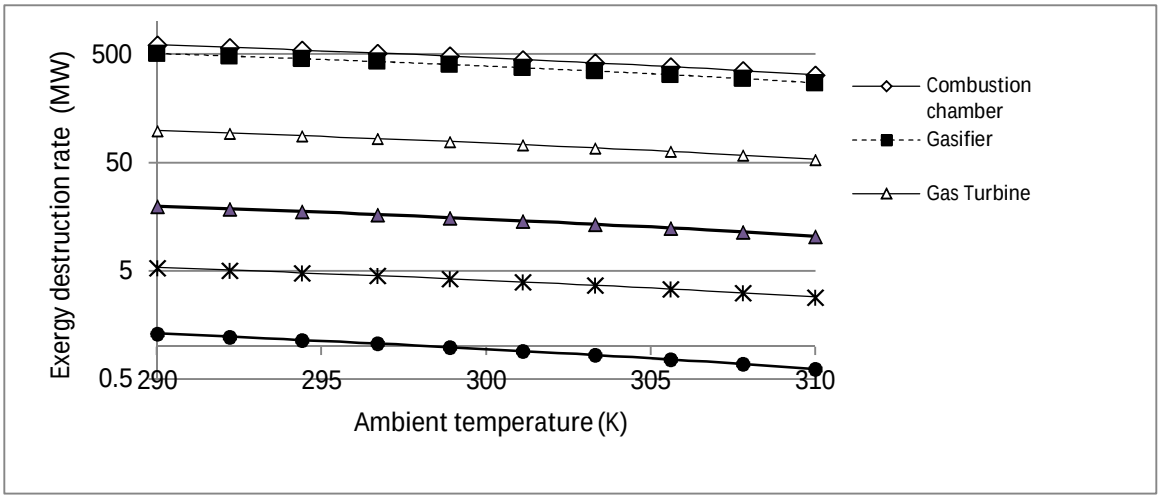

Figure 5.33 Effects of variation in the ambient temperature on the exergy destruction of the major components of the system 2

5.4 Results of Proposed System 3

This system can be employed to meet the electricity, heating, cooling, hot water and fresh water demand of a refinery anywhere in the world but the composition of produced syngas

will depend upon the composition of the feedstock available at that location. The performance of the developed system 3 is assessed for a refinery in Saudi Arabia due to the abundant availability of waste feed stock (heavy oil).

The energy and exergy efficiencies of the major sub-systems of the proposed IGCC system 3 are depicted in Fig. 5.34. The energy and exergy efficiencies of the cold gas, overall, Gas turbine and steam turbine for the proposed systems 3 are found to be 58.17% and 57.6%, 55.9% and 32.1%, 29.8% and 26.7%, 34.1% and 60.1%, respectively.

The exergy destruction rate, rate of work input and rate of work out are discussed in this section. In addition to this, sensitivity analysis is carried out against the variation in the mass flow rate of steam, combustor temperature, inlet temperature of gas turbine and ambient temperature.

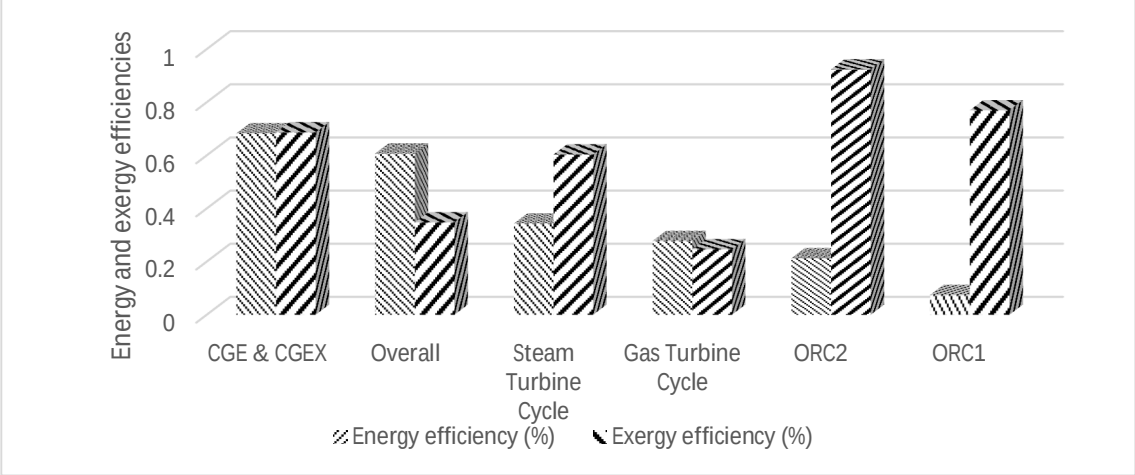

Figure 5.34 Energy and exergy efficiencies of the major sub-systems of the proposed system 3

The rate of exergy destruction in the major components of the proposed IGCC system 1 is represented in Fig. 5.35. The highest magnitude of exergy destruction in the order of 658.6 MW is associated with the syngas combustion chamber followed by the gasifier in the order of 327.1 MW Gibbs reactor in this case. The third and fourth highest amount of exergy destruction are in the order of 98.1 MW and 90.3 MW in space heater and Gas turbine, respectively. The least amount of exergy destruction is found to be 163.5 kW in the evaporator 1 of absorption chiller 1 due to smaller temperature difference between the inlet and exit of the generator 1. The percentage of exergy destruction is shown

in Fig. 5.36. It is important to note that almost half (48%) of the system irreversibilities are associated with combustion chamber followed by about one quarter (27%) in the gasifier.

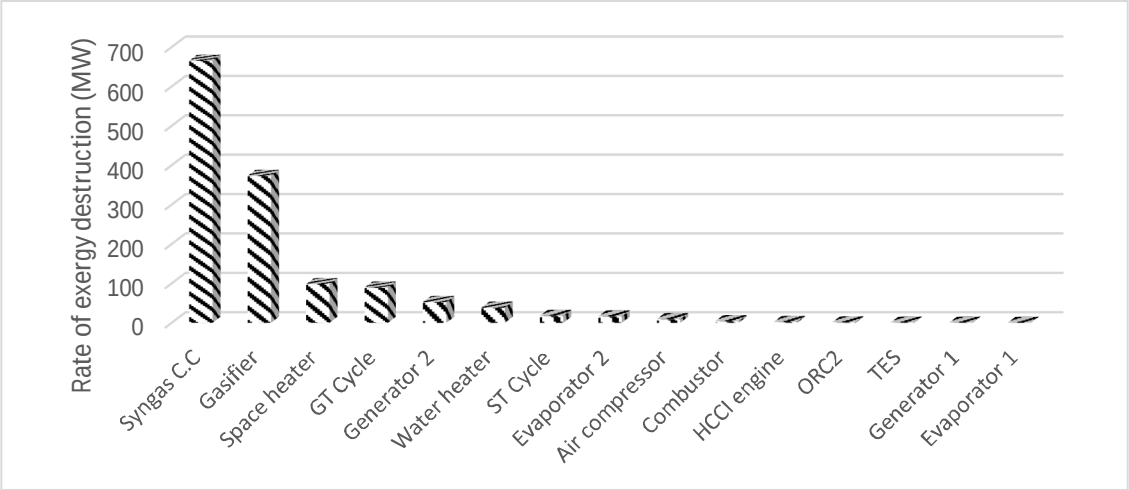

Figure 5.35 Rate of exergy destruction in the major sub-systems of the proposed system 3

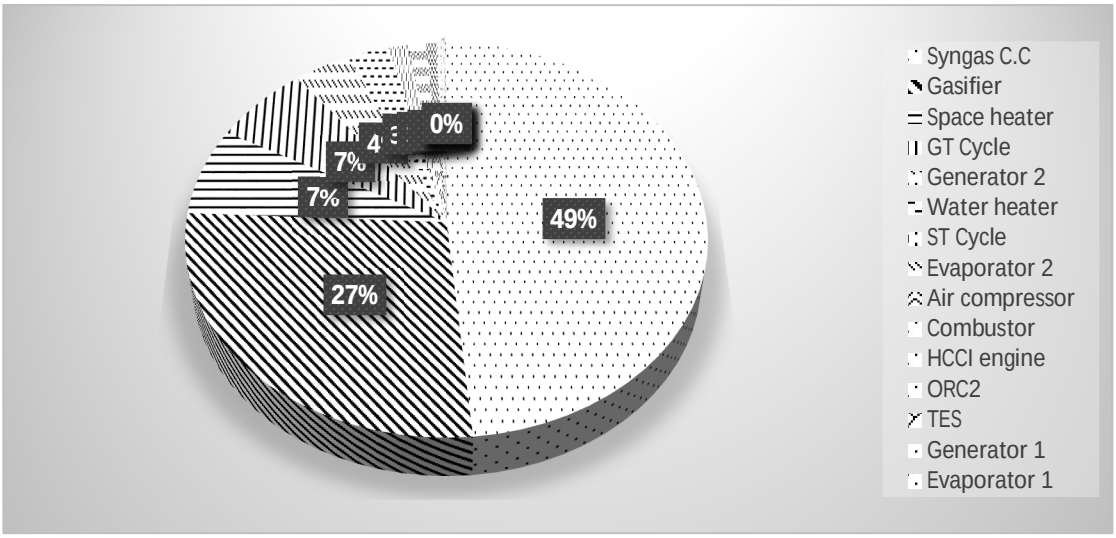

Figure 5.36 Percentage of exergy destruction rate in the major sub-systems of the system 3

The rate of work input required to drive the compressor of the Gas turbine is found to be highest with a magnitude of 121.3MW followed by the pump of steam turbine with a magnitude of 3.13 MW as plotted in Fig. 5.37. The least amount of work rate required is 54 kW associated with the pump of ORC 1.

It is important to note that the Figures 5.35 and 5.36 represent exergy destruction but in different forms. The amount of exergy destruction in a specific sub-system can be

found in Fig. 5.35 but it is not easy to figure out quickly that how much percentage of exergy destruction is occurring in that particular unit. Therefore, Fig 5.36 is presented to show the percentage share of the subunits in exergy destruction.

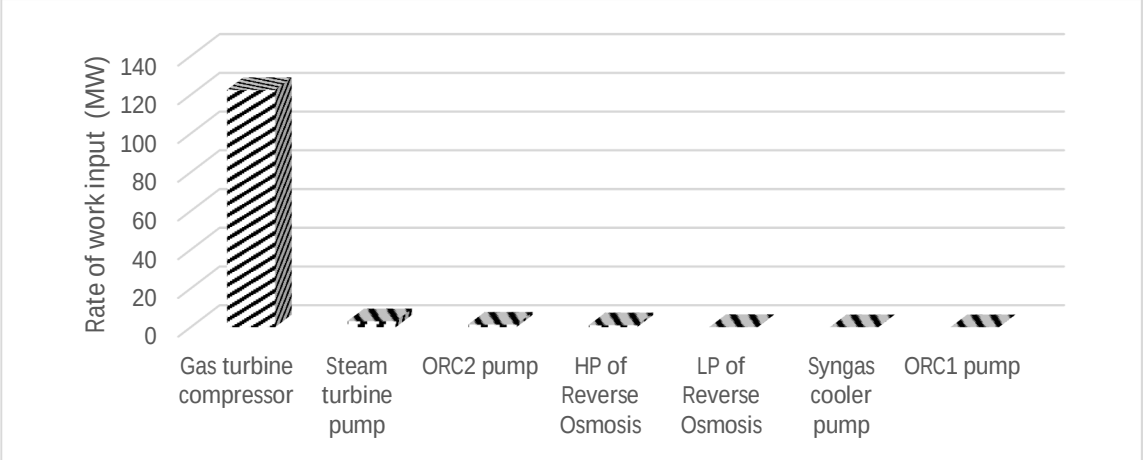

Figure 5.37 Rate of work input required to drive the major sub-systems of the system 3

The rate of work output is found to be highest in the Gas turbine cycle with a magnitude of 269 MW followed by the steam turbine cycle with a magnitude of 177 MW as shown in Fig 5.38. The ORC 2 has the third highest rate of work output with an amount of 14.32 MW. The least amount of output work rate is associated with the ORC of the HCCI engine.

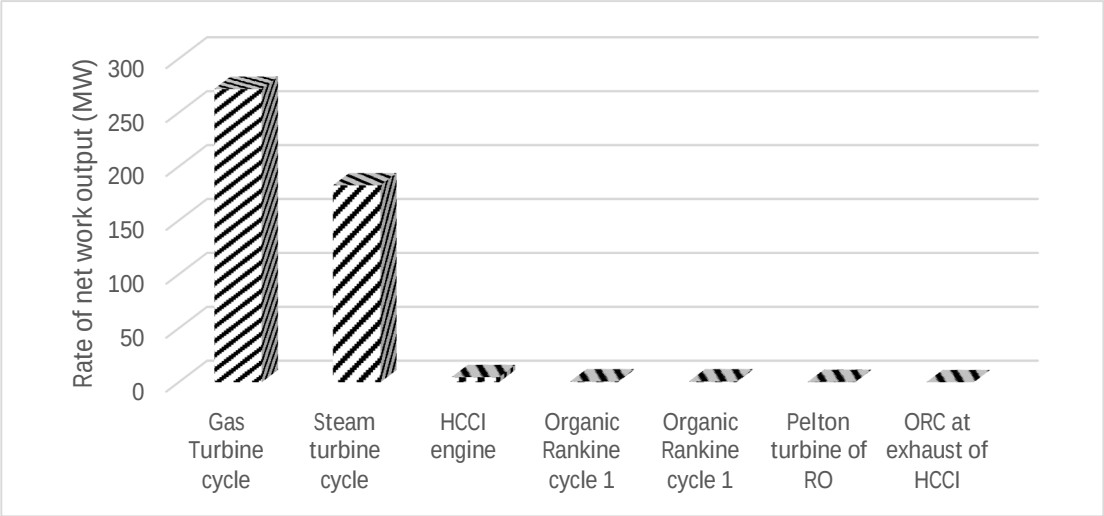

Figure 5.38 Rate of work output by the major sub-systems of the proposed system 3

The effects of fluctuation of mass flow rate of steam in the gasifiers of the proposed system 3 on the volume fraction based composition of the syngas are illustrated in Fig. 5.39.

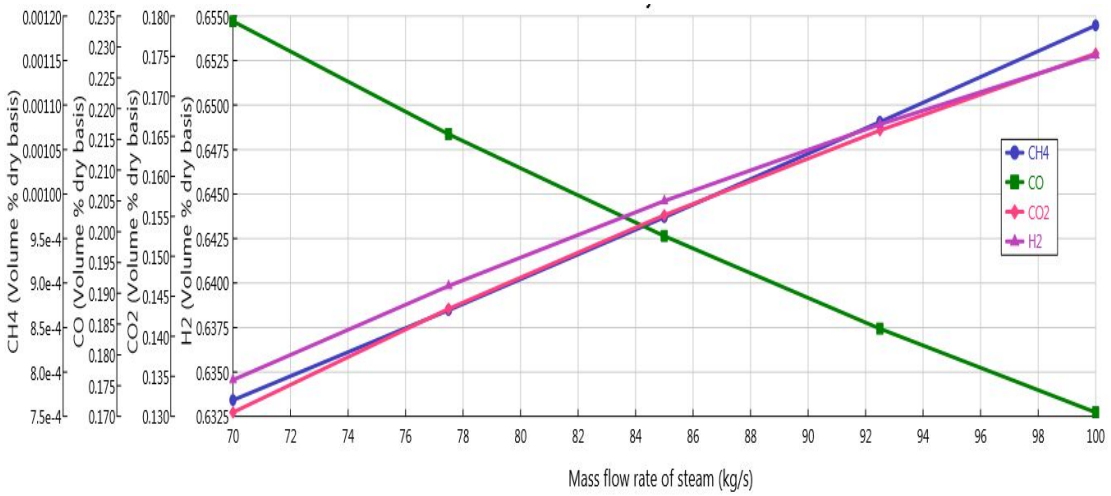

Figure 5.39 Effects of variation in the mass flow rate of steam on gas yield for the system 3

The yield of methane and carbon dioxide and hydrogen in this model increases when the mass flow rate of steam is increased from 70 kg/s to 100 kg/s whereas, the yield of carbon monoxide is decreased with the increase in mass flow rate of steam. This trend follows same pattern as of system 1 and system 2 with slight variation in the gas yield. This trend is observed because of the reason that more amounts of hydrogen and oxygen are available in the gasifier to convert these into methane, carbon dioxide and hydrogen.

The yield of methane and carbon dioxide and hydrogen in system 3 follow the same trend as in system 1 and system 2 with some variation in the volume fraction based yield as depicted in Fig. 5.40. The yield of gases CH_4, CO_2 and H_2 is enhanced with the rise in the temperature of combustion reactor whereas, the yield of CO decreases with the increase in the combustion reactor. This is due to the same reason heat of the combustion reactor is the driving factor of the gasifier and the temperature of the gasifier increases with the increase in the combustion temperature which in turn favors the heterogeneous reaction 1 in Table 4.7 as compared to the other reactions. On the other hand, the yield of carbon monoxide decreases because of the same reason as discussed in system 1 and system 2.

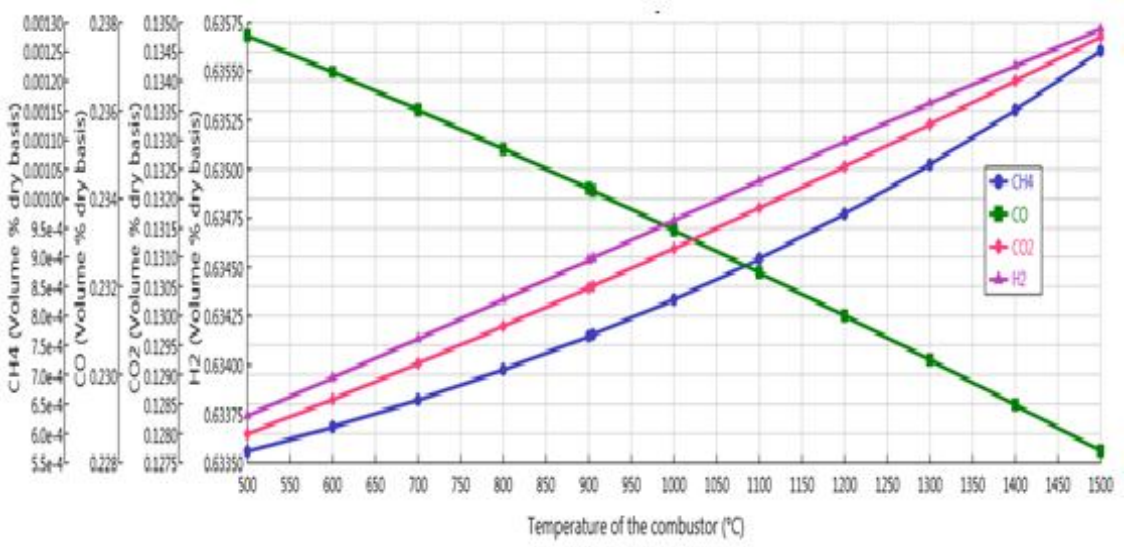

Figure 5.40 Effects of variation in the combustion temperature on gas yield for the system 3

The fluctuations in the LHV and HHV of syngas of system 3 are observed against the variation in the mass flow rate of the steam from 70 kg/s to 100 kg/s as depicted in Fig. 5.41. The lower heating value and higher heating value of the produced syngas are decreased from 16.2 MJ and 18.3 MJ to 14.9 MJ and 17.1 MJ, respectively.

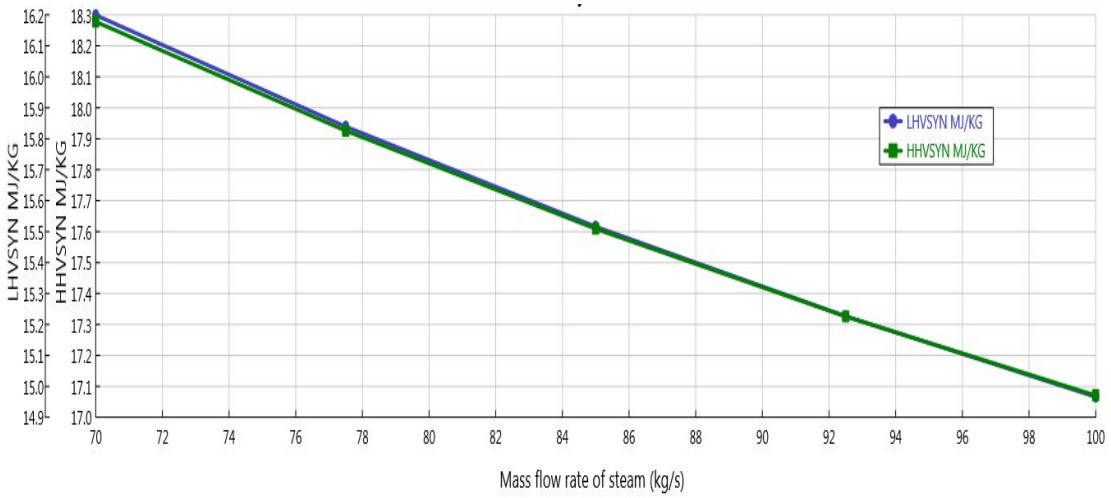

Figure 5.41 Effects of variation in the mass flow rate of steam on calorific values of the syngas for the system 3

The cold gas energy efficiency of the syngas and work rate of Gas turbines are plotted against the fluctuation in the mass flow rate of water from 70 kg/s to 100 kg/s as shown in Fig. 5.42. Cold gas energy efficiency and the work rate of turbines decrease with

the increase in the mass flow rate of water. This is because of the reason that the lower heating value of the syngas reduces with the increase in the mass flow rate of the water.

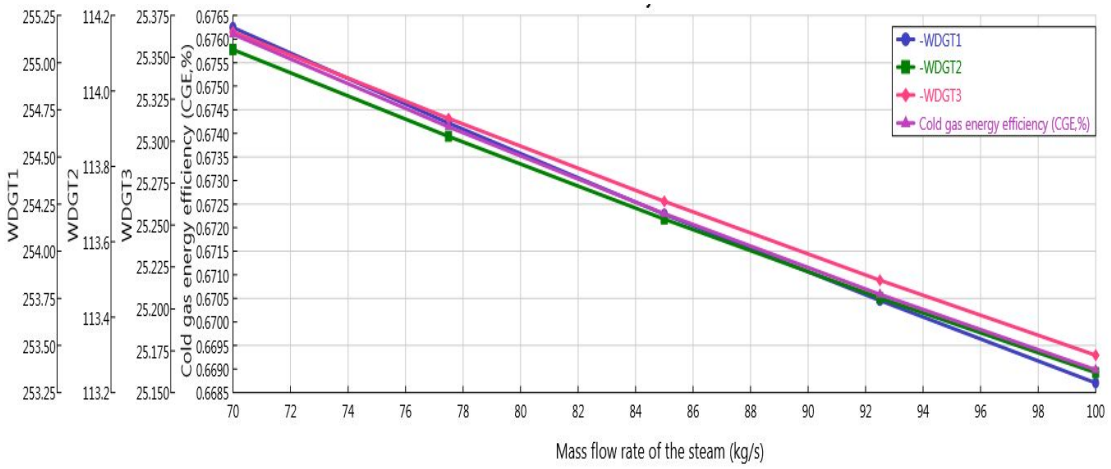

Figure 5.42 Effects of variation in the mass flow rate of steam on the syngas efficiencies and work rate of GT for the system 3

The inlet temperature of gas turbine is varied from 1600 to 1873K to make an assessment of its effects on overall energy and exergy efficiencies of proposed system 3 as depicted in Fig. 5.21. The magnitude of energetic and exergetic efficiencies of the proposed system 3 are increased from 58% to 60.5% and from 32% to 34.7%, respectively, with the rise in temperature from 1600 K to 1873 K. The syngas at high temperature has high enthalpy, which is the main reason for this enhancement.

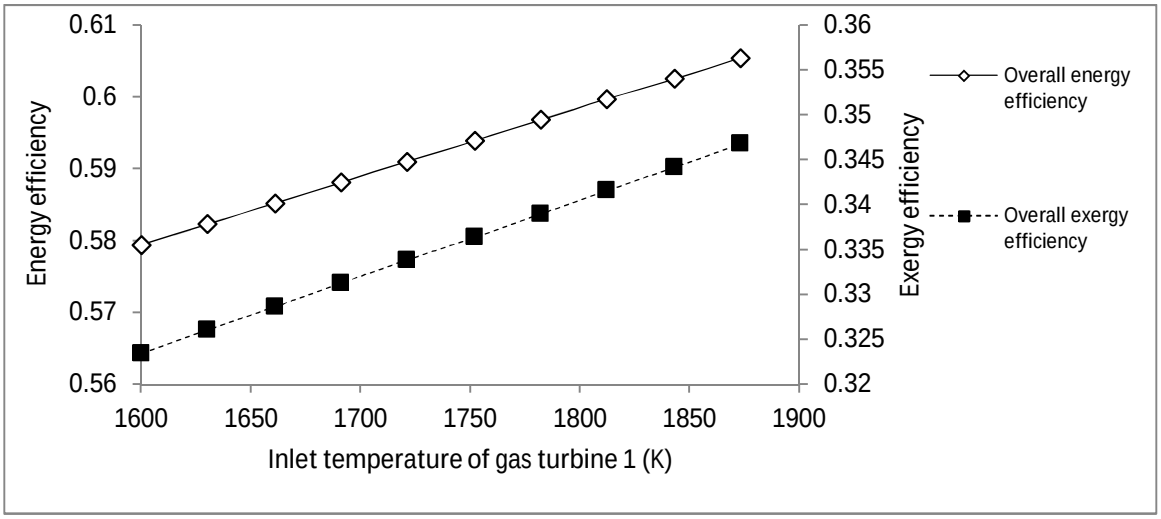

Figure 5.43 Effects of variation in the inlet temperature of gas turbine 1 on overall efficiencies of the system 3

The effects of fluctuation in the ambient temperature are plotted against the exergy destruction rate in the major sub-systems of the proposed system 3 as shown in Fig. 5.44. The magnitude of exergy destruction rate in syngas combustion chamber, biomass combustor, gasifier, gas turbine, organic Rankine cycle 2 and steam turbine decreases with the increase in the ambient temperature. This pattern is observed because of the reduced finite temperature difference between operating temperatures of these sub-systems and ambient.

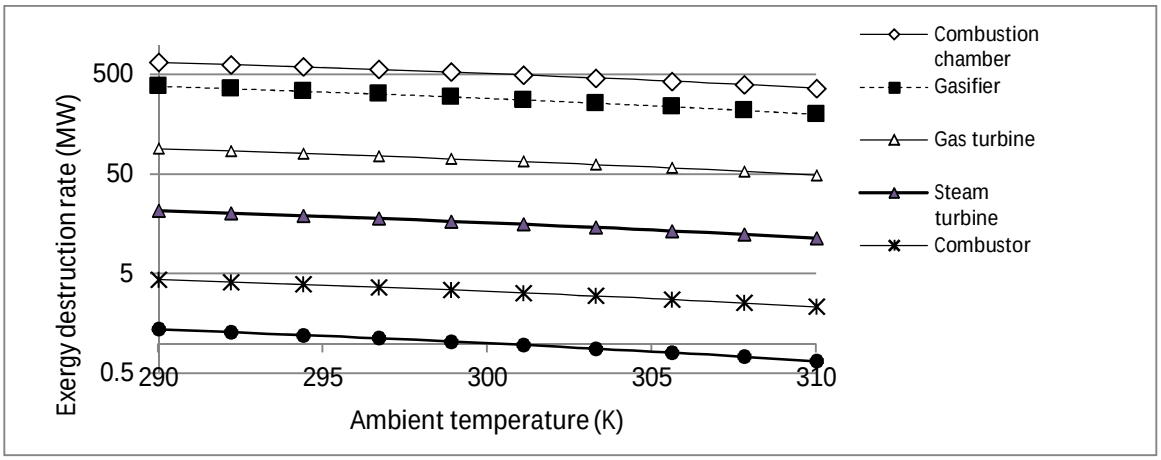

Figure 5.44 Effects of variation in the ambient temperature on the exergy destruction of the major components of the system 3

Islam et al. [58] successfully developed an integrated multigeneration system including HCCI engine which is a sub-system of the proposed system 3. Each subsystem is modeled and governing equations are analyzed using Engineering Equation Solver (EES) which is a numerical solver function to solve algebraic equations. The performance analyses of the proposed system are carried out for given operating conditions. In the exergy analysis the dead state is defined to have a pressure P_0=101.325 kPa and temperature T_0=298 K. The components of the proposed HCCI engine are considered to be as a control volume and steady state open system. Overall burn rates in HCCI are fast so these are approximated as ideal Otto cycle. The energy and exergy efficiencies of overall system without RO plant are increased from 42.7% and 37.9%, to 53.4% and 46.8%, respectively. This huge increase in the energy and exergy efficiencies of overall system excluding RO plant is mainly due to the effective utilization of the waste heat in ORC turbines, absorption chillers, heat pump and thermal energy storage system.

In addition to this, engine exhaust is used for raising the temperature of working fluid R113 which runs turbine and then absorption refrigeration system 3. The exergy efficiencies of the reverse osmosis (RO) plant and overall system including RO plant are increased from 6.4% to 8.7% and 44.1% to 45.01%, respectively, after integrating Pelton turbine. It is important to note that the exergy efficiency of overall system decreases after incorporating RO plant which is due to the high exergy destruction associated with RO module and high pressure pump. In this case, the demand of sweet water is met at the expense of the high exergy destruction in the system. The energy and exergy efficiencies of ORC turbine are 14.2% and 16.8%, respectively. Moreover, the maximum power produced by the HCCI is 4805 kW. This high power output is because of high temperature and pressure produced as result of combustion in the power stroke. The high temperature and pressure is due to the high calorific value (120 MJ/kg) of hydrogen blended as a fuel for combustion. Another reason for this is the high capacity (2.4 liter) of each cylinder and coupling of four cylinder engine with the turbocharger which helps to generate high pressure of 33369 kPa during the work stroke of the HCCI engine.

Fig. 5.45 shows the effects of increasing the engine exhaust from 682 K to 725 K on the energy and exergy efficiencies of the ORC turbine and overall system with and without absorption chiller.

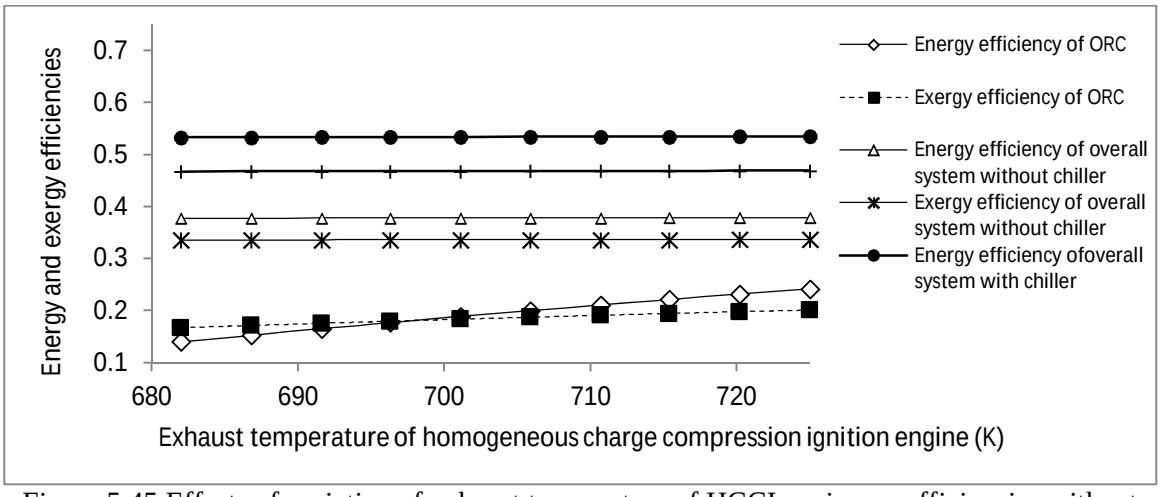

Figure 5.45 Effects of variation of exhaust temperature of HCCI engine on efficiencies without chiller

The energy and exergy efficiencies of the ORC turbine increase from 14% to 24% and 16.8% to 20.2%, respectively. This is because of the increase in the inlet enthalpy of the ORC turbine because the exhaust temperature is increased while keeping the mass flow

rate of ORC working fluid R133 constant. The energy and exergy efficiencies of the overall system with and without absorption chiller also increase with the increase in the temperature of engine exhaust. The effects of increasing the mass flow rate of engine exhaust from 0.29kg/s to 0.35kg/s on the energy and exergy efficiencies of the ORC turbine and overall system with absorption chiller are presented in Fig. 5.46. The energy and exergy efficiencies of the ORC turbine increase from 14.2% to 26.4% and 16.8% to 20.9%, respectively. The energy and exergy efficiencies of the overall system with absorption chiller also increase with the increase in the temperature of engine exhaust.

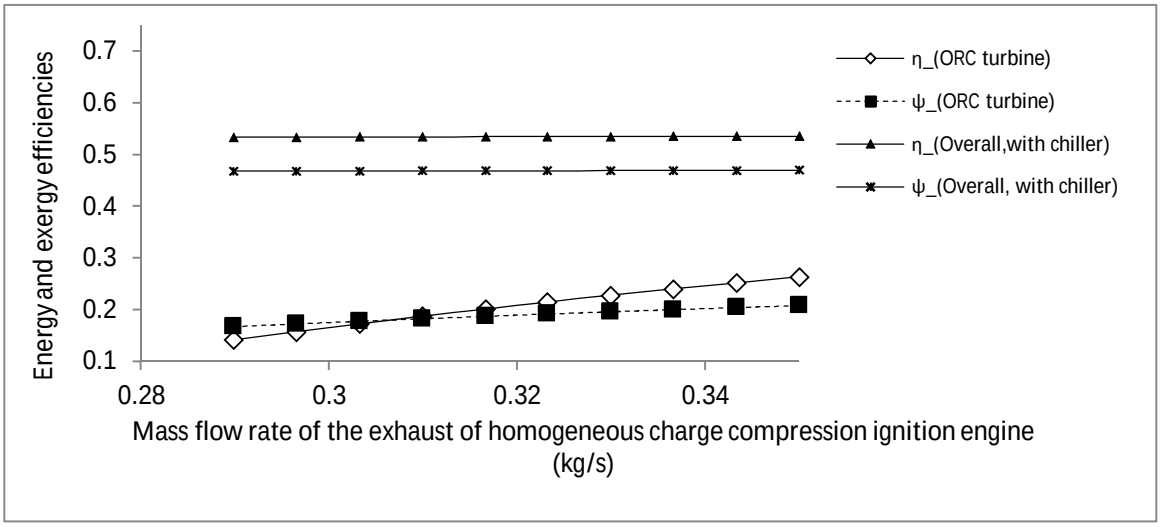

Figure 5.46 Effects of variation of mass flow rate of the exhaust of HCCI engine on efficiencies with chiller

The effects of variation of cylinder volume on energy and exergy efficiencies are presented in Fig. 5.47. The energy and exergy efficiencies and output power of the HCCI engine increase by increasing the cylinder volume due to the increase in the amount of air fuel mixture.

The reference environment temperature is another critical parameter that has a significant impact on the performance of the system. The effects of varying ambient temperature on the exergy destruction in the components of homogeneous charge compression ignition engine are shown in Fig. 5.48.

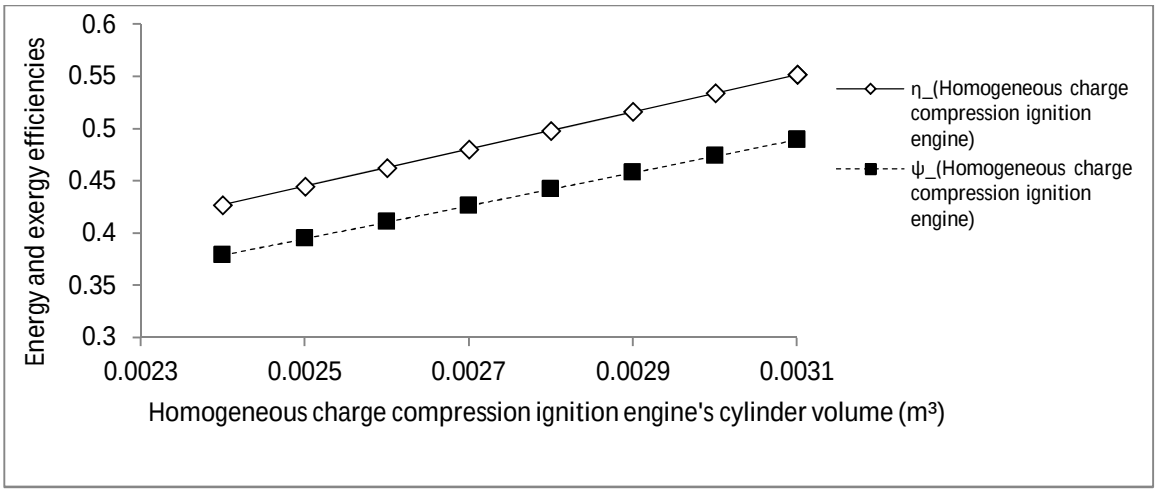

Figure 5.47 Effects of variation of cylinder volume on efficiencies of HCCI engine

It can be seen that the exergy destruction in all components of HCCI engine decreases with the increase of ambient temperature from 298 K to 310 K. This is because the entropy generation in these sub units is decreased due to the reduction in the finite temperature difference between operating and environment conditions.

The effects of increasing the mass flow rate of the fresh water from 100kg/s to 500kg/s on the net power input to RO plant, work input to low pressure and high pressure pump, and power output by Pelton turbine are presented in Fig. 5.49.

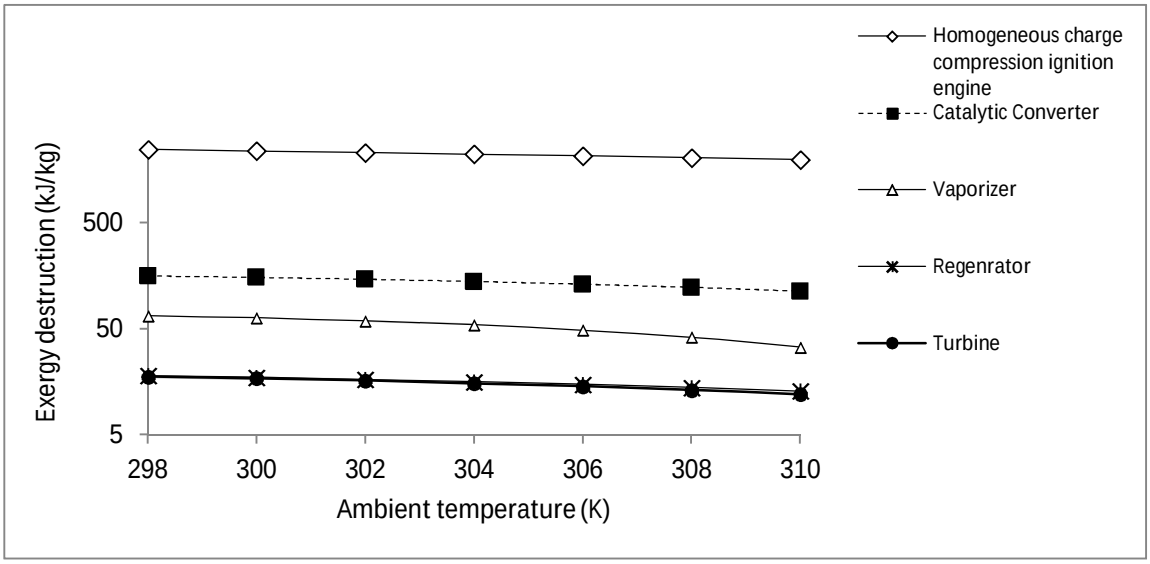

Figure 5.48 Effects of variation of ambient temperature on exergy destruction in engine components

The work done by all components increases with the increase in the mass flow rate, but the work input to the high pressure pump has a steep increase as compared to other units. This is because of the fact that the volume flow rate of the saline increases with the increase in the fresh water. Moreover, the pressure difference between exit and inlet states of this pump is very high. Therefore, the net work done follow the same pattern because the work input to the high pressure pump has a major contribution in the net work done required to run the RO plant.

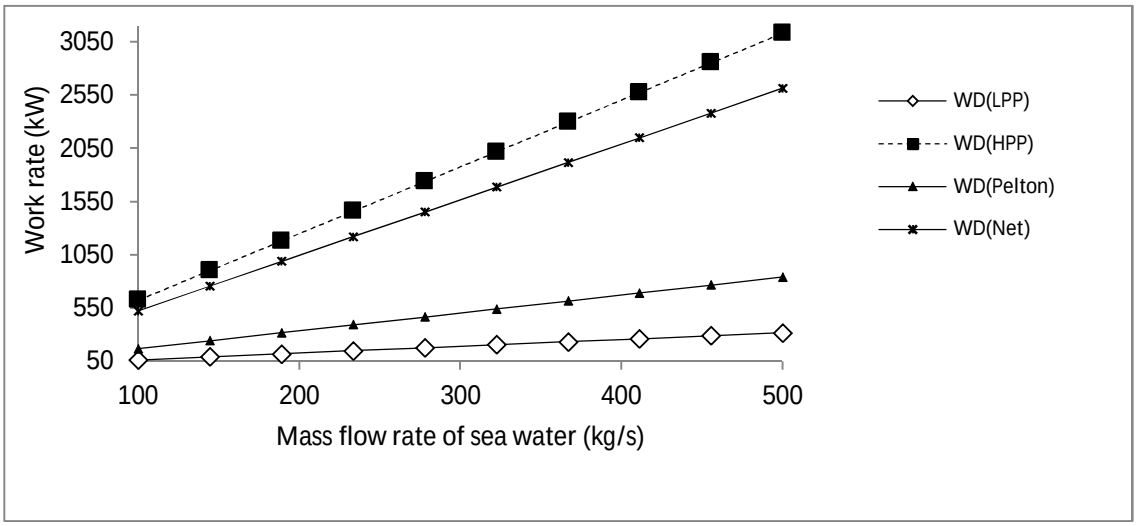

Figure 5.49 Effects of variation of mass flow rate of seawater on work done by the pumps and Pelton turbine

Fig. 5.50 represents the effects of increasing the recovery ratio from 0.35 to 0.75 on the net power input to RO plant, work input to low pressure and high pressure pump, and power output by Pelton turbine. The power required to drive low and high pressure pumps decreases with the increase in the recovery ratio. This is due to the fact that recovery ratio is increased while keeping the feed water rate constant. It is important to note that the power required to drive the high pressure pump is almost equal to the net power required to drive the RO plant. This is due to the fact that, at this state, the input power to the low pressure pump is almost equal to the power recovered by the Pelton turbine.

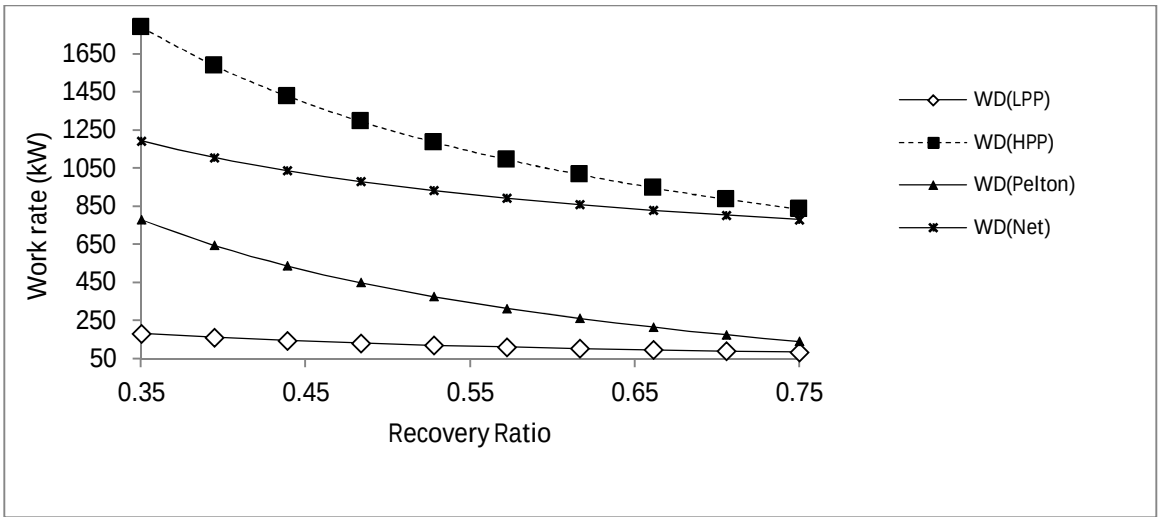

Figure 5.50 Effects of variation of recovery ratio on work done by the pumps and Pelton turbine

The properties of hydrogen used for the analyses of HCCI engine are tabulated in Table 5.1. The lower heating values and the higher heating values for the hydrogen are the highest as compared to other fossil fuels. The lower heating value and research octane number of hydrogen is significantly high as compared to other fuels. The density of ethanol and gasoline are very close to each other whereas, the density of hydrogen is significantly low.

Table 5.1 Comparison of fuel properties of ethanol, gasoline and hydrogen

Property	**Ethanol**	**Gasoline**	**Hydrogen**
Chemical formula	C_2H_5OH	C_8H_8	H_2
Molecular weight (kg/kmol)	46	114	2
Oxygen percent (weight %)	34.8	Nil	Nil
Density (kg/m^3)	785	760	0.08
Boiling temperature at 1 atm (°C)	78.3	145.1	34.2
Latent heat of vaporization (kJ/kg)	840	305	461
Stoichiometric air/fuel ratio	9.0	14.6	34.2
Lower heating value of fuel (MJ/kg)	26.9	44.0	120
Research octane number (RON)	107	92-98	130
Motor octane number (MON)	89	80-90	-

Source: [115]

The design and operating parameters used for the reverse osmosis plant are presented in Table 5.2. The fresh water production is targeted to 100 kg/s and membrane recovery factor for the base case is selected 0.6. The isentropic efficiencies of low pressure and high pressure pumps as well as Pelton turbine are taken to be 85%. The salinity of the water and ambient temperature for the base case are selected as 35,000 PPM and 25°C, respectively.

Table 5.2 Operating and design parameters of RO plant

Parameter	**Values**
Product water flow rate	100 kg/s
Salinity of product water	450 PPM
Sea water salinity	35,000 PPM (base case)
Sea water feeding temperature	25 ^{0}C (base case)
High pressure pump efficiency, η_{HPP}	85%
Low pressure pump efficiency, η_{LPP}	85%
Pelton turbine efficiency, η_{PT}	85%
Plant load factor f_l	90%
Membrane recovery ratio, r_r	0.6 (base case)
Membrane replacement factor, r_m	10%
Membrane salt rejection ratio	99%
Salt water permeability constant, k_s	2.03×10^{-5} m^3/m^2 s kPa
Water permeability constant, k_w	2.05×10^{-6} m^3/m^2 s kPa

Source: [126].

5.5 Comparative Analysis

A comparative study of all three proposed systems reveals that the energy and exergy efficiencies of the Gas turbine of system 1 is found to be the highest followed by system 2 as depicted in Table 5.3.

The comparison of rate of work input required by the sub-systems of all three proposed systems is represented in Table 5.4. The highest rate of work input required is by the compressor of the Gas turbine cycle followed by the pump of steam turbine cycle.

It is obvious that the rate of work input required by the compressor is same in all three systems because of the reason that the flow of air and exit pressure of the air is kept

same in all systems for the comparison. The pump of the organic Rankine cycle is the third in rate of work input to the system. The least amount of work input required is 54 kW by the pump of ORC 1.

Table 5.3 Comparison of efficiencies of major sub-systems of the all three proposed systems

Component	**System 1**		**System 2**		**System 3**	
	Energy efficiency (%)	**Exergy efficiency (%)**	**Energy efficiency (%)**	**Exergy efficiency (%)**	**Energy efficiency (%)**	**Exergy efficiency (%)**
Gas Turbine Cycle	29.8	26.7	29.2	25.9	27.81	24.65
Steam Turbine Cycle	34.11	60.13	33.65	61.66	34.37	60.35
ORC1	9.8	68.75	9.8	68.75	7.5	77
ORC2	21.62	93	21.25	92.2	21.3	92.4
ORC3	-	-	18.82	75.56	-	-
Overall	55.92	32.14	57.94	33.27	60.71	34.83
CGE & CGEX	58.17	57.6	62.08	61.41	68.32	68.71

The comparison of rate of work output obtained from sub-systems of all three proposed systems is tabulated in Table 5.5. The highest rate of work output is by the Gas turbine cycle followed by the steam turbine cycle. The highest rate of work output by the Gas turbine cycle is because of the high inlet enthalpy of the combustion gases entering turbine.

Table 5.4 Comparison of the input power required to drive major compressors and pumps of all three proposed systems.

Parameter	**System 1 (MW)**	**System 2 (MW)**	**System 3 (MW)**
Gas turbine compressor	122.6	122.6	122.6
Steam turbine pump	3.1	3.1	3.1
Syngas cooler pump	0.07	0.07	0.07
ORC1 pump	0.054	0.054	0.054
ORC2 pump	1.4	1.4	1.4
ORC3 pump	-	1.4	-
LP of (RO)	-	0.11	0.11
HP of (RO)	-	1.1	1.1
RO (net)		0.87	0.87

The reverse osmosis plant is not included in system 1 whereas, it is incorporated in food industry. Desalination plant and HCCI engine both are integrated with system 3 to meet the fresh water and additional load requirements of the refinery.

Then, the heat of the gas turbine exhaust is recovered to produce steam to run steam turbine. The organic Rankine cycle 2 has the third highest rate of work output as it recovers the waste heat of the exhaust gas coming out of the steam generator. The homogeneous charged compression ignition (HCCI) engine in proposed system 3 produces additional amount of power output 4806 kW.

Table 5.5 Comparison of the net rate of work output by the major sub-systems of all three proposed systems

Rate of work output by major sub-systems	**System 1(MW)**	**System 2 (MW)**	**System 3 (MW)**
Gas Turbine cycle	268.9	251.9	272.1
Steam turbine cycle	176.75	164.7	182.7
Organic Rankine cycle 1	1.308	1.31	0.84
Organic Rankine cycle 2	14.3	14	14
Organic Rankine cycle 3	-	-	-
Pelton turbine of RO	-	0.28	0.28
HCCI engine	-	4.81	4.81
ORC at exhaust of HCCI	-	0.018	0.018

Table 5.6 tabulates the comparison of the capacities of producing cooling and heating rates by the major sub-systems of all three proposed systems. It is important to note that significant saving in electricity is possible due to the huge amount of cooling produced through absorption chillers, which would otherwise be produced through electricity driven air conditioners.

The system irreversibilities are investigated to figure out the sub-systems responsible for the losses. The ranking of the sub-systems with respect to the exergy destruction occurring in them shows the same pattern in all proposed systems with some deviated in the amount of exergy destruction.

Table 5.6 Comparison of the production of heating, cooling and hot water by the major sub-systems of all three proposed systems

Sub-system	**System 1 (MW)**	**System 2 (MW)**	**System 3 (MW)**
Absorption Chiller (cooling rate)	213.5	185.3	214.8
Space heater (heat rate)	170.6	166.5	162.8
TES	4.8	4.8	4.8
Water heater (heat rate)	16.7	16.7	16.7
Heat Pump (heat rate)	-	1.6	-

All proposed systems have the highest exergy destruction in the syngas combustion chamber due to the irreversibilities associated with the combustion. The gasifier which converts the feedstock into syngas is ranked 2 in exergy destruction.

Table 5.7 Comparison of the exergy destruction in the major sub-systems of all three proposed systems

Rank	**Major sub-systems**	**System 1**	**System 2**	**System 3**
		Exergy destruction (MW)	Exergy destruction (MW)	Exergy destruction (MW)
1	Syngas C.C	658.624	604.484	665.405
2	Gasifier	372.051	508.748	373.295
3	Space heater	98.128	98.128	98.128
4	GT Cycle	90.326	98.268	89.525
5	Generator 2	52.578	45.557	52.868
6	Water heater	38.406	44.201	38.733
7	ST Cycle	17.982	19.476	17.872
8	Evaporator 2	16.395	14.206	16.485
9	Air compressor	9.615	9.615	9.615
10	Combustor	5.312	5.312	4.328
11	HCCI engine	-	-	2.478
12	Heat pump	-	1.498	-
13	ORC2	1.444	1.254	1.284
14	TES	0.683	0.683	0.683
15	Generator 1	0.524	0.524	0.524
16	Evaporator 1	0.163	0.163	0.163

The amount of carbon in the inlet feedstock is responsible for the carbon dioxide emissions. The emission of CO_2 produced by the all proposed systems are compared against a biomass based IGCC system as represented in Fig. 5.51. The comparative study reveals imperative results for system 1 and system 2. It is important to note that the mix feedstock ratio 2 of animal manure to biomass is highly environmental benign as compared to other compositions $\left(\frac{Animal\ Manure}{Biomass} = 2\right)$.

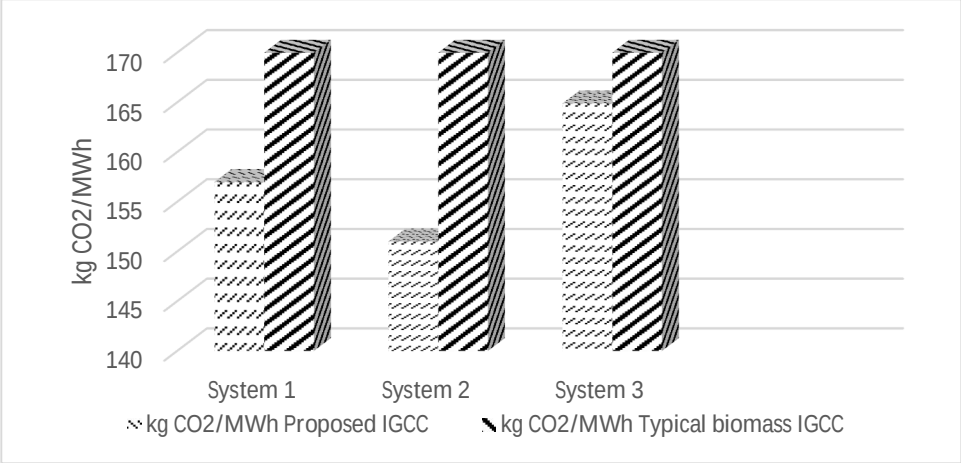

Figure 5.51 Comparison of emissions between conventional biomass based IGCC and proposed systems

The amount of CO_2, SO_2, NO and NO_2 produced per MWh of electricity for the proposed system 1, system 2 and system 3 is tabulated in Table 5.8. The production of carbon dioxide is compared with a typical biomass based IGCC plant reported in literature [127], whereas, the production of SO_2, NO, NO_2 and CO is compared with the research reported by Brown et al. [8]. It can be seen that carbon dioxide emission is low for system 1 and system 2 whereas, for system 3 emission is marginally low due to addition of heavy oil which contains 87% carbon. The emission of other species is also less in proposed systems as compared to the reported in literature.

Nevertheless, the CO_2 emissions are less in all proposed systems as compared to the typical biomass based integrated combined cycles. It is important to note that the carbon, nitrogen and sulfur based emissions are the least in system 2 as compared to the other two developed systems.

Table 5.8 Comparison of the emissions produced between a conventional biomass based IGCC system and proposed systems

Emission/Power	**Biomass IGCC Ref.** [127]**,** [8]	**System 1**	**System 2**	**System 3**
$\frac{kg\ CO_2}{MWh}$	170	157	151	164.9
$\frac{kg\ SO_2}{MWh}$	0.07	0.06	0.05	0.06
$\frac{kg\ (NO + NO_2)}{MWh}$	0.05	0.04	0.03	0.045
$\frac{kg\ (CO)}{MWh}$	0.015	0.012	0.01	0.013

5.6 Model Validation

The existing biomass based IGCC systems reported in the literature are not similar to the developed systems therefore, the data of a typical biomass based IGCC system from literature [128] is selected and fed in the developed model to validate the composition of the syngas produced. Dry basis syngas composition free of NH_3, H_2S and HCl and lower heating value of syngas are tabulated in Table 5.9. All the results obtained from the developed model for the typical biomass feedstock are in line with the research reported to date.

Table 5.9 Model validation for syngas composition against a typical biomass operated IGCC

Parameter	**Literature** [122,104, 125]		**Model results**
Syngas composition (Vol % dry and free of NH_3, H_2S, HCL)	H_2	45.8	46.3
	CO	21.6	21.4
	CH_4	10	10.73
	CO_2	21.2	20.07
	N_2	1.4	1.5
Syngas LHV (dry at 0°C and 1 atm)	11.3 MJ/m^3		11.7 MJ/m^3
CGE (LHV and mass basis	71.5%		68.71%

The input parameters like mass flow rate and temperature of organic cycle and gas turbine in the developed model are set same as reported in literature to validate net amount of output work rate of organic Rankine cycle, and energy and exergy efficiencies of the gas turbine. The results tabulated in Table 5.10 are within good agreement as compared to the literature.

Table 5.10 Comparison of the results obtained from present modelling with the results reported in the literature

Parameter	**Present Work**			**Literature**
	System1	**System2**	**System3**	Ref. [18], [131]
$\dot{W}_{net,ORC,total}(ORC1 + ORC2)\ kW_e/kW_{th}$	0.26	0.27	0.255	0.25
η_{gt} (%)	29.8	29.2	27.8	30.4
ψ_{gt} (%)	26.7	25.9	24.7	28.8

The capital cost analyses are outlined and compared with literature in Table 5.11. The cost of an IGCC system ranges between \$1100/kW to over \$1700/kW [132]. The overall plant cost for system 1, system 2 and system 3 is found to be in the order of \$1554/kW, \$1609/kW and \$1544/kW, respectively. It can be seen that total cost of the proposed system is within the cost range of an IGCC system reported in the literature despite the fact that extra heat exchanger and sub-systems are needed for multigeneration.

Table 5.11 Comparison of total capital cost of proposed system with literature

Equipment	**System 1 USD (M)**	**System 2 USD (M)**	**System 3 USD (M)**	**Sources**
Gasifier	395	395	395	[133]
Heat exchangers	6.1	6.1	6.1	[134]
Heat recovery steam generator	30.5	30.5	31	[133]
Steam turbines & generators	36.9	35	36.9	[133]
Gas turbines & generators	69.2	69.2	69.2	[133]
Steam condenser	3.7	3.5	3.7	[133]
Deaerator	1	1	1	[133]
Drums	1	1	1	[135]
Reactors	0.5	0.5	0.5	[135]
Recirculated cooling	1.9	1.7	1.9	[135]
Waste water treatment	5.1	5.1	5.1	[135]
Glycol drying unit	1.7	1.7	1.7	[136]
Pumps	4.7	4.5	4.7	[135]
Absorption chiller	40	34.73	40.3	[137]
Reverse osmosis		1.2	1.2	[138]
HCCI engine	-	-	0.9	[139]
Total Capital cost	597.3	580.73	600.2	
Operating and maintenance cost = 0.2*Capital Cost	119.5	116.15	120.04	[132]
Total Cost	716.8	697	720.24	

The built-in function in Aspen (Plus) V9 and Thermoflow Suite 26 are used to determine the cost of the major components of the proposed systems. The cost of some components are also taken from literature. The cost of electricity is calculated and depicted in Table 5.12. It can be seen that the cost of electricity for each kWh produced for system 1, system 2 and system 3 is found to be 5 cents, 4.7 cents and 5.1 cents, respectively.

Table 5.12 Comparison of cost of electricity of the proposed systems

Estimated Cost of Energy	**System 1**	**System 2**	**System 3**
O & M (cent/kWh)	0.8	0.8	0.9
Fuel (cent/kWh)	0.7	0.5	0.7
Capital (cent/kWh)	3.5	3.4	3.5
Cost of electricity (cent/kWh)	5	4.7	5.1

The power generated in MW, thermal energy produced and exergy destroyed per kg of the fuel input are compared and validated with the results of comprehensive exergy analyses conducted by Siefert et al. [140]. The amount of exergy destruction in the gasifier of the proposed system is little higher than the literature but the overall exergy destruction is in line with the literature as depicted in Table 5.13.

Table 5.13 Model validation of power and exergy destruction associated with heat transfer

Parameter	**Gasifier**				**Overall**			
	Sys1	**Sys2**	**Sys3**	**Ref.**[140]	**Sys1**	**Sys2**	**Sys3**	**Ref.**[140]
Power (MW/kg)	-	-	-	-	8.5	8	13	9.1
Heat (MW/kg)	2.3	2.4	2.3	2.5	11.9	10.8	14	12.9
Exergy destroyed (MW)	6	7	8	4.9	18.4	17.8	19.1	16.1

5.7 Optimization

The optimization of all three proposed systems is done using built-in function Genetic algorithm in Engineering Equation Solver. The genetic algorithm is able to solve optimization problems related to both constrained and unconstrained. It is a process that drives biological evolution and it is based on natural selection. The genetic algorithm is a global solution rather than localized solution means it keeps checking even if the optimized values are found to make sure that there is no better solution beyond. It repeatedly modifies a population of individual solutions.

Three objectives used in developing an optimization function include the following:

1. Maximize exergy efficiency
2. Minimize cost
3. Minimize emissions

The mass flow rate of feedstocks, at the inlet of Gas turbines, steam turbine cycle and temperatures at the inlet of Gas turbines, steam turbine cycle and absorption chiller 2 are optimized for system 1 and results are presented in Table 5.14

Table 5.14 Optimized values of the syngas mass flow rate and inlet temperatures for the proposed system 1

Parameter	**Optimised Values**
Mass flow rate at Gas turbine inlet (kg/s)	520
Mass flow rate at steam turbine inlet (kg/s)	75
Mass flow rate of animal manure (kg/s)	10
Mass flow rate of biomass (kg/s)	10
Mass flow rate of food waste (kg/s)	10
Inlet temperature at Gas turbine 1 (K)	1800
Inlet temperature at Gas turbine 2 (K)	1400
Inlet temperature at Gas turbine 3 (K)	1300
Inlet temperature at steam turbine cycle (K)	1000
Inlet temperature at absorption chiller 2 (K)	325

The mass flow rate of feedstocks, at the inlet of Gas turbines, steam turbine cycle and temperatures at the inlet of Gas turbines, steam turbine cycle and absorption chiller 2 are optimized for system 2 and results are presented in Table 5.15

Table 5.15 Optimized values of the syngas mass flow rate and inlet temperatures for the proposed system 2

Parameter	**Optimised Values**
Mass flow rate at Gas turbine inlet (kg/s)	510
Mass flow rate at steam turbine inlet (kg/s)	130
Mass flow rate of animal manure (kg/s)	30
Mass flow rate of biomass (kg/s)	12
Inlet temperature at Gas turbine 1 (K)	1750
Inlet temperature at Gas turbine 2 (K)	1401
Inlet temperature at Gas turbine 3 (K)	1253
Inlet temperature at steam turbine cycle (K)	950
Inlet temperature at absorption chiller 2 (K)	389

The mass flow rate of feedstocks, at the inlet of Gas turbines, steam turbine cycle and temperatures at the inlet of Gas turbines, steam turbine cycle and absorption chiller 2 are optimized for system 3 and results are presented in Table 5.16

Table 5.16 Optimized values of the syngas mass flow rate and inlet temperatures for the proposed system 3

Parameter	**Optimised Values**
Mass flow rate at Gas turbine inlet (kg/s)	450
Mass flow rate at steam turbine inlet (kg/s)	100
Mass flow rate of heavy oil (kg/s)	10
Mass flow rate of biomass (kg/s)	10
Mass flow rate of food waste (kg/s)	10
Inlet temperature at Gas turbine 1 (K)	1800
Inlet temperature at Gas turbine 2 (K)	1450
Inlet temperature at Gas turbine 3 (K)	1300
Inlet temperature at steam turbine cycle (K)	1060
Inlet temperature at absorption chiller 2 (K)	350

The depletion factor and sustainability index for all proposed systems are tabulated in Table 5.17. The depletion factor is highest for system 1 and least for proposed system 3. Sustainability index is inverse of depletion factor hence, it can be seen that the system 1 is highly sustainable whereas, system 3 is least sustainable based on exergy analysis.

Table 5.17 Depletion factor and sustainability index of all proposed systems

Systems	**Depletion factor**	**Sustainability Index**
System 1	0.678	1.47
System 2	0.667	1.5
System 3	0.652	1.53

CHAPTER 6 CONCLUSIONS AND RECOMMENDATIONS

The refinery waste (heavy oil) mixed with biomass driven IGCC multigeneration system is an alternative for energy sustainability. This study has performed thermodynamic analyses based on energy and exergy to investigate the performance of the multigeneration system and determine the extent of the system components to be enhanced for higher efficiency. Orimulsion is selected for assessment as its properties are available in the literature and its composition is almost same as heavy refinery residue.

6.1 Conclusions

In this thesis study, three new IGCC multigeneration systems are developed and analyzed for community, food industry and oil refinery. In this regard, the energy, exergy and thermal analyses are conducted for three types of feedstocks for gasification. The operating conditions are varied to analyze the effects on the composition of syngas, Gas turbine, steam turbine, space heating, hot water, thermal energy storage system and overall system efficiencies. The integration of renewable energy resources and comprehensive energy and exergy investigations yield imperative results. The overall and cold gas energy and exergy efficiencies for a mixed feedstock of biomass, food waste and heavy oil based system are found to be highest as compared to other two proposed systems. The second highest overall and cold gas energy and exergy efficiencies are found to be for a mixed feedstock of biomass and animal manure based system. The least magnitude of overall and cold gas energy and exergy efficiencies are found to be for a mixed feedstock of biomass, food waste and animal manure based system. The parametric study shows that the LHV and HHV of the syngas produced through all types of feedstock mix are enhanced with the rise in the combustion temperature whereas, overall energetic and exergetic efficiencies of the all three developed models follow a decreasing trend with the increase in the mass flow rate of steam and combustion temperature. Furthermore, some of the significant conclusive remarks are summarized as follows:

1. The costs of electricity for system 1, system 2 and system 3 are found to be 5 cents/kWh, 4.7/kWh cents and 5.1 cents/kWh, respectively.
2. System 1, system 2 and system 3 produce 8.54 MW, 8.02 MW and 13.3 MW, respectively, against 1 kg/sec feed which is significantly high as compared to conventional biomass based IGCC.

3. The amount of CO_2 in kg produced per MWh of electricity for system 1, system 2, and system 3 is found to be 7.6%, 11.1% and 3%, respectively.
4. The highest amount of exergy destruction in the order of 6.65 MW occurs in the combustion chamber of system 3 due to irreversibilities associated with combustion.
5. The highest magnitude of energy and exergy efficiencies of the cold gas and overall system are found to be 68.3% and 68.7%, and 60.7% and 34.8%, respectively, for system 3 as compared to other two developed systems.
6. Energy recovery through Pelton turbine recovers 24.3% of the input power required to drive RO plant.
7. The LHV and HHV of wood (Birch) based system are found to be 12026 kJ/kg and 13628 kJ/kg, respectively. Also, the LHV and HHV of olive waste based system are found to be 12033 kJ/kg and 13614 kJ/kg, respectively.
8. The overall energy efficiencies of wood (Birch) and olive waste based systems are in the order of 35.8%% and 44.5%, respectively.
9. On-site H_2 consumption in HCCI engine reduces the huge cost of compression, storage and transportation.
10. The overall exergy efficiencies of wood (Birch) and olive waste based systems are found to be 71% and 61.5%, respectively.
11. The feedstock composition of 33% biomass and 67% animal manure is highly environmental benign.
12. The major system irreversibilities are associated with the combustion chamber of syngas followed by the gasifier with exergy destruction of 89% and 5.73%, respectively.
13. The largest exergy destructions related to RO plant appear to be in the order of 992.9 kJ/kg and 101.3 kJ/kg for the high-pressure and low pressure pumps, respectively.

6.2 Recommendations

The three developed novel systems can be used anywhere in the world with adjustment to composition of the feedstock. It is recommended to select the system that best fits the type of available waste. Further improvements can be investigated in future studies which can include experimental results to validate the predictions of analytical studies. It is crucial to transform the waste into useful outputs including hydrogen with less CO_2 emissions to mitigate global warming. Hence, it is imperative to integrate multigenerational sub-systems with IGCC to achieve high energy and exergy efficiency. Future studies should complement and integrate these resourceful integrated gasification combined cycles for multigenerational systems with the following

- A prototype of proposed model should be built to investigate and compare its performance with the results of this study.
- The potential of integration of developed systems with renewable energy resources like solar and geothermal should be conducted and assessed.
- A study should be conducted using built-in plug reactor in Aspen which requires detailed chemical reaction kinetics based on experimental results and provides results which are comparable to an actual reactor.
- The feedstocks composed of used tires, hospital waste, leather waste and sunflower residue should also be investigated for IGCC multigeneration applications. This kind of investigation requires a custom built gasifier.
- The reinjection of CO_2 to the gasifier should be investigated to assess its effects on syngas production as well the emissions.
- The low cost CO_2 compression techniques should be explored to sell it to the oil exploration companies as compressed CO_2 is injected in oil wells with low levels to enhance the oil recovery.
- The technological advancement in gas turbine design and material need to be improved to enable it to operate solely on the hydrogen as a fuel as well as its ability to handle working fluid at a temperature higher than 1700°C.

REFERENCES

[1] "Renewables 2014 Global Status Report," 2014. [Online]. Available: http://www.ren21.net/portals/0/documents/resources/gsr/2014/gsr2014_full report_low res.pdf. [Accessed: 07-May-2015].

[2] M. Ratner and C. Glover, "U.S. energy: Overview and key statistics," *Congressional Research Service*. 2014.

[3] "Energy Information Administration US, Annual energy outlook report." [Online]. Available: https://www.eia.gov/outlooks/aeo/pdf/0383(2017).pdf. [Accessed: 20-Mar-2017].

[4] H. Liu, W. Ni, Z. Li, and L. Ma, "Strategic thinking on IGCC development in China," *Energy Policy*, vol. 36, no. 1, pp. 1–11, 2008.

[5] M. Pérez-Fortes, A. D. Bojarski, E. Velo, J. M. Nougués, and L. Puigjaner, "Conceptual model and evaluation of generated power and emissions in an IGCC plant," *Energy*, vol. 34, no. 10, pp. 1721–1732, 2009.

[6] N. Lior, "Energy resources and use: The present situation and possible paths to the future," *Energy*, vol. 33, no. August 2006, pp. 842–857, 2008.

[7] S. Shelley, "IGCC Power Generation – Down But Not Out," 2008. [Online]. Available: http://www.redorbit.com/news/business/1570518/igcc_power_generation__down_ but_not_out/. [Accessed: 05-May-2016].

[8] J. A. Ratafia-Brown, L. M. Manfredo, J. W. Hoffmann, and M. Ramezan, "An environmental assessment of IGCC power systems," in *Nineteenth annual Pittsburgh coal conference*, Pittsburgh., 2002, p. 27.

[9] R. M. Jones and N. Z. Shilling, "IGCC gas turbines for refinery applications." [Online]. Available: https://powergen.gepower.com/content/dam/gepower-pgdp/global/en_US/documents/technical/ger/ger-4219-igcc-gas-turbines-for-refinery-applications.pdf. [Accessed: 06-May-2016].

[10] J. Thompson, "Integrated gasification combined cycle (IGCC) – Environmental performance," Platts IGCC Symposium, Pittsburgh., 2005.

[11] "National Energy Technology Department." [Online]. Available: http://www.netl.doe.gov/research/coal/energy-systems/gasification/gasifipedia/igcc-config. [Accessed: 19-May-2016].

[12] N. Lapa, J. F. Santos Oliveira, S. L. Camacho, and L. J. Circeo, "An ecotoxic risk assessment of residue materials produced by the plasma pyrolysis/vitrification (PP/V) process," *Waste Manag.*, vol. 22, no. 3, pp. 335–342, 2002.

[13] I. Marbee, "New opportunities and system consequences for biomass integrated gasification technology in CHP applications.," Chalmers University of Technology, 2005.

[14] "Types of gasifiers." [Online]. Available: http://www.enggcyclopedia.com/2012/01/types-gasifier/. [Accessed: 01-May-2016].

[15] S. Islam and I. Dincer, "Development, analysis and performance assessment of a combined solar and geothermal energy-based integrated system for multigeneration," *Sol. Energy*, vol. 147, pp. 328–343, 2017.

[16] S. Islam and I. Dincer, "Comparative performance study of an integrated air-cycle refrigeration and power generation system," *Appl. Therm. Eng.*, 2016.

[17] F. Suleman, I. Dincer, and M. Agelin-Chaab, "Development of an integrated renewable energy system for multigeneration," *Energy*, vol. 78, pp. 196–204, 2014.

[18] F. Khalid, I. Dincer, and M. A. Rosen, "Energy and exergy analyses of a solar-biomass integrated cycle for multigeneration," *Sol. Energy*, vol. 112, pp. 290–299, 2015.

[19] "GSTC: Map of facilities." [Online]. Available: http://www.gasification-syngas.org/resources/map-of-gasification-facilities. [Accessed: 01-May-2016].

[20] "The Future of Coal: Options for a carbon-constrained world," 2007. [Online]. Available: http://web.mit.edu/coal/The_Future_of_Coal_Summary_Report.pdf. [Accessed: 12-May-2016].

[21] E. Shoko, B. McLellan, A. L. Dicks, and J. C. D. da Costa, "Hydrogen from coal: Production and utilisation technologies," *Int. J. Coal Geol.*, vol. 65, no. 3–4, pp. 213–222, 2006.

[22] L. Jiang, R. Lin, H. Jin, R. Cai, and Z. Liu, "Study on thermodynamic characteristic and optimization of steam cycle system in IGCC," *Energy Convers. Manag.*, vol. 43, pp. 1339–1348, 2002.

[23] H. C. Frey and Y. Zhu, "Improved system integration for integrated gasification combined cycle (IGCC) systems," *Environ. Sci. Technol.*, vol. 40, no. 5, pp. 1693–1699, 2006.

[24] A. Valero and S. Usón, "Oxy-co-gasification of coal and biomass in an integrated gasification combined cycle (IGCC) power plant," *Energy*, vol. 31, no. 10–11, pp. 1643–1655, 2006.

[25] Z. Yuehong, W. Hao, and X. Zhihong, "Conceptual design and simulation study of a co-gasification technology," *Energy Convers. Manag.*, vol. 47, no. 11–12, pp. 1416–1428, 2006.

[26] A. V. Bridgwater, "Renewable fuels and chemicals by thermal processing of biomass," *Chem. Eng. J.*, vol. 91, no. 2–3, pp. 87–102, 2003.

[27] K. Stahl and M. Neergaard, "IGCC power plant for biomass utilisation, Värnamo, Sweden," *Biomass and Bioenergy*, vol. 15, no. 3, pp. 205–211, 1998.

[28] M. K. Cohce, I. Dincer, and M. A. Rosen, "Energy and exergy analyses of a biomass-based hydrogen production system.," *Bioresour. Technol.*, vol. 102, no. 18, pp. 8466–74, 2011.

[29] M. A. Mujeebu, S. Jayaraj, S. Ashok, M. Z. Abdullah, and M. Khalil, "Feasibility study of cogeneration in a plywood industry with power export to grid," *Appl. Energy*, vol. 86, no. 5, pp. 657–662, 2009.

[30] S. Assima, G. P. Dell'Orco, J. M. Navaee-Ardeh and S. Lavoie, "Catalytic

conversion of residual fine char recovered by aqueous scrubbing of syngas from urban biomass gasification," *Biomass and Bioenergy*, vol. 100, pp. 98–107, 2017.

[31] D. A. Landis, C. Gratton, R. D. Jackson, K. L. Gross, D. S. Duncan, C. Liang, T. D. Meehan, B. A. Robertson, T. M. Schmidt, K. A. Stahlheber, J. M. Tiedje and B. P. Werling, "Biomass and biofuel crop effects on biodiversity and ecosystem services in the North Central US," *Biomass and Bioenergy*, 2017.

[32] D. Martyniak, G. Żurek, and K. Prokopiuk, "Biomass yield and quality of wild populations of tall wheatgrass [Elymus elongatus (Host.) Runemark]," *Biomass and Bioenergy*, vol. 101, pp. 21–29, 2017.

[33] P. Basu, *Biomass Gasification, Pyrolysis and Torrification, Practical Design and Theory*, Second edi. Academic Press, 2013.

[34] V. Wilk, H. Kitzler, S. Koppatz, C. Pfeifer, and H. Hofbauer, "Gasification of residues and waste wood in a dual fluidised bed steam gasifier," *Proc. Int. Conf. Polygeneration Stategies (ICPS 10)*, 2010.

[35] H. Hofbauer, R. Rauch, K. Bosch, R. Koch, and C. Aichernig, "Biomass CHP Plant Güssing - A Success Story," *Expert Meet. Pyrolysis Gasif. Biomass Waste*, 2002.

[36] R. K. Thapa and B. M. Halvorsen, "Stepwise analysis of reactions and reacting flow in a dual fluidized bed gasification reactor," *Adv. Fluid Mech.*, vol. 82, pp. 37–48, 2014.

[37] H. C. Frey and N. Akunuri, "Probabilistic modeling and evaluation of the performance, emissions, and cost of texaco gasifier-based integrated gasification combined cycle systems using ASPEN," 2001. [Online]. Available: http://www4.ncsu.edu/~frey/reports/Frey_Akunuri_2001.pdf. [Accessed: 16-Mar-2016].

[38] G. Ordorica-Garcia, P. Douglas, E. Croiset, and L. Zheng, "Technoeconomic evaluation of IGCC power plants for CO2 avoidance," *Energy Convers. Manag.*, vol. 47, no. 15–16, pp. 2250–2259, 2006.

[39] P. E. Campbell, J. T. McMullan, and B. C. Williams, "Concept for a competitive coal fired integrated gasification combined cycle power plant," *Fuel*, vol. 79, no. 9, pp. 1031–1040, 2000.

[40] M. Kanniche and C. Bouallou, "CO2 capture study in advanced integrated gasification combined cycle," *Appl. Therm. Eng.*, vol. 27, no. 16, pp. 2693–2702, 2007.

[41] S. Arienti, L. Mancuso, and P. Cotone, "IGCC plants to meet the refinery needs of hydrogen and electric power," in *Seventh European gasification conference*, Barcelona, Spain., 2006.

[42] U. Desideri and A. Paolucci, "Performance modelling of a carbon dioxide removal system for power plants," *Energy Convers. Manag.*, vol. 40, no. 18, pp. 1899–1915, 1999.

[43] C. Descamps, C. Bouallou, and M. Kanniche, "Efficiency of an Integrated Gasification Combined Cycle (IGCC) power plant including CO2 removal," *Energy*, vol. 33, no. 6, pp. 874–881, 2008.

[44] L. Zheng and E. Furinsky, “Comparison of Shell, Texaco, BGL and KRW gasifiers as part of IGCC plant computer simulations,” *Energy Convers. Manag.*, vol. 46, no. x, pp. 1767–1779, 2005.

[45] O. Holopainen, “IGCC plant employing heavy-petroleum residues,” *Bioresour. Technol.*, vol. 46, no. 1–2, pp. 125–128, 1993.

[46] F. Emun, M. Gadalla, T. Majozi, and D. Boer, “Integrated gasification combined cycle (IGCC) process simulation and optimization,” *Comput. Chem. Eng.*, vol. 34, no. 3, pp. 331–338, 2010.

[47] M. Ashizawa, S. Hara, K. Kidoguchi, and J. Inumaru, “Gasification characteristics of extra-heavy oil in a research-scale gasifier,” *Energy*, vol. 30, no. 11–12, pp. 2194–2205, 2005.

[48] J. Davison, S. Arienti, P. Cotone, and L. Mancuso, “Co-production of hydrogen and electricity with CO2 capture,” *Energy Procedia*, vol. 1, no. 1, pp. 4063–4070, 2009.

[49] Y. Kansha, M. Ishizuka, C. Song, and A. Tsutsumi, “An innovative methanol synthesis process based on self-heat recuperation,” *Appl. Therm. Eng.*, vol. 70, no. 2, pp. 1189–1194, 2014.

[50] M. Vaezi, M. Passandideh-Fard, M. Moghiman, and M. Charmchi, “Gasification of heavy fuel oils: A thermochemical equilibrium approach,” *Fuel*, vol. 90, no. 2, pp. 878–885, 2011.

[51] K. Gerdes, R. Stevens, T. Fout, J. Fisher, G. Hackett, and W. Shelton, “Current and Future Power Generation Technologies: Pathways to Reducing the Cost of Carbon Capture for Coal-fueled Power Plants,” *Energy Procedia*, vol. 63, pp. 7541–7557, 2014.

[52] P. Ahmadi, M. A. Rosen, and I. Dincer, “Multi-objective exergy-based optimization of a polygeneration energy system using an evolutionary algorithm,” *Energy*, vol. 46, no. 1, pp. 21–31, 2012.

[53] M. Al-Ali and I. Dincer, “Energetic and exergetic studies of a multigenerational solar-geothermal system,” *Appl. Therm. Eng.*, vol. 71, pp. 16–23, 2014.

[54] I. Dincer and C. Zamfirescu, “Renewable-energy-based multigeneration systems,” *Int. J. Energy Res.*, vol. 36, no. 15, pp. 1403–1415, 2012.

[55] F. A. Al-Sulaiman, I. Dincer, and F. Hamdullahpur, “Exergy modeling of a new solar driven trigeneration system,” *Sol. Energy*, vol. 85, pp. 2228–2243, 2011.

[56] T. A. H. Ratlamwala and I. Dincer, “Comparative energy and exergy analyses of two solar-based integrated hydrogen production systems,” *Int. J. Hydrogen Energy*, vol. 40, no. 24, pp. 7568–7578, 2015.

[57] Y. Bicer and I. Dincer, “Development of a new solar and geothermal based combined system for hydrogen production,” *Sol. Energy*, vol. 127, pp. 269–284, 2016.

[58] S. Islam, I. Dincer, and B. S. Yilbas, “Energetic and exergetic performance analyses of a solar energy-based integrated system for multigeneration including thermoelectric generators,” *Energy*, vol. 93, pp. 1246–1258, 2015.

[59] F. Yilmaz, M. T. Balta, and R. Selbaş, "A review of solar based hydrogen production methods," *Renew. Sustain. Energy Rev.*, vol. 56, pp. 171–178, 2016.

[60] M. Šingliar, "Solar Energy Using for Hydrogen Production," *Pet. Coal*, vol. 49, pp. 40–47, 2007.

[61] "Hydrogen-Bellona Rapport Nr.6-2002," 2002. [Online]. Available: http://bellona.org/filearchive/fil_Hydrogen_6-2002.pdf.

[62] D. Dini, "Hydrogen production through solar energy water electrolysis," *Int. J. Hydrogen Energy*, vol. 8, no. 11, pp. 897–903, 1983.

[63] H. Ozcan and I. Dincer, "Energy and exergy analyses of a solar driven Mg-Cl hybrid thermochemical cycle for co-production of power and hydrogen," *Int. J. Hydrogen Energy*, vol. 39, no. 28, pp. 15330–15341, 2014.

[64] A. Ursua, L. M. Gandia, and P. Sanchis, "Hydrogen Production From Water Electrolysis: Current Status and Future Trends," *Proc. IEEE*, vol. 100, no. 2, pp. 410–426, 2012.

[65] A. Yilanci, I. Dincer, and H. K. Ozturk, "A review on solar-hydrogen/fuel cell hybrid energy systems for stationary applications," *Prog. Energy Combust. Sci.*, vol. 35, no. 3, pp. 231–244, 2009.

[66] D. MacPhee and I. Dincer, "Thermodynamic Analysis of Freezing and Melting Processes in a Bed of Spherical PCM Capsules," *J. Sol. Energy Eng.*, vol. 131, no. 3, p. 31017, 2009.

[67] I. Dincer, "On thermal energy storage systems and applications in buildings," *Energy Build.*, vol. 34, no. 4, pp. 377–388, 2002.

[68] I. Dincer and S. Dost, "A perspective on thermal energy storage systems for solar energy applications," *Int. J. Energy Res.*, vol. 20, pp. 547–557, 1996.

[69] A. A. AlZahrani and I. Dincer, "Performance assessment of an aquifer thermal energy storage system for heating and cooling applications," *J. Energy Resour. Technol.*, vol. 138, no. 1, pp. 011901–011908, 2015.

[70] R. Soltani, I. Dincer, and M. A. Rosen, "Thermodynamic analysis and performance assessment of an integrated heat pump system for district heating applications," *Appl. Therm. Eng.*, vol. 89, pp. 833–842, 2015.

[71] R. Soltani, I. Dincer, and M. A. Rosen, "Comparative performance evaluation of cascaded air-source hydronic heat pumps," *Energy Convers. Manag.*, vol. 89, pp. 577–587, 2015.

[72] A. I. Kalina and H. M. Leibowitz, "Application of the Kalina cycle technology to geothermal power generation," *Geotherm. Resour Counc. Trans*, vol. 13, pp. 605–611, 1989.

[73] P. Ahmadi, I. Dincer, and M. A. Rosen, "Exergo-environmental analysis of an integrated organic Rankine cycle for trigeneration," *Energy Convers. Manag.*, vol. 64, pp. 443–457, 2012.

[74] J. Hogerwaard, I. Dincer, and C. Zamfirescu, "Analysis and assessment of a new organic Rankine cycle with/without cogeneration," *Energy*, vol. 62, pp. 300–310,

2013.

[75] J. H. Mack, S. M. Aceves, and R. W. Dibble, “Demonstrating direct use of wet ethanol in a homogeneous charge compression ignition (HCCI) engine,” *Energy*, vol. 34, no. 6, pp. 782–787, 2009.

[76] S. Saxena, S. Schneider, S. Aceves, and R. Dibble, “Wet ethanol in HCCI engines with exhaust heat recovery to improve the energy balance of ethanol fuels,” *Appl. Energy*, vol. 98, pp. 448–457, 2012.

[77] D. L. Flowers, S. M. Aceves, and J. M. Frias, “Improving ethanol life cycle energy efficiency by direct utilization of wet ethanol in HCCI engines,” *SAE Technical Paper No. 2007-01-1867*. 2007.

[78] A. Khaliq, S. K. Trivedi, and I. Dincer, “Investigation of a wet ethanol operated HCCI engine based on first and second law analyses,” *Appl. Therm. Eng.*, vol. 31, no. 10, pp. 1621–1629, 2011.

[79] M. Wilf and K. Klinko, “Performance of commercial seawater membranes,” *Desalination*, vol. 96, no. 1–3, pp. 465–478, 1994.

[80] M. Wilf and K. Klinko, “Effective new pretreatment for seawater reverse osmosis systems,” *Water Supply*, vol. 17, no. 1, pp. 117–125, 1999.

[81] M. Wilf and K. Klinko, “Optimization of seawater RO systems design,” *Desalination*, vol. 138, no. 1–3, pp. 299–306, 2001.

[82] W. Zhou, L. Song, and T. K. Guan, “A numerical study on concentration polarization and system performance of spiral wound RO membrane modules,” *J. Memb. Sci.*, vol. 271, no. 1–2, pp. 38–46, 2006.

[83] I. H. Aljundi, “Second-law analysis of a reverse osmosis plant in Jordan,” *Desalination*, vol. 239, no. 1–3, pp. 207–215, 2009.

[84] Y. Cerci, “Exergy analysis of a reverse osmosis desalination plant in California,” *Desalination*, vol. 142, no. 3, pp. 257–266, 2002.

[85] E. Drioli, E. Curcio, G. Di Profio, F. Macedonio, and A. Criscuoli, “Integrating Membrane Contactors Technology and Pressure-Driven Membrane Operations for Seawater Desalination,” *Chem. Eng. Res. Des.*, vol. 84, no. 3, pp. 209–220, 2006.

[86] “Global Waste on Pace to Triple by 2100,” 2013. [Online]. Available: http://www.worldbank.org/en/news/feature/2013/10/30/global-waste-on-pace-to-triple. [Accessed: 22-Sep-2017].

[87] O. K. M. Ouda, S. A. Raza, R. Al-Waked, J. F. Al-Asad, and A. S. Nizami, “Waste-to-energy potential in the Western Province of Saudi Arabia,” *J. King Saud Univ. - Eng. Sci.*, vol. 29, no. 3, pp. 212–220, 2017.

[88] “Biomass potential of Date Palm Waste.” [Online]. Available: http://www.ecomena.org/biomass-date-palm-wastes/. [Accessed: 10-Sep-2016].

[89] “Saudi Arabia burns 900,000 barrels of oil per day for electricity,” 2014. [Online]. Available: https://www.ohio.com/akron/pages/saudi-arabia-burns-900-000-barrels-of-oil-per-day-for-electricity. [Accessed: 25-Sep-2017].

[90] A.-S. Nizami, “Waste-to-Energy Potential in Saudi Arabia,” 2015. [Online].

Available: https://www.ecomena.org/wastetoenergy-saudiarabia/. [Accessed: 05-Oct-2017].

[91] R. Zanzi, K. Sjöström, and E. Björnbom, "Rapid pyrolysis of agricultural residues at high temperature.," *Biomass and Bioenergy*, vol. 23, no. 5, pp. 357–366, 2002.

[92] T. Pröll, R. Rauch, C. Aichernig, and H. Hofbauer, "Fluidized Bed Steam Gasification of Solid Biomass - Performance Characteristics of an 8 MWth Combined Heat and Power Plant," *Int. J. Chem. React. Eng.*, vol. 5, no. 1, 2007.

[93] W. Doherty, A. Reynolds, and D. Kennedy, *Materials and processes for energy: communicating current research and technological developments*. A. Méndez-Vilas (Ed.), Formatex Research Centre, 2013.

[94] D. R. Reinhart, "Determining the Chemical Composition of Solid Waste Problem Statement," 2004.

[95] H. H. . Haugen, B. M. . Halvorsen, and M. S. Eikelnd, "Simulation of gasification of livestock manure with Aspen Plus," *Proc. 56th SIMS*, pp. 271–277, 2015.

[96] A. Malek, M. N. A. Hawlader, and J. C. Ho, "Design and economics of RO seawater desalination," *Desalination*, vol. 105, no. 3, pp. 245–261, 1996.

[97] M. L. Crowder and C. H. Gooding, "Spiral wound, hollow fiber membrane modules: A new approach to higher mass transfer efficiency," *J. Memb. Sci.*, vol. 137, no. 1–2, pp. 17–29, 1997.

[98] J. Marriott and E. Sørensen, "A general approach to modelling membrane modules," *Chem. Eng. Sci.*, vol. 58, no. 22, pp. 4975–4990, 2003.

[99] M. N. A. Hawler, J. C. Ho, and A. Malek, "An experimental and analytical study of Permasep B10 separation characteristics," *J. Memb. Sci.*, vol. 87, no. 1–2, pp. 1–21, 1994.

[100] H. Huang, N. Young, B. P. Williams, S. H. Taylor, and G. Hutchings, "COS hydrolysis using zinc-promoted alumina catalysts," *Catal. Letters*, vol. 104, no. 3, pp. 17–21, 2005.

[101] C. Rhodes, S. A. Riddel, J. West, B. P. Williams, and G. J. Hutchings, "The low-temperature hydrolysis of carbonyl sulfide and carbon disulfide: a review," *Catal. Today*, vol. 59, no. 3–4, pp. 443–464, 2000.

[102] T.-C. Hung, "Waste heat recovery of organic Rankine cycle using dry fluids," *Energy Convers. Manag.*, vol. 42, pp. 539–553, 2001.

[103] E. L. Keating, *Applied Combustion*, Second Edi. New York, USA: Taylor & Francis, 2007.

[104] F. Suleman, I. Dincer, and M. Agelin-Chaab, "Energy and exergy analyses of an integrated solar heat pump system," *Appl. Therm. Eng.*, vol. 73, pp. 557–564, 2014.

[105] S. Islam and I. Dincer, "Comparative performance study of an integrated air-cycle refrigeration and power generation system," *Appl. Therm. Eng.*, vol. 106, pp. 493–505, 2016.

[106] I. Dincer and M. A. Rosen, *Exergy, environment and sustainable development*. Elsevier Ltd, 2013.

[107] J. Szargut, D. R. Morris, and F. R. Steward, *Exergy analysis of thermal, chemical, and metallurgical process*. Hemisphere Publishing Corporation, USA, 1988.

[108] J. Szargut, *Exergy Method: technical and ecological applications*. Boston: WIT Press, 2005.

[109] M. G. Gronli, M. C. Melaaen, M. Grønli, and M. C. Melaaen, "Mathematical model for wood pyrolysis - Comparison of experimental measurements with model predictions," *Energy & Fuels*, vol. 14, no. 4, pp. 791–800, 2000.

[110] T. Proll and H. Hofbauer, "Development and application of simulation tool for biomass gasification based processes," *Int. J. Chem. React. Eng.*, vol. 6, pp. 1–56, 2008.

[111] Y. A. Cengel and M. A. Boles, *Thermodynamics an Engineering Approach*, 7th ed. McGraw-Hill, New York, 2011.

[112] T. J. Kotas, *The Exergy Method of Thermal Plant Analysis*. Butterworth, London, 1985.

[113] M. J. Moran, H. B. Shapiro, D. D. Boettner, and M. Bailey, *Fundamentals of Engineering Thermodynamics*, 7th ed. John Wiley and Sons Ltd, 2011.

[114] I. Dincer, "The role of exergy in energy policy making," *Energy Policy*, vol. 30, no. 2, pp. 137–149, 2002.

[115] J. B. Heywood, *Internal Combustion Engines Fundamentals*. McGraw Hill, New York, 1988.

[116] F. Ma and Y. Wang, "Study on the extension of lean operation limit through hydrogen enrichment in a natural gas spark-ignition engine," *Int. J. Hydrogen Energy*, vol. 33, no. 4, pp. 1416–1424, 2008.

[117] C. R. Ferguson and A. T. Kirkpatrick, "Internal Combustion Engines," Second, Ed., Wiley, New York, 2004.

[118] P. Ahmadi, I. Dincer, and M. A. Rosen, "Thermoeconomic multi-objective optimization of a novel biomass-based integrated energy system," *Energy*, vol. 68, pp. 958–970, 2014.

[119] A. Bejan, G. Tsatsaronis, and M. J. Moran, "Thermal Design and Optimization," New York: John Wiley & Sons, 1996.

[120] F. Mohammadkhani, N. Shokati, S. M. S. Mahmoudi, M. Yari, and M. A. Rosen, "Exergoeconomic assessment and parametric study of a Gas Turbine-Modular Helium Reactor combined with two Organic Rankine Cycles," *Energy*, vol. 65, pp. 533–543, 2014.

[121] J. Sadhukhan, K. . Ng, and E. . Hernandez, *Biorefinereis and Chemical Processes*. West Sussex, UK: John Wiley & Sons, Ltd, 2014.

[122] R. Jayakumar, "Analysis of power Generation Process Using Petcoke," Texas A&M University, College Sation, TX, USA, 2008.

[123] D.-H. Jang, S.-P. Yoon, H.-T. Kim, Y.-C. Choi, and C. Lee, "Simulation analysis of hybrid coal gasification according to various conditions in entrained-flow gasifier," *Int. J. Hydrogen Energy*, vol. 40, no. 5, pp. 2162–2172, 2015.

[124] J. Xie, W. Zhong, J. B, S. Y, and H. Y, “Eulerian-Langrangian method for three-dimensional simulation of fluidized bed coal gasification.,” *Adv. Powder Technol.*, vol. 24, pp. 382–392, 2013.

[125] K. Umeki, K. Yamamoto, T. Namioka, and K. Yoshikawa, “High temperature steam-only gasification of woody biomass,” *Appl. Energy*, vol. 87, pp. 791–798, 2010.

[126] R. S. El-emam and I. Dincer, “Thermodynamic and thermoeconomic analyses of seawater reverse osmosis desalination plant with energy recovery,” *Energy*, vol. 64, pp. 154–163, 2014.

[127] A. Corti and L. Lombardi, “Biomass integrated gasification combined cycle with reduced CO 2 emissions : Performance analysis and life cycle assessment (LCA),” *Energy*, vol. 29, pp. 2109–2124, 2004.

[128] C. Wu, X. Yin, L. Ma, Z. Zhou, and H. Chen, “Design and Operation of A 5 . 5 MW e Biomass Integrated Gasification Combined Cycle Demonstration Plant,” *Energy and Fuels*, vol. 22, no. 13, pp. 4259–4264, 2008.

[129] T. Proll, R. Rauch, C. Aichering, and H. Hofbauer, “Coupling of biomass steam gasification and SOFC-gas turbine hybrid system for highly efficient electricity generation.,” in *ASME Turbo Expo: Power for Land Sea and Air*, 2004.

[130] M. Gassner and F. Marechal, “Thermodynamic comparison of the FICFB and Viking gasification concepts,” *Energy*, vol. 34, pp. 1744–1753, 2009.

[131] “Current and Future Technologies for Gasification- Based Power Generation,” USA, 2010.

[132] “IGCC Economics and Impact of 3Party Covenant.” [Online]. Available: http://www.belfercenter.org/sites/default/files/legacy/files/igcc financing chapter 5.pdf. [Accessed: 28-Jul-2017].

[133] “Aspen Plus V9.” Aspen Tech, 2016.

[134] “Thermoflow Suite 26 (TFLOW26).” Thermoflow Inc. USA, 2016.

[135] M. S. Peters, K. D. Timmerhaus, and R. E. West, *Plant Design and Economics for Chemical Engineers*. McGraw-Hill, Inc., 2003.

[136] T. J. Falcke, A. F. A. Hoadley, D. J. Brennan, and S. E. Sinclair, “The sustainability of clean coal technology: IGCC with/without CCS,” *Process Saf. Environ. Prot.*, vol. 89, no. 1, pp. 41–52, 2011.

[137] “Commercial Energy Systems: Compare - Installed Costs - Chillers.” [Online]. Available: http://c03.apogee.net/contentplayer/?coursetype=ces&utilityid=northwestern&id=1084. [Accessed: 26-Jul-2017].

[138] S. Loutatidou, B. Chalermthai, P. R. Marpu, and H. A. Arafat, “Capital cost estimation of RO plants: GCC countries versus southern Europe,” *Desalination*, vol. 347, pp. 103–111, 2014.

[139] D. B. Makel and B. Blizman, “Biogas-Fuelled HCCI Power Generation System for Distributed Generation,” California Energy Comission Report, Publication number:

CEC-500-2016-033, 2014.

[140] N. S. Siefert, S. Narburgh, and Y. Chen, “Comprehensive exergy analysis of three IGCC power plant configurations with CO2 capture,” *Energies*, vol. 9, no. 9, 2016.